Summer 8-1-2021

Sedimentology and Shallow Groundwater Responses of a Coastal Marsh Along a Salinity Gradient: A Case Study In Grand Bay National Estuarine Research Reserve, Mississippi

James Thompson

SEDIMENTOLOGY AND SHALLOW GROUNDWATER RESPONSES OF A COASTAL MARSH ALONG A SALINITY GRADIENT: A CASE STUDY IN GRAND BAY NATIONAL ESTUARINE RESEARCH RESERVE, MISSISSIPPI

by

James Thompson

A Thesis
Submitted to the Graduate School,
the College of Arts and Sciences
and the School of Biological, Environmental, and Earth Sciences
at The University of Southern Mississippi
in Partial Fulfillment of the Requirements
for the Degree of Master of Science

Approved by:

Dr. Franklin T. Heitmuller, Committee Chair
Dr. Patrick D. Biber
Dr. Kevin A. Kuehn
Dr. George T. Raber

August 2021

ABSTRACT

Climate change and relative sea level rise is resulting in saltwater intrusion and inundation of coastal marshes. This study investigates factors affecting marsh hydrology, including sediment composition, seasonal variability, and coastal storms in Grand Bay National Estuarine Research Reserve (NERR) near Pascagoula, Mississippi. Analysis of sediment includes color, organic matter, carbonate, magnetic susceptibility, and particle size. Shallow groundwater hydrologic trends between Summer 2015 and Fall 2016 are established along a salinity gradient at four sites using water levels, temperature, and conductivity monitored at the surface and in piezometers at depths of 0.75m, 1.5m, and 2.25m.

Sediment analysis indicates reducing conditions throughout with redoximorphic concentrations of iron oxides and oxidation colors. Sediment is typically high in organic matter (avg 4.6% and up to 18.5%) and below 5% carbonate. Magnetic susceptibility increases seaward. The relative abundance of sand particles is a controlling factor for permeability in the clay and silt rich marsh sediments. Shallow groundwater levels fluctuate corresponding to diurnal tidal cycles, seasonal cycles, and short-term storm influences. Temperature and salinity fluctuate slowly, and do not have strong tidal signals indicating a distinction between the marine surface and terrestrial subsurface. The salinity gradient generally follows expected trends. However, the salinity gradient shifts to the middle of the marsh in drier periods such that salinity is higher than in outer marsh areas. Salinity generally decreases with depth suggesting that seaward flow of fresher water in the shallow subsurface coupled with low permeability fine-grained sediments resists the seepage of higher density saline surface water.

ACKNOWLEDGMENTS

There are many people to whom I owe a great deal of thanks. Foremost, I would like to acknowledge my advisor, Dr. Franklin Heitmuller, for his endless patience, support, and guidance. I would like to thank Dr. Patrick Biber and Dr. Kevin Kuehn, for their advice and support throughout the duration of the project including many hours of fieldwork. Thanks to Dr. George Raber, for guidance and for help with GIS. I would also like to thank the Grand Bay NERR staff for guidance and access, especially Jay McIlwain and Lindsay Spurrier. Thanks to the USM Office of the Vice President for Research for seed funding.

Additional thanks go to Dr. Micheal Davis, for support, advice, and access to equipment at the Lake Thoreau Environmental Center. Fellow USM graduate students, Matt Lodato, Jay Price, and Brandy Purdy, deserve thanks for their invaluable assistance in the installation and maintenance of the piezometers. I am grateful for USM geology undergraduate students, especially Austin Cannon, for enduring hours of fieldwork in rough conditions. Finally, I would like to extend my gratitude to Dr. Davin Wallace for the generous use of his lab and laser granulometer at Stennis Space Center.

DEDICATION

I would like to thank my friends and family, especially my mother and sister, for their understanding, patience, and support. Thanks go out to my friend Lloyd Throop for dropping everything to help when this project was literally stuck in the mud. Furthermore, thanks are also extended to Dr. Grant Harley, Dr. David Patrick, and Dr. Maurice Meylan for their helpful wisdom and encouragement.

TABLE OF CONTENTS

LIST OF TABLES

LIST OF ILLUSTRATIONS

LIST OF ABBREVIATIONS

BHER	Bayou Heron Site
CTD	Conductivity, Temperature, Depth
GCRL	Gulf Coast Research Lab
GNDNERR	Grand Bay National Estuarine Research Reserve
LALLS	Low Angle Laser Light Scattering
LOI	Loss On Ignition
LTEC	Lake Thoreau Environmental Center
MBAY	Middle Bay Juncus Site
NERR	National Estuarine Research Reserve
NERRS	National Estuarine Research Reserve System
NOAA	National Oceanic and Atmospheric Administration
PSU	Practical Salinity Units
SALT	Salt Pan Site
SLR	Relative Sea Level Rise
SPAR	Spartina Site
SWMP	Surface Water Monitoring Program
USGS	United States Geological Survey
USM	The University of Southern Mississippi
WQBH	Water Quality Monitoring Station at Bayou Heron
WQPC	Water Quality Monitoring Station at Point aux Chenes

CHAPTER I – INTRODUCTION

1.1 Introduction

This research is part of a collaborative effort among coastal scientists, ecologists, and geologists at The University of Southern Mississippi (USM) to develop a model for vegetation responses, organic degradation, nutrient fluxes, and greenhouse gas emissions associated with sea-level rise along a gradient from terrestrial freshwater environments to brackish estuarine marshes. The climate and sea-level changes predicted in the National Climate Assessment (2014) could result in severe deviations from current hydrologic conditions along the gradient thereby affecting sediment deposition and groundwater salinity in coastal marshes.

Coastal marshes offer a large range of ecosystem services including storm protection, flood control, essential habitat for many aquatic species, carbon sequestration, nutrient regulation, water quality improvements, and shoreline stabilization, among others (Barbier et al., 2011). Climate change and relative sea level rise (SLR) is already and will continue to result in salt-water intrusion into these vital coastal habitats, affecting biotic productivity and healthy ecosystem function. The effects of salt-water intrusion into coastal marsh habitats could include altered productivity, litter decomposition, reduced species diversity, and impaired ecosystem functionality in the near-term. In the long-term, urban and industrial encroachment on wetlands could potentially result in the loss of extensive areas of coastal marsh habitat. As the water level rises and the inundation frequency increases, the natural response of the ecosystem is typically characterized by vegetation retreat (Hilbert, 2006). A lack of undeveloped upland habitat would restrict this process and further impair an already stressed habitat.

Furthermore, geologically rapid changes in sea level could overwhelm species with limited mobility.

The southeastern United States is predicted to have increased temperatures, more extreme rainfall events, and more frequent coastal inundation/storm surge events within this century (Melillo et al., 2014). Even at current sea level conditions, this prediction is concerning and reason for emphasis of the preservation of coastal environments, which naturally serve to mitigate storm energy and flooding. However, predictions for Mississippi suggest substantial areas of the coast will experience between 1 to 2 m of SLR by 2100, resulting in coastal flooding of property and loss of extensive infrastructure and coastal marsh habitats (Melillo et al., 2014). This rate of change is roughly an order of magnitude faster than typical geologic interglacial cycles that correspond to past sea level changes (Milliken et al., 2008).

The research site for this study, Grand Bay National Estuarine Research Reserve (GNDNERR), is located in southeastern Jackson County on Mississippi's Gulf Coast adjacent to the state border with Alabama highlighted in the map below (Figure 1.1). GNDNERR was established as a protected estuary in 1999 under the National Oceanic and Atmospheric Administration's (NOAA) National Estuarine Research Reserve System (NERRS). A joint effort of private and public agencies, GNDNERR properties create a combined 18,000 acres of protected coastal, wetland, and terrestrial habitats. The current research goals of GNDNERR include advancements "relating to habitat protection, climate change, and water quality" to improve management of coastal resources and scientific understanding (Grand Bay National Estuarine Research Reserve, 2013). The NOAA Sentinel Site Program began at GNDNERR in 2012 and evolved from the

System-Wide Monitoring Program that established guidelines for collecting and sharing data from protected lands. Ongoing operations in GNDNERR include “tidal marsh, mangrove, submerged aquatic vegetation, wetland surface elevation change, water level, surface water quality, and meteorological data monitoring” (Office of Ocean and Coastal Resources, 2012). Some sentinel stations are relevantly associated to this research effort and will aid in other multi-disciplinary research efforts as well.

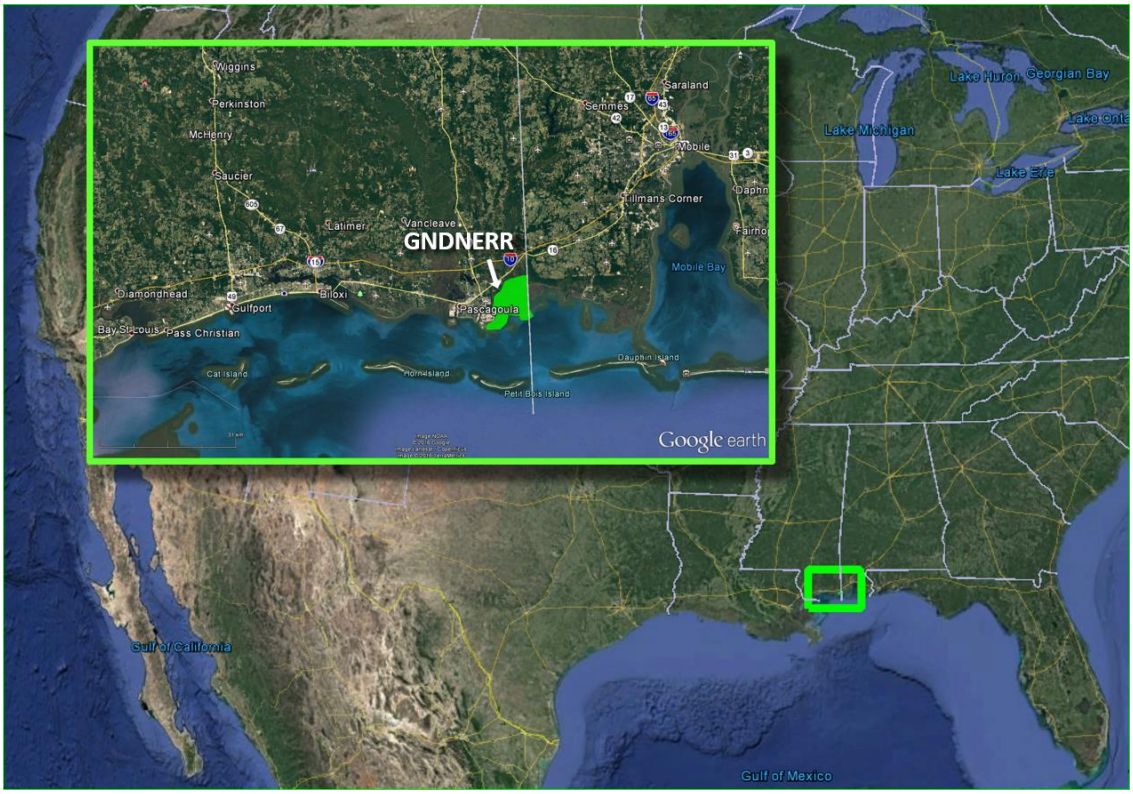

Figure 1.1 *Grand Bay National Estuarine Research Reserve Regional Map*

The GNDNERR is located on the Gulf Coast in Jackson County, Mississippi adjacent to the state border of Alabama.

Very little research has been done on the sedimentology and hydrologic processes of Gulf Coast estuarine and marsh environments. A past tendency in academia to segregate terrestrial and marine systems has resulted in limited understanding of processes across the freshwater-saltwater transition. There are large gaps in knowledge

crucial to understanding potential changes in the salt marsh environment caused by relative SLR. One such knowledge gap exists in the understanding of groundwater hydrology throughout the marsh. Second, the geologic history of the study area is loosely understood as an abandoned retrogradational delta, but no work has been done to characterize the sedimentology of the subsurface in GNDNERR. These two knowledge gaps are inextricably intertwined and necessary for the understanding of how water and sediment move in the system.

1.2 Goals

The overall goal for this study is to contribute to a greater understanding of marsh sedimentology and hydrology with regards to how the predicted changes in relative sea level and climate change might affect the GNDNERR and its underlying geologic processes. This overall goal fits well with the National Oceanic and Atmospheric Administration's (NOAA) goal for the GNDNERR to foster research that improves the understanding of estuarine resources including water quality, habitat protection, and climate change (Grand Bay National Estuarine Research Reserve, 2013). Although the intention of this research was not to attempt validation of current predictions for the effects of SLR, aspects of this research most certainly advance the ongoing multidisciplinary research working to identify factors of, and responses to, SLR. The research results here should be combined with collaborative investigations of salt-tolerance mechanisms and responses by vegetation to changing salinity, spatial modeling of shoreline and vegetation changes, as well as new restoration and preservation techniques for a more complete interdisciplinary understanding of the marsh system.

1.3 Objectives

In support of this study's overall goal, this research fulfilled tangible objectives. The first objective was to collect and analyze sediment cores to establish sediment composition and characteristics of the subsurface. The second objective was the identification of spatial and temporal trends in groundwater hydrology along a salinity gradient. Third, external factors (e.g., coastal storms, tidal fluctuations, rainfall events) that directly affect changes in hydrology and sedimentation have been identified for further research. The final objective was to create a dataset for reference by collaborative interdisciplinary investigations. Fulfillment of these objectives has addressed the research questions below.

1.4 Research Questions

This study answers three primary research questions. What is the basic spatial and temporal nature of shallow groundwater salinity in the salt marshes of GNDNERR? How does subsurface sediment composition affect shallow groundwater properties in the salt marshes of GNDNERR? How might the sedimentology and hydrology influence or be influenced by tides, storms, and vegetation communities regarding SLR?

It is important to note that focusing on only one of these questions would not adequately address its subject. The sedimentology of the subsurface is a controlling factor of the groundwater hydrology. Also, an understanding of the hydrology revealed how the salinity of the groundwater differs from surface waters. If a less saline groundwater source is available to vegetation communities, the vegetation may be more resilient or less affected by surface inundation events. Thereby, a more resilient vegetation may resist erosion longer. This corresponds with questions left from earlier studies by Schmid

(2000) and Hilbert (2006). In addition, understanding the sediment structure could allow for more accurate assessment of the potential rates of erosion and the potential rates of saline infiltration into the shallow groundwater. This knowledge is crucial to ongoing sediment flux research and water resource management plans, both of which are interests for multiple private and public agencies. So, the three primary research questions taken together have formed the basis of this thesis and served to fill a knowledge gap essential to future research.

CHAPTER II – PREVIOUS RESEARCH

2.1 Previous Coastal Research

From the 1950s to the 1970s, processes associated with estuarine and salt marsh environments were frequently overlooked. Most past research put heavy emphasis on beaches and barrier islands because of population density and economic value associated with these environments (Hoyt, 1967; Gosselink et al., 1974; Dolan et al., 1980). Though much of this research is applicable to coastal environments in general, conclusions drawn from linear systems such as beaches and barrier islands can lead to gross over-simplification in transitional estuarine systems. Furthermore, variables such as geomorphology and regional coastal slope must be weighted differently depending on the scale of study (Pendleton et al., 2010). Thus, scientists were disinclined to focus on estuarine systems.

Since the early 1970s, rapid and increasing growth of populations and infrastructure on coastal properties led to an increased interest in coastal environments and ecosystem health (Gosselink et al., 1974; Morton et al., 2004). The Coastal Zone Management Act of 1972 established the National Estuarine Research Reserve System to protect estuarine ecosystem areas. United States Geological Survey (USGS) and Landsat surveys were conducted regularly on all potential NERR sites including Grand Bay (Hilbert, 2006). A multidisciplinary effort spearheaded by NASA led to a categorical risk index database using a combination of marine, weather, and geologic variables. This database established 30 percent of the Gulf Coast as very high risk to SLR (Gornitz et al., 1994). In 1996, the Intergovernmental Panel on Climate Change documented a 2 mm/yr rate of global sea-level change through the previous century. This highlighted the need

for further investigation of coastal systems believed to be most vulnerable to high rates of change (Scavia et al., 2002). In 1998, the USGS began using advanced surveying techniques including LIDAR and GPS to track shoreline changes to help predict the vulnerability to erosion (Morton et al., 2004). By 2003, the USGS established the National Assessment of Shoreline Change Project using historical shoreline changes from archival and recent surveys and provided a vital means of data dissemination (Morton et al., 2005).

Until recently, the Bruun and Swift rules (Schwartz, 1967) were used to understand shoreline processes. The Bruun rules states that shoreline changes in response to sea level rise are a complex reaction of the entire shoreface, not just a retreat of sand (Nicholls et al., 1995). Additionally, Swift states that the shoreface response to sea level rise depends on "grain size, wave conditions, sediment supply, and several other factors" (Cooper and Pilkey, 2004). However, the process of shoreline and marsh evolution are much more complicated than Bruun and Swift accounted for. These oversimplifications hold true only on the simplest beach type coasts and assume too much control based on the sediment grain size parameter.

Generally, marsh evolution is poorly defined on a site-by-site basis. In detail, wetland losses comprise a complex sequence of processes involving reduced wetland productivity and ultimate death of the individual plants, which in turn allows a range of other destructive processes to occur (Nicholls et al., 1995). While it is clear that fundamental research has provided explanations for certain shoreline environments, there is a lack of knowledge of the evolution of the marsh environment. Specifically, studies

regarding sediment composition, salinity, and fluctuations of the water table would better inform predictions of estuarine responses to SLR.

2.2 Previous Sedimentological Research of Study Area

Specific to the sedimentology of this thesis in GNDNERR, Schmid (2000) completed an analysis of shoreline change using GPS and historic survey maps based on the hypothesis that the GNDNERR has been sediment starved for centuries due to a natural redirection of the Escatawpa River into the Pascagoula River (Otvos, 1985). Schmid (2000) hypothesized that significant erosion and loss of land was occurring on the marsh and local barrier islands from the 1980s to 1999. Using available data and GIS, Schmid determined a minimum approximate loss of 10 acres of land annually in the GNDNERR area and noted several hurricanes occurred during this period. Furthermore, a cursory comparison of these results with another nearby marsh revealed that there were two primary factors contributing to this land loss: human development and wave energy erosion. However, Schmid went no further other than to suggest detailed understanding of the sediment fluxes in GNDNERR could help pinpoint the underlying process of shoreline loss (Schmid, 2000).

Since 2010, updates to Schmid's work and similar research performed by the USGS and the National Oceanic and Atmospheric Administration (NOAA) have included adding newly available LIDAR data into models and utilizing higher resolution tidally adjusted input data (Strauss et al., 2002). With higher resolution, evaluations of short-term erosion and land loss becomes more complicated, but valuable understandings of how sediment movement affects the shoreline are gained. Schmid's (2000) work and more recent projects by others have laid the framework for understanding the

sedimentological processes in GNDNERR and provide a means of meaningful interpretation to the sediment composition to be examined in this thesis.

Additionally, a recent pilot study conducted by NERR staff demonstrated a potential method for monitoring sediment deposition using trap stations and surface elevation tables (SETs) in GNDNERR allowing overwash sediments to become trapped and collected periodically. This ongoing research hopes to address the knowledge gap of sediment flux, which persists leaving the current understanding of land erosion and deposition limited to a comparison of shorelines. The SETs are semi-permanent and have become part of the NOAA Sentinel Site Program (Office of Ocean and Coastal Resources, 2012). In an effort to decipher sediment fluxes, other researchers will correlate data from the SETs with findings documented in this thesis from nearby research sites.

Sediment fluxes are the key to deciphering submergence and land loss. However, land loss is not synonymous with marsh loss. Marshes can often retreat landward if unimpeded as many studies have shown. Some work has focused on distinguishing between submergence from SLR and submergence from subsidence. Submergence in general represents an insufficient rate of sediment accretion to maintain a level above the water. Subsidence is sinking or lowering of the ground irrespective of changes in sea level or sediment input (White and Tremblay, 1995). Well understood causes of subsidence include the depletion of oil and water reservoirs, faulting, dissolution, compaction, and settling. White and Tremblay (1995) examined subsidence in Texas and Louisiana estuaries and calculated that actual coastal accretion rates have been drastically lower than the maximum due to human structures preventing sediment from reaching the

estuaries. White and Tremblay (1995) established general sediment fluxes for different environments but acknowledged a need for precise elevation monitoring to verify sediment accretion deficits relative to sea level. The SETs or surface elevation tables in GNDNERR should enable precise measurements of sediment accretion, enabling calculation of a sediment deficit, and measure any subsidence present, which can be combined with research results in this thesis.

Although previous and ongoing research has focused on sediment flux at the surface, the research documented in this thesis focuses on sediment structure and composition below the surface. This provides a holistic understanding of marsh sediment processes, which include both short-term and long-term effects of SLR.

2.3 Previous Hydrologic Research of Study Area

Whereas there are obvious preambles to the sedimentological component of this research in GNDNERR, very few studies have considered the hydrologic components beyond tidal or storm inundation. The only existing hydrologic data for Grand Bay is from ongoing surface water monitoring and limited pore-water sampling; no groundwater data exist. Kent Hilbert at NASA used Landsat imagery to study land cover changes from 1974 to 2001. Hilbert (2006) related observed changes in plant communities to geomorphic changes such as land subsidence and inundation from saline surface water. This work highlighted the need for further multidisciplinary studies including vegetation responses and hydrologic conditions (Hilbert, 2006). Logically, shallow groundwater hydrology could be significant to the biodiversity and resilience of vegetative communities.

As of Spring 2015, very few studies have begun to investigate more complex processes in estuarine salt marshes such as shallow groundwater salinity. Although not geographically associated with the study area, the most relevant research is part of a study in North Inlet, South Carolina, which used electrical resistivity to survey subsurface conductivity along several transects (Carter et al., 2008). The study noted seasonal variance in the freshwater-brackish interface and modeled a predictive relationship between the water table and interface position. Although the position of the interface was recorded in a spatially continuous manner along the transects, it could only be recorded approximately once per month at the lowest tide. Therefore, no correlations to tidal cycles or precipitation events could be made. Furthermore, the setting of the transects at North Inlet is protected by a sand beach and is subject to larger tidal fluctuations and more freshwater surface flow than the targeted positions in Grand Bay (Carter et al., 2008). So in an effort to expand the holistic understanding of marsh hydrology, this thesis research continuously monitored conductivity, temperature, and subsurface depth of the groundwater in order to reveal the effects of tidal cycling, storm events, and potential SLR.

2.4 Description of Study Area

Research site selections within GNDNERR, as depicted in Figure 2.1, was based on collaborative input and a variety of required factors. Of primary importance, site selection focused on spanning the assumed coastal salinity gradient. Also, the locations needed to be accessible by boat or rugged-terrain-vehicle to enable long-term installation viability and ease of access for routine visits and data retrieval. Emphasis on the transition zones of various vegetative communities including Spartina alterniflora and

Juncus roemerianus allowed for interdisciplinary study. For increased scientific impact, installations are also near existing NOAA Sentinel Sites, which include various installations such as sediment elevation tables or surface water monitoring stations.

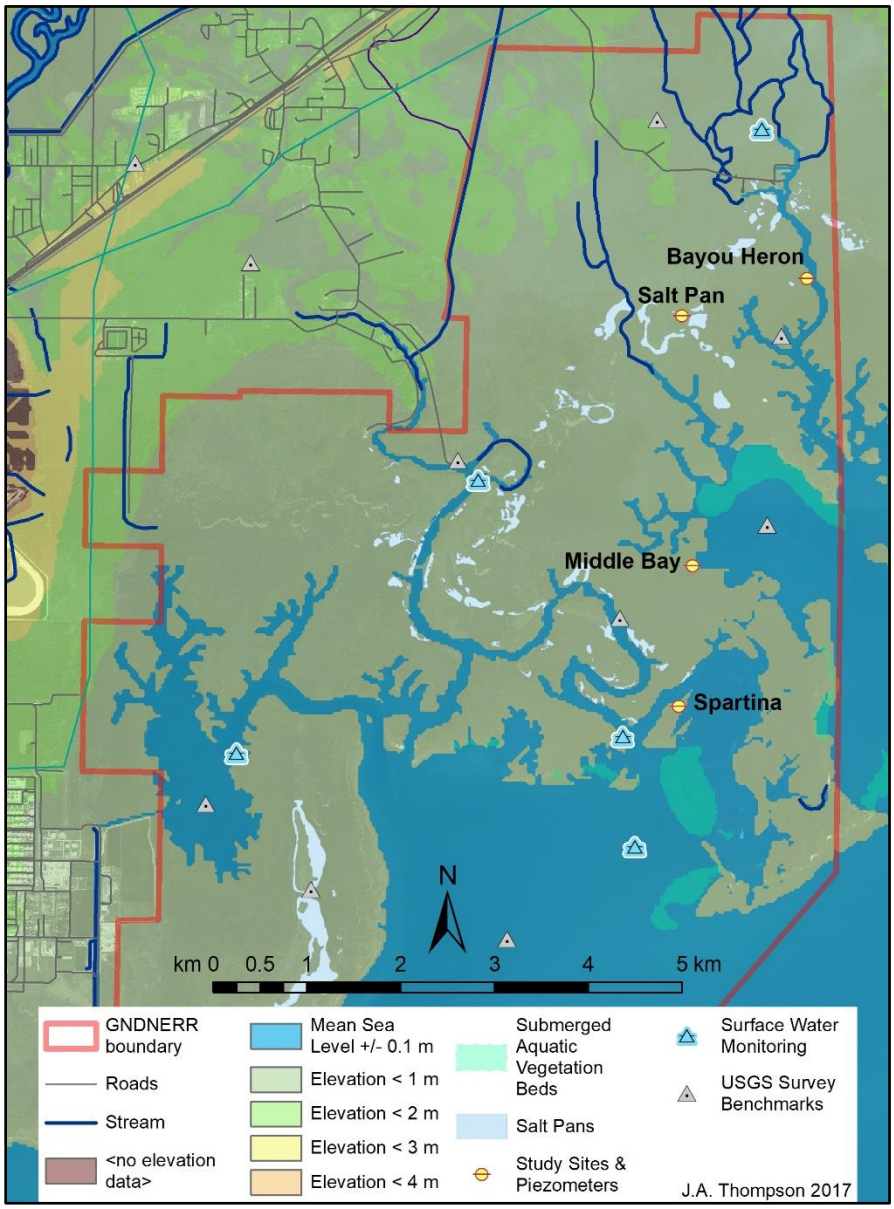

Figure 2.1 *GNDNERR Local Area Elevation Map*

NERR boundary is denoted in red. Points indicate current and ongoing research locations. Elevations based on USGS National Elevation Dataset 7.5' digital elevation models, 2012.

Study sites selected for this research include the Spartina (North Rigolets), Middle Bay, Salt Pan, and Bayou Heron sites (Figure 2.2). Bayou Heron is the most northerly site and the only site not immediately adjacent to a Sentinel station. This site is approximately 1 km downstream from the nearest Sentinel station and has brackish and highly tannic surface waters. The Salt Pan site is about 1.5 km west-southwest of Bayou Heron. It features uniquely stagnant and often desiccating surface conditions that precipitate salts and restrict vegetative growth. Middle Bay and Spartina (North Rigolets) areas are the intermediate and southernmost sites, respectively. Surface inundation frequency and marine exposure are higher at these seaward sites.

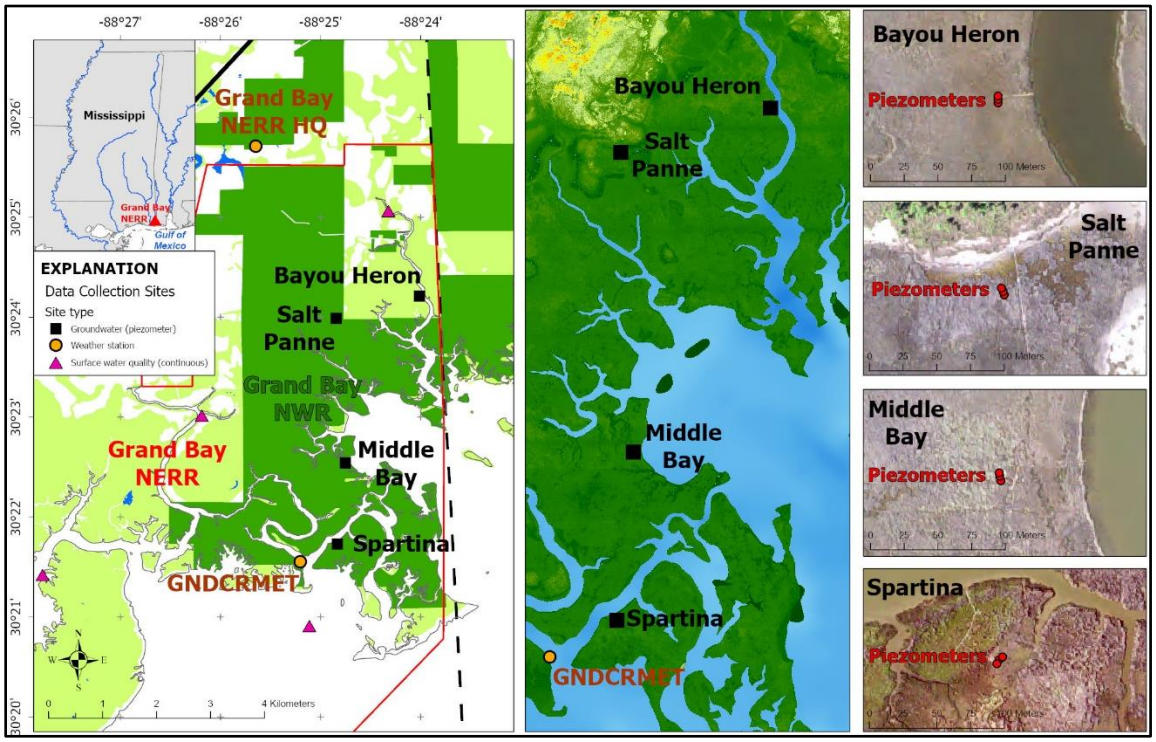

Figure 2.2 *Site Map*

Each groundwater site has 4 stations comprised of 3 piezometers and 1 surface station.(Aerial imagery from ESRI, 2016)

The northern area of the former Escatawpa delta is dominated by pine savannas and brackish marshes with tidally-influenced tannic waters. The southern area is comprised of more saline marshes and is subject to higher energy conditions from Mississippi Sound. All sites are frequently inundated by seasonal tidal events and storm surge events, include those during hurricane season between June and November. The diurnal tide range around Pascagoula averages 0.46 meters. Annually, the astronomical tides range approximately 1.1 meters (Eleuterius and Criss, 1991). These tidal and storm related events both erode and deposit sediments. Onshore migration of coarse lagoonal sediments from Mississippi Sound constitutes one consistent source of inorganic sediment input for GNDNERR. Suspended sediment loads from Mobile Bay and the Pascagoula River likely constitute a significant fine-grained inorganic sediment source. Given the lack of current fluvial deposition, most inorganic deposition occurs with hurricane storm surge bringing sediment from shallow areas just offshore from the marsh (Turner et al., 2006). However, Infrequent extreme flooding events and more frequent moderate flow events—bringing organic-rich sediments from nearby riverine and terrestrial sources—likely supply significant nutrient deposition and fine grained sediment volume to the marsh (Tornqvist et al., 2007). The biology and geology of the marsh environment responds to gradual changes, such as warming temperatures and saltwater intrusion. Nevertheless, the marsh is threatened by erosion and marine inundation (Scavia et al., 2002).

The GNDNERR habitat provides critical refuge areas for wildlife and vegetation. Throughout the study area, there is a variety of vegetation communities and habitats depicted in Figure 2.3 and Figure 2.4. Black needle rush (Juncus roemerianus) occurs in

nearly pure stands at Bayou Heron and Middle Bay, but cordgrass (Spartina alterniflora) is uniquely common at the North Rigolets area leading to the site name, Spartina. The Salt Pan site, named for the areas of high surface salinity, transitions from a marsh community dominated by J. roemerianus to pine savannah within a few hundred meters. These salt flats or "pannes" occur throughout the marsh and are commonly found to occur near marsh-forest margins (Figure 2.4). Typical vegetation unique to salt flats includes 'glasswort' (Salicornia bigelovii), 'seablite' (Suaeda linearis), and 'saltwort' (Batis maritimus) (Eleuterius and Criss, 1991). The vegetation at each site was noted to study long-term changes.

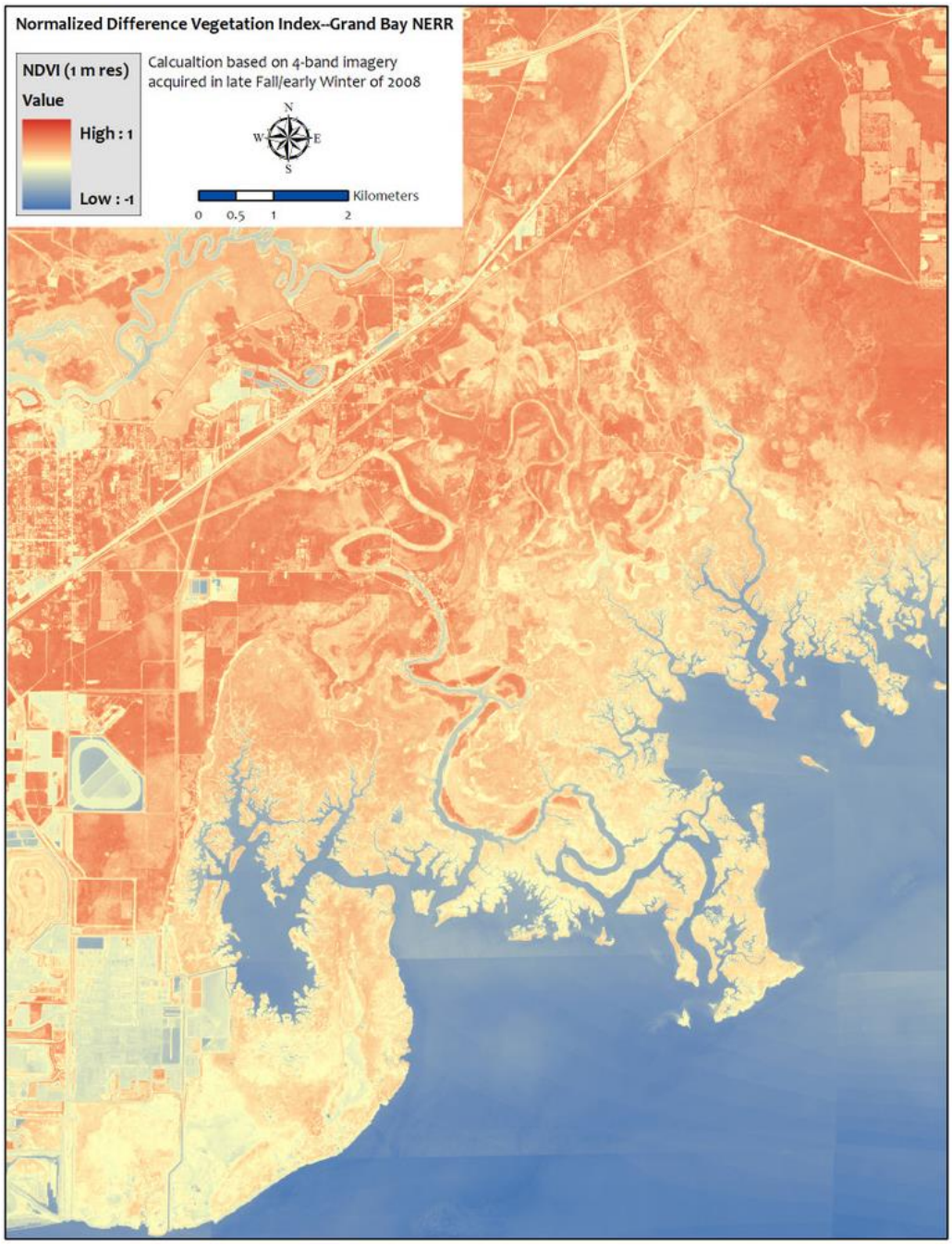

Figure 2.3 *GNDNERR Normalized Difference Vegetation Index*

The warmer colors are an indication of healthy, dense vegetation. (Provided by MS Department of Marine Resources).

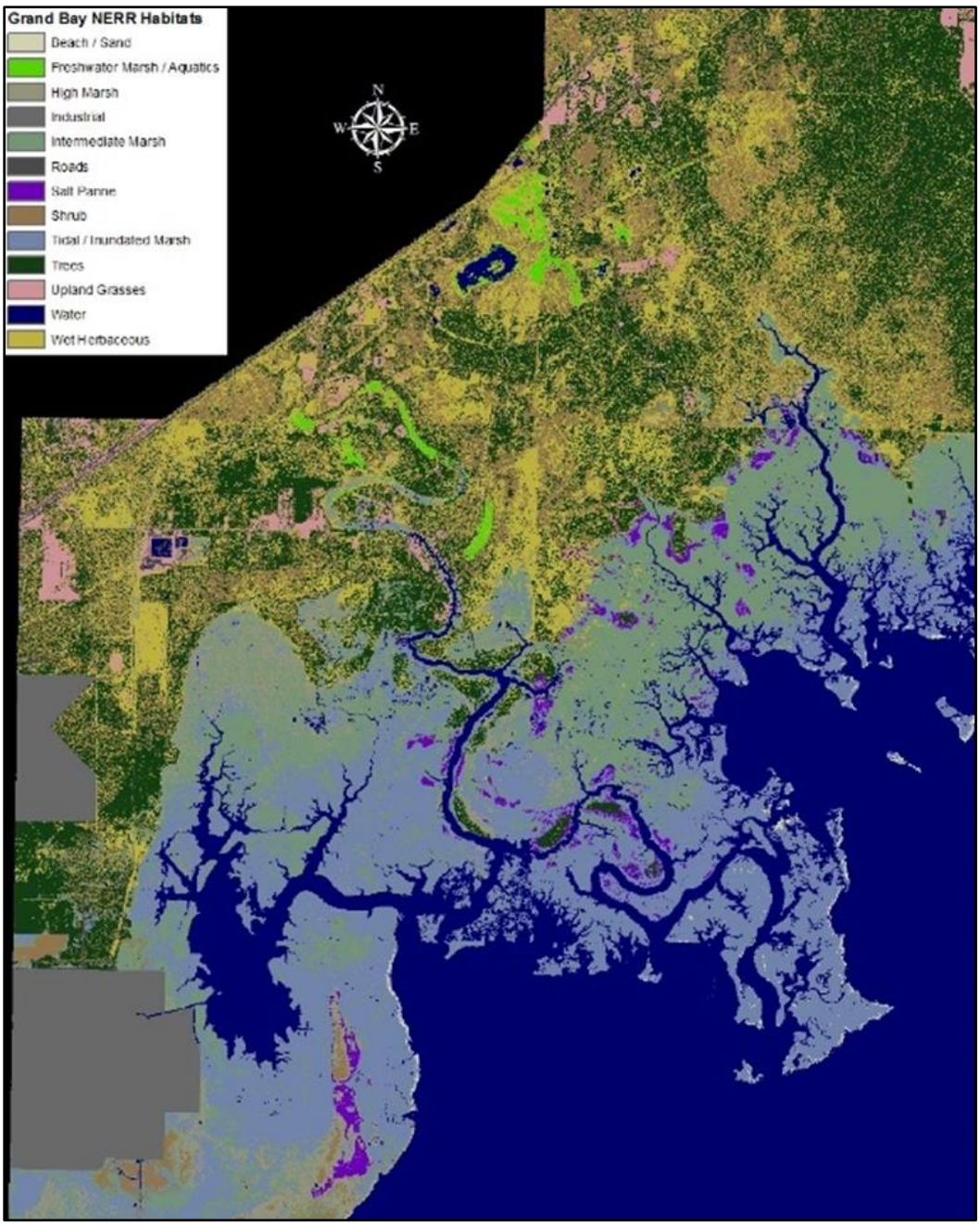

Figure 2.4 *GNDNERR Habitat Map*

Each color represents a different habitat. Of particular note, the purple color represents Salt Panne environments. (Provided by MS Department of Marine Resources).

2.5 Geologic History of Study Area

The geologic history of the study area is important to understand its formation and evolution through time. Beginning in the Middle Pliocene epoch, the Citronelle Formation was initially deposited approximately 3.6 Ma across the northern Gulf Coastal Plain. The Citronelle Formation is comprised of fluvial and deltaic deposits and remain as the oldest deposits exposed along the immediate coast. During the Early Pleistocene, beginning approximately 2.58 Ma, there was cyclical regional uplift and erosion of some of the Citronelle Formation causing river deltas such as the Pascagoula, Escatawpa, and Mobile to move seaward (Eleuterius and Criss, 1991). This was followed by deposition of fluvial sediments from the study area to the present-day extent of the Mississippi Sound. A period of erosion occurred resulting in substantial removal of early deposits during the Calabrian (1.8 Ma) through approximately the end of the Middle Pleistocene (126 ka). The Late Pleistocene initiated with the Sangamon interglacial period and associated melting of continental glaciers. During the Sangamon interglacial period, marine isotope stage "MIS" 5 (125ka – 75ka), the study area was inundated by seawater (Otvos, 2004). Figure 2.5 illustrates the sea level during this period.

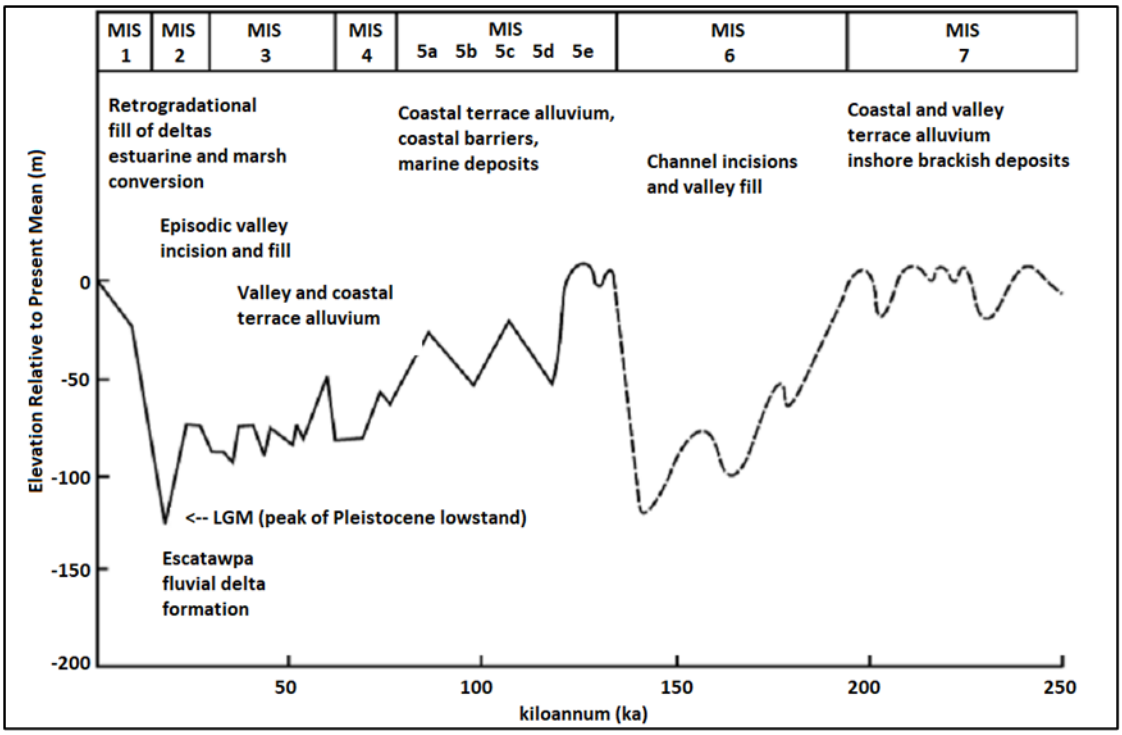

Figure 2.5 *Mississippi Coast Sea Level Plot*

Sea level along the Northern Gulf Coast interpreted from marine isotope data for the last 250,000 years. Modified from Otvos (2004).

During the Sangamon interglacial, deposition of the Biloxi marine sediments as well as Prairie Formation fluvial sediments occurred. Following the Sangamon, the Wisconsin glaciation (approximately 85 ka – 11 ka) resulted in sea-level decline causing deposition of the Prairie Formation to progress southward. The current southern limit of the continental shelf located about 100 km offshore corresponds to the extent of sediment deposition at the peak of the Wisconsin (Eleuterius and Criss, 1991). The MIS 2 (approximately 22 ka – 17 ka) is characterized as the sea level lowstand with the last glacial maximum (LGM) occurring around 18 ka. The Prairie Formation prograded as stream erosion occurred cutting deeply incised valleys through previously deposited units as deep as the Biloxi. The Grand Bay area was formed as a lowstand fluvial delta of the

Escatawpa River. As glacial melt increased at the end of the Pleistocene, sea level rise began (Schmid and Otvos, 2004).

The Holocene epoch marked the beginning of the current interglacial. With the post-glacial sea level rise (MIS 1), erosion of the Prairie Formation brought high loads of coarse sediments to the coast slowly filling valleys and widening bays. Peninsulas and barrier island evolution helped reduce sediment exchange with the gulf and enhanced sediment deposition within the bays and deltas. The shift in climate caused a period of transgressive delta growth and increased riverine sediment flux resulting in fluvial, estuarine, and tidal deposition (Anderson, et al., 2016).

During the early Holocene, valleys were filled, and the Grand Bay study area transitioned from a hydrologically fresh to a brackish environment and eventually into a marine environment during the Late Holocene. The beginning of marsh development occurred through a combination of northward barrier island migration and fluvial deposition. Point aux Chenes Bay and Grand Bay formed the sizeable delta of the Escatawpa River extending to the now submerged Batture Islands and seaward shoals (Eleuterius and Criss, 1991). The marshes continued to prograde in the early Holocene until the flow of the Escatawpa was captured and diverted to the Pascagoula River leaving Grand Bay as a transgressive or retrogradational delta starved of sediments and lacking substantial freshwater inflow (Otvos, 1985).

The exact timing of the Pascagoula's capture of the Escatawpa is not well constrained. The river capture occurred when stream flow eroded through weak lithological units. As a point of erosion migrated upstream it laterally intersected the established watershed of the Escatawpa (Maher et al., 2007). The Pascagoula River is

likely to have undergone such significant headward and lateral erosion several times including the early Holocene. The Pascagoula confluence has remained the dominant outflow of the Escatawpa River except during rare flood conditions when the Escatawpa can temporarily reconnect partial outflow to Bayou Heron. In addition, the Grand Bay shoreline was eroded and reshaped over time because of the lack of barrier island protection from storm events (Passeri et al., 2015).

CHAPTER III – METHODOLOGY

3.1 Research Design

The research for this thesis was designed to contribute to a multidisciplinary exploratory study. Because of a lack of existing data for exact comparison or a thorough understanding of the system, the exploratory framework allowed for maximum flexibility in studying the Grand Bay area with goals set forth in this thesis. Simply disproving or supporting a set of hypotheses would limit the potential understanding of the system for the entire multidisciplinary investigation. With the exploratory approach, yet unseen questions are more easily addressed. Furthermore, the exploratory approach was ideal for the related but distinct geological focus of this research: the hydrological and the sedimentological investigations.

Methodologies for this study included quantitative analyses of field and laboratory data coupled with qualitative analyses (e.g., sediment color). For hydrology, shallow groundwater was monitored for temperature, conductivity, depths, and other variables. Quantification of sediment characteristics include depth below surface, organic matter composition, carbonate content, and sediment particle size ratios. Finally, predictions and conclusions about underlying processes and their significance was based on understanding of geologic principles and statistical treatment of the observations made across the Grand Bay study area.

3.2 Data

3.2.1 Primary Data

Primary data include sedimentary datasets and hydrological datasets. Sedimentary properties were evaluated through a combination of field work and laboratory analyses. Field work included extraction of sediment cores from boreholes designated for installation of shallow groundwater piezometers and hydrologic sensors (see below). Laboratory evaluations of sediment color, organic matter content (% mass), weight percent of inorganic particle size (mm) fractions, and calcium carbonate content (% mass) were done in the USM Sedimentology Laboratory and the USM Coastal Hazards Laboratory. Specific methodological details are disclosed in subsequent sections of this chapter.

Hydrological variables were continuously monitored using sensors in the field. Variables included time series of absolute pressure (kPa) as measurement of groundwater depth (m), atmospheric pressure (kPa), groundwater conductivity (microsiemens) as a numerical proxy for salinity, and groundwater temperature (°C). Conductivity, temperature, and water depth measurements were collected at a maximum interval of 15-minutes over a minimum period of 6 months spanning summer through spring conditions. At a minimum, hourly resolution was necessary to establish tidal trends. More frequent data sampling was useful for identifying rapid changes commonly associated with storm influences. However, data storage and battery power onboard the sensor were limited. Increasing the sampling frequency was a tradeoff with the monetary cost of travel associated with servicing the sensor. The 6-month minimum term was determined by the seasonal cycles of precipitation. Southern Mississippi has two wet cycles occurring

January through March and June through September intermittent with two dry cycles occurring April through May and October through December (NCDC, 2021). Thus to ensure a scientifically representative set of data for approximating average conditions, the dataset needed to cover at a minimum one full dry cycle and one full wet cycle or half a year. Any less time would skew the averages and reduce applicability of conclusions.

Specific physical instrumentation was required for primary data collection and field measurements. Sediment core samples required a spade auger for vegetated material, a bucket auger for sandy or loose material, and an open-faced auger for clays or densely packed material. A measuring tape with metric and imperial units was used for measuring core depths. Munsell soil color charts were used for describing sediment colors. Hydrologic instrumentation included Solinst® Levelogger sensors, which were deployed in piezometers as depicted in Figure 3.1.

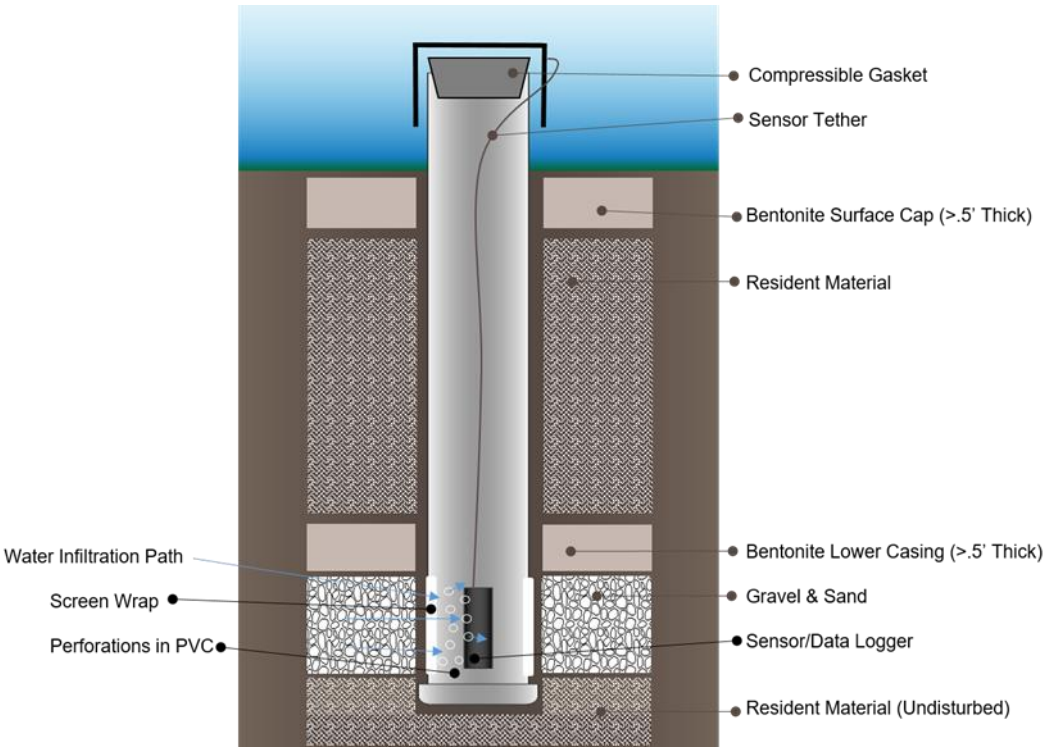

Figure 3.1 *Piezometer Diagram*

This illustration represents the typical configuration and ideal material fill surrounding the standpipe. Installation of shallow piezometers used only a thick bentonite cap/casing due to surface proximity. Diagram is not to scale.

Piezometers are shallow wells constructed to sample groundwater at specific depths. Construction for this research was based on a design example from the U.S. Army Corps of Engineers (2000) as well as from practical field experience. These piezometers were constructed using 2-inch diameter schedule-40 PVC tubing and screened with non-corrosive fiberglass mesh attached with plastic zip ties. Perforations were drilled in the PVC spanning from the bottom to approximately 0.4 meters up the standpipe on each piezometer, and included a drain hole in the bottom cap. The perforations allowed for fluid to transfer and collect inside the well where the sensors are deployed. The fiberglass screen prevented large debris from clogging the perforations. At the top of the pipe, a rubber stopper prevented the ingress of debris and over wash. The

stopper was protected by a larger loose-fitting schedule-40 PVC cap secured to the pipe with a corrosion resistant bolt (Wetlands Regulatory Assistance Program, 2000). This design ensured security in storm conditions and was easily removable without tools for frequent sensor access.

3.2.2 Secondary Data

Secondary data sources were used primarily for planning with limited use as post-collection reference data sources. Existing data available at USM and through Grand Bay NERR include tide data (NOAA), water quality data from the SWMP (http://cdmo.baruch.sc.edu/), vegetation and sediment dynamics and characteristics (e.g., SET tables) from the permanent monitoring plots established in 2010-2011 as part of the Sentinel Site Program (Office of Ocean and Coastal Resources, 2012), as well as digital elevation models and USGS coastal survey datasets.

Additional reference sources included expert faculty and staff at USM from the departments of Biological Sciences, Coastal Sciences, and Geography & Geology who are Co-PIs for the overarching multidisciplinary research and served as references for planning and interpretation of data. The following experts are noted by their research interest in the multidisciplinary effort: Frank Heitmuller (GHY/GLY) – sedimentary and hydrogeological processes; Patrick Biber (COA/GCRL) and Mike Davis (BIO) – primary production assessment of both above- and below-ground fractions; Kevin Kuehn (BIO) – detrital and microbial dynamics, POC and DOC, of “dead” carbon; and Wei Wu (COA/GCRL) – landscape scaling and spatial/temporal modeling.

3.3 Field Methods

Field methods initiated with pre-deployment preparations, which included securing scheduled access with NERR staff to aid in familiarization to the NERR property and procedures for access to Sentinel Site locations. General areas of interest within the NERR were discussed between several of the researchers to ensure study sites optimal for addressing research questions. Following the selection of four or more target areas using available satellite or aerial imagery, groundwork included a reconnaissance trip to observe potential sites for installations of nested shallow groundwater wells or piezometers in accordance with vegetation, existing research installations, and ease of access.

For access to outer marsh sites, a skiff boat was required to transport equipment and personnel. For access to the salt pan, the use of a 4x4 or all-terrain vehicle was required as seen in Figure 3.2. The boat and ATV as well as any necessary truck and trailering equipment were provided by the Department of Geography and Geology. Final pre-deployment preparations included preparation of the piezometers.

Figure 3.2 *Aspects of Fieldwork*

Top Left: Installation of the boardwalks with Dr. Pat Biber and others. Top Right: Dr. Frank Heitmuller demonstrating collection of a sample from the auger with Matt Lodato. Middle: Using the RTV to access the Salt Pan site with Matt Lodato (photo credit: FTH). Bottom Left: The RTV covered in marsh muck after fieldwork. Bottom Right: Dr. Frank Heitmuller pulling the skiff away from the marsh shoreline.

Field methods involved both sampling during piezometer installations and long-term monitoring techniques. Each study site includes three piezometers of different depths. The target depths of 1m, 3m, and 5m were chosen based on a literature review (Carter et al., 2008). However, these depths proved untenable for installation, and shallower depths of 0.75m, 1.5m, and 2.25m were used across all installation sites.

During piezometer installation, sediments were sampled as seen in Figure 3.2. Beginning at the marsh surface horizon, sediment samples were collected at regular intervals – approximately every 30 to 35 cm. Surface samples were scraped using a bladed garden trowel and placed in a labeled sample bag for laboratory analysis.

Subsurface samples were collected from the coring augers used to excavate a borehole for the piezometer. Each time the auger was lifted to be sampled or emptied, the depth of the hole was measured with a folding rule. Sample intervals were constrained by the length of the auger bit. Thus, a sample was labeled with the depth at which the bottom of the auger bit reached. Immediately after bagging and labeling, the samples were placed in a cooler, which prevented desiccation and decay, for transport to the lab as seen in Figure 3.3. When a target depth was reached, a final sample was collected, and the piezometer was installed.

Figure 3.3 *Sediment Samples*

Sediment samples being transported on ice before being loaded into laboratory freezers.

Piezometer installation entailed insertion of the PVC standpipe and filling any surrounding void space with appropriate materials. Small gravel or very coarse sand was used around the screened section to permit infiltration of groundwater through the porous and permeable material. This material was topped with a layer of bentonite clay (Figure 3.1). Bentonite swells on contact with water creating an impermeable seal that prevents vertical migration of shallower waters alongside the PVC standpipe (Wetlands Regulatory Assistance Program, 2000). This was critical to ensure that the piezometer would only fill with water from the screened depth interval. Additional resident material or filler was used above this bentonite seal to fill the distance up to a surface cap of bentonite. For shallow piezometers, there was insufficient depth to have more than a single thick layer of bentonite at the surface. When enough bentonite was used, the piezometer was firmly cemented in place by the swelling of the clay. Even if the ground surface was inundated by tide or storm surge, the sample interval was only affected by natural patterns of groundwater movement.

Groundwater was intermittently sampled by manual and automated techniques. Manual methods required physical collection of water with a vacuum or bailer tube followed by water-quality analysis using a laboratory-calibrated YSI multiparameter meter. This method was only performed as a seasonal confirmation of the measurements recorded by the deployed sensors. Solinst Levelogger and Hobo CTD sensor models were deployed in selected piezometers as indicated below in Table 3.1.

Sensors recorded absolute pressure (kPa), conductivity (mS), and temperature (°C) of the shallow groundwater. Absolute pressure was used to measure the depth (m) of the water in the piezometer by subtracting atmospheric pressure (kPa) (monitored by a

Solinst BaroLogger sensor at the GBNERR headquarters) from the reading to determine hydrostatic pressure (kPa). Measured conductivity is a direct proxy for salinity. These conductivity, temperature, and depth (CTD) sensors were programmed to record every 15 minutes. This frequency adequately captured short storm events of any strength as well as daily tidal cycles. Data stored internally was collected periodically by retrieving the sensor with a Steelon® tether attached to the PVC well cap. The records were downloaded on-site using a laptop and specialized software. The sensors were then redeployed, and the data were analyzed in the lab.

Table 3.1 *Sensor Deployment*

STATION	PZ. DEPTH BELOW SURFACE	SENSOR BRAND	SENSOR MODEL	SERIAL ID	REC START	REC END	EGM96 SENSOR ELEV.	SENSOR DEPTH BELOW SURFACE
BAYOU HERON								
surface	0m	Hobo	***	***	8/28/15	10/31/16	0.17m	-0.05m
shallow	0.75m	Solinst	Levelogger	1071022	7/25/15	4/7/16	-0.42m	0.62m
intermediate	1.5m	Solinst	Levelogger	1071144	11/12/15	8/26/16	-1.12m	1.35m
deep	2.25m	Solinst	Levelogger	1071144	7/25/15	11/12/15	-1.93m	2.10m
MIDDLE BAY JUNCUS								
surface	0m	Hobo	***	***	8/28/15	10/31/16	0.04m	-0.05m
intermediate	1.5m	Solinst	Levelogger	1071154	7/25/15	8/3/16	-1.23m	1.27m
deep	2.25m	Solinst	Levelogger	1071154	8/3/16	8/26/16	-2.06m	2.10m
SALT PAN								
surface	0m	Hobo	***	***	8/29/15	10/29/15	0.33m	-0.05m
deep	2.25m	Solinst	Levelogger	1071200	10/2/15	4/2/16	-1.73m	2.06m
***	***	Hobo	U24-002 Conductivity	9945047	8/25/16	3/6/17	***	***
SPARTINA								
surface	0m	Hobo	***	***	8/28/15	10/31/16	0.06m	-0.05m
shallow	0.75m	Solinst	Levelogger	1071152	7/25/15	8/26/16	-0.41m	0.47m
intermediate	1.5m	Solinst	Levelogger	1071136	7/25/15	8/26/16	-1.20m	1.40m

Sensor deployments for surface and groundwater stations listed by site. Missing data is indicated by ***. Only stations with successful sensor deployments are listed. Missing piezometer depths indicate that no sensor was successfully deployed.

3.4 Sediment Laboratory Methods

Laboratory procedures focused on the analysis of sediment core samples. Upon returning from the field, sediment core samples were cataloged and prepared for various analytical methods. Samples were frozen to prevent decay or off-gassing while waiting to be processed. Samples collected were of sufficient volume for redundant and multiple analyses, including color, organic content (% mass), carbonate content (% mass), magnetic susceptibility (units), and particle size (units). These methods are described in the following sections.

3.4.1 Munsell Soil Color

All samples were visually described while naturally damp using Munsell soil color charts. Color is commonly used as a means of identifying reduction and oxidation characteristics and other environmental processes. The Munsell color system is a standardized color space for the identification and naming of colors. The Munsell color system breaks down every color into three components: hue, value, and chroma (Figure 3.4) (Munsell, 1907). Recorded together, typically something like 2.5YR 7/1, which is described as light reddish grey, any color can be determined and given a consistent meaningful name. For digitally printing or displaying the color, a conversion app Munverter can translate Munsell notation to RGB and Hexachromic values (Stratton, 2014).

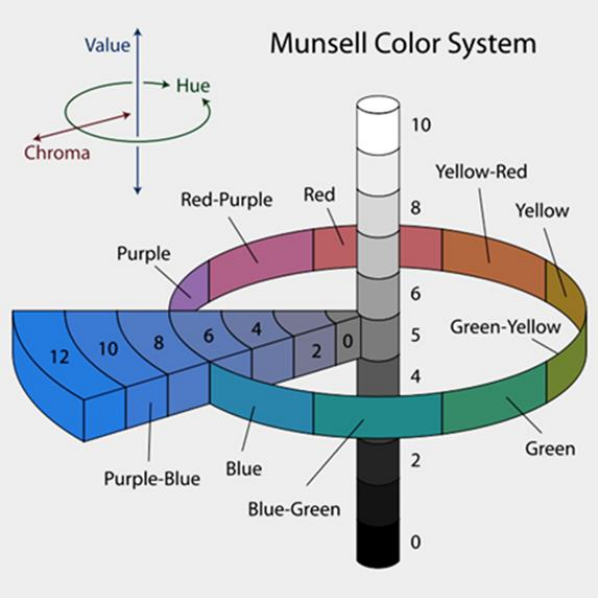

Figure 3.4 *Munsell Color System*

Munsell Color System describes colors using Value to indicate light amplitude, Hue to indicate RGB color group and Chroma to indicate color saturation. Illustration from Wiki Commons.

Factors affecting color include organic carbon content, the presence of active bacteria, time, sediment material and mineral content, Fe/Mn content and oxidation state, available gasses such as oxygen, and water content or saturation. Neither oxidation nor reduction can easily occur without organic matter for the bacteria to digest. The accumulation of organic matter darkens a soil. Other ions and minerals may also impart a color characteristic on a soil. Most notably in soil, iron and magnesium when in a reduced state are rather grey or colorless but are red to yellow when oxidized. Most sediment containing iron is originally deposited in an oxidized or insoluble form. Oxidation depends on the availability of gases such as the name sake oxygen. Under dry conditions, gasses exchange readily through soil pores, and oxidation easily occurs. Under saturated conditions, oxygen is very slow to diffuse through soil. The available oxygen is therefore dependent on the flow of water through the soil. A stagnant water

will rapidly become anoxic and promote anaerobic processes leading to reducing conditions. The duration of saturation or conditions determines how much reduction or oxidation occurs. Seasonal water tables can often be determined based on the depth to grey soil colors indicating saturated and reducing conditions. Water can also cause a change in the value, darker when wet or lighter when drier.

3.4.2 Organic Matter

Organic matter content is typically determined by chemical decomposition using hydrogen peroxide or loss-on-ignition (LOI). Organic content is important because of the many roles organic material has on soil properties including stability, water capacity, nutrient availability, and even the pH-buffering capacity of the soil water (Brady and Weil, 2010). Leaching a sample with hydrogen peroxide is a method of removing organic material from a sample through oxidation of organic carbon to form carbon dioxide, which is released from the sample (Schmidt, 1965).

The sediment core samples were prepared by measuring a minimum of 50g of oven dried (105oC overnight), physically disaggregated sediment, which was transferred to a pre-weighed beaker. The combined weight was measured so that weight of the sediment before processing was known. Then a 30% hydrogen peroxide solution was added gradually to the beaker over a period of hours, while the reaction occurred. Once the sample was no longer reactive, the beaker was placed in a gravity oven at 85oC for a minimum of 8 hours and until all water was removed. Then the sample was reweighed. However, leaching was determined to be untenable for organic content testing due to unforeseen chemical reactions. Samples with visible amounts of salt sometimes gained mass likely due to chloride and ferrous ions present in marsh sediment (Craft et al.,

1991). The results of leaching were not used, but the leached sample materials were retained for particle size analysis.

Loss-on-ignition is an alternative method to leaching. The LOI method required subsamples to be prepared by gravity-oven drying at 105oC. To begin, 4g of physically disaggregated sample material and a ceramic crucible were weighed and placed in a muffle furnace at a temperature of 500oC for at least 4 hours. Organic material was determined by weighing the sample and crucible again. The resulting difference in mass was the amount of organics, which was then converted to percentage (ASTM, 2011).

3.4.3 Carbonate Content

Carbonate content was determined using a modified gravimetric method in which a sediment sample of known mass was reacted with an acid solution of known mass to consume carbonate (CO3) and release carbon dioxide (CO2) over a period of time. The relative loss in mass was then attributed to the inorganic carbon content (Goh, Arnaud, & Mermut, 1993). This low-cost method provides an acceptable estimation of inorganic carbon content comparable to more advanced LOI and XRD methods but includes limited errors introduced by the presence of salts, high organic content, and specific mineralogy (Santisteban et al., 2004).

Sediment from each interval was used for carbonate content (percent) testing. Each sample was oven dried, disaggregated, and 10g were measured. Unlike the organic matter testing, the 10g samples were neither treated by hydrogen peroxide nor subjected to a muffle furnace to avoid potential underestimation of carbonate content in accordance with the calculation method. A hydrochloric acid, ferrous chloride solution was prepared immediately prior to testing to reduce volatilization of the hydrochloric acid. Ferrous

chloride tetrahydrate was used as an antioxidant, which reduced error from the oxidation of manganese oxide and re-bonding of released ions of calcium and magnesium (Allison and Moodie, 1965). Granular ferrous chloride tetrahydrate ($FeCl2 \cdot 4H2O$) was dissolved at a measure of 3g per 100mL of 4 mol L-1 hydrochloric acid (HCl). Then, 10mL of the acid reagent solution was added to an Erlenmeyer flask and weighed. A pre-weighed sediment sample was added to the flask and capped with a rubber stopper. Flasks were periodically agitated and vented to allow for dispersion of released carbon dioxide gas while also limiting the errors due to evaporation of water. Flasks were carefully monitored to avoid excessive boiling, which would increase the involvement of organic material in the reaction.

Total weight was measured every 30 minutes to monitor the rate of change. A rapid change in the first 30 minutes would indicate calcite dominated carbonates; a rapid change after 30 minutes could indicate the presence of dolomitic carbonates. Reaction observations were concluded after a minimum of 4 hours and when no observable change in mass had occurred for the duration of the last hour. The proportion of mass lost to the original sample mass is multiplied by a factor of 2.273—the ratio of the molecular weights of calcium carbonate to carbon dioxide—and by 100 to calculate the percent equivalent calcium carbonate content. Organics would need a longer duration to significantly react with this dilution and thus can be ignored (Goh et al., 1993) (ASTM, 2011).

Typically, recommended accuracy is 0.01g or better when used with 1g samples. Goh et al. (1993) further recommend an instrument accuracy of 0.003g and a test duration of 2 hours or when no change is detectable for 30 minutes. The measurement accuracy of

available equipment was limited to 0.1 grams (1% of sample mass). Thus, I chose a larger sample mass of 10g, and a 4-hour duration was chosen as a safe benchmark to reduce the chance of undetected significant changes in mass without including significant organic release.

3.4.4 Magnetic Susceptibility

Samples were analyzed for magnetic susceptibility using a Bartington MS3 meter and MS2B dual-frequency sensor. This system uses electrical circuitry and magnets to record the sample's ability to temporarily resist or maintain an induced magnetic field. Although of limited use for this thesis, these data can be useful for evaluating bulk mineralogy, comparing sediment provenance, and distinguishing areas in an environment with higher erosion potential even within the same lithologic unit (Maher et al., 2007). Thus, all samples were analyzed for provenance implications and to provide a basis of comparison for further study.

Preparation began with the calibration of the Bartington MS2B dual-frequency sensor by using the Bartsoft software to establish a baseline magnetic value for an empty plastic specimen container. This value was compared to a second measurement of an integrated calibration mass within the meter followed by a final measurement of the empty specimen container. This established sensor drift and correction values as a baseline for all sample measurements.

Sediment samples were oven dried and were untreated to preclude oxidation of potentially magnetic minerals. A three-step measurement process was applied to each sample. The first and third measurements are simply the empty specimen container. For the second measurement, each sample, weighing 10g, was placed into the specimen

container and subjected to the magnetic measurement. Each measurement step occurred for half a minute and was repeated three times to obtain an average value. The software then applied its corrected values and returned the final value in Susceptibility Index (SI) units.

3.4.5 Particle Size

Size analysis of sediment particles was done to provide information useful for determining source environment, vertical sequence changes, and relative permeability. Examination of particle size results for each sample and the changes from one interval to another allowed for soil characterization. The general type of grains—sand, silt, and clay—and mineralogy narrowed the possible environmental sources of the material. The sorting or similarity in size of grains helped determine under what conditions the material was deposited. The previous tests of color, organics, carbonates, and magnetic susceptibility are all inextricably related to the particle size. Thus, these analyses were considered together to make reasonable conclusions about marsh soil stratigraphy and history of the depositional environment. In turn, these findings shed light on possible sedimentological responses to local change.

It is important to understand the principles applied to particle size analysis. First, the particle dimensions were constrained to "bins" for classification based on the Udden-Wentworth sediment classification system used by the USGS (Appendix A). This particle size classification should not be confused with soil texture classification as defined by the U.S. Department of Agriculture to identify soils of mixed particle sizes. Second, particle size distribution (PSD) can be illustrated in a variety of ways. Traditional particle size distribution curves are useful for calculations of sorting and skewness of a given sample.

These curves illustrate the percent of a sample relative to particle size—typically referred to as “undersize distribution” as used by geologists or “oversize distribution” as used by engineers. Each sediment sample was analyzed and illustrated in this manner.

Sediment samples were analyzed for particle size by using a Malvern Mastersizer3000 with a HydroLV cell in the Coastal Hazards Laboratory at the USM Department of Marine Science. This instrument applies low angle laser light scattering (LALLS) and statistical algorithms to calculate the approximate shape and dimensions of sediment particles as they passed between a scanning laser of variable frequency and sensor plate. This method allowed for high accuracy and precision much faster than the traditional method of hydrometer analysis and sieving, and LALLS requires significantly less sample material and preparation.

Approximately 20g of oven dried, physically disaggregated, and H2O2 leached sediment was transferred to a 400mL beaker. Then, 250mL of distilled water and 100mL of 5% sodium hexametaphosphate ((NaPO3)6) solution were added to the beaker. The sample was mechanically mixed until evenly disaggregated in the solution (ASTM, 2007). The sample was covered and left overnight to allow the sodium hexametaphosphate adequate time to act as a deflocculant for any clays in the sample and for any salts to re-dissolve. Immediately prior to testing, the sample was vigorously mixed to suspend all particles. The aqueous mixture was then drawn by pipette and deposited into the HydroLV cell of the LALLS instrument. The cell is a conical vat containing distilled water under constant motion induced by a small blending propeller. As the aqueous sediment mixture was added to the cell, the sediment suspension continually passed through the detector. The sample mixture was added until the detector

reached optimal light occlusion—around 10 to 15 percent as indicated by the Malvern Mastersizer (ver. 3.10) software. The sample mixture was analyzed for several minutes using three laser light wavelength ranges. Then the three results were averaged together for the final values of the particle-size distribution. The Malvern software generated frequency curves for particle sizes ranging from 4mm to 0.1µm (Malvern, 2015). These data were processed using Microsoft Excel to create frequency "bins" equivalent to grain size classifications of the Udden-Wentworth Scale.

3.5 Hydrological Laboratory Methods

Hydrological data include conductivity (µS/cm), temperature (°C), and water table depth (m) in the shallow subsurface of the marsh. It is difficult to directly measure salinity, and an accepted method is to measure conductivity of the groundwater or soil solutions. A variety of conductivity, temperature, and depth (CTD) sensors were considered. Battery life, onboard data storage, resistance to corrosion, software, and price were leading considerations. Ultimately, a combination of readily available Hobo CTDs and newly purchased Solinst Levelogger CTD sensors were deployed (Table 3.1).

Prior to deployment, all sensors underwent laboratory sensor calibrations, software updates, and data storage setup. Laboratory sensor calibrations were performed by Dr. Pat Biber at GCRL using calibration solutions of known values to check and adjust sensor measurements through software input. Both Hobo and Solinst use proprietary software to interface with the sensor packages and data storage aspects of the CTD units. Sensors and sensor software of each brand are comparable and updated periodically. Thus, only the Solinst Levelogger software methods are discussed for an overview of setup and interfacing with the data loggers. When setting up data loggers

with the software, each Levelogger unit serial number was recorded and assigned a name describing the site and piezometer depth in which it was to be deployed. The software synchronized the data logger clock time and any parameters for record keeping. As mentioned previously, absolute pressure, temperature, and conductivity were typically set to record once every 15 minutes. A sampling interval of 10 min was used during a few short deployments to determine if there was significant benefit to the increased frequency for the resolution of storm events. Sampling intervals of 15 minutes are common among national meteorological data sets including the nearby SWMP stations and were determined to be the optimal interval for storage, battery life, and data resolution tradeoffs (National Data Buoy Center, 2009).

Maintaining calibration was vital throughout the duration of the project. At initial deployment and redeployments, calibration checks were performed by collecting water samples from each piezometer with a handheld YSI ProPlus multimeter. Conductivity and temperature measured by the YSI unit were compared to the last sampling record of the piezometer sensor. Though no significant deviations were found in any sensor, the possibility of sensor calibration drift or failure had to be checked. Pressure sensor calibration was not a concern as the sensor measures absolute rather than vented pressure and is corrected for barometric pressure through the software by means of an additional Barologger sensor deployed on a weather platform onsite near the GNDNERR headquarters.

Data from sensors were recovered by removing each sensor from the piezometer and optically interfacing with a computer connected saddle. Sensor retrieval was facilitated by a tether suspending sensors approximately 5 cm from the bottom of the

piezometer. Steelon, nylon-coated braided stainless-steel fishing line was tied around a screw at the piezometer cap and tightened down between two washers and attached to the sensor cap using fishing tackle clips. Steelon of 40lb-test was originally used but failed to last the duration of the study. Repairs were made with Steelon of 80lb-test was used with more success. Due to a few tether failures, a technique was devised using a lightbulb grabber on an extension pole to collect a detached sensor from the bottom of the piezometer. The lightbulb grabber is comprised of metal bands like fingers held tight together by a coil spring, which was modified to wrap around the bundle twice for a tighter fit around the smooth sensor. The bundle slides over end of sensor and friction provided by the spring holds the sensor as the tool is lifted from piezometer.

Data analysis using the Hobo or Solinst software was limited. These programs were used primarily for sensor setup, data retrieval, and basic processing and export to Microsoft Excel. The basic processing included value correction for barometric pressure, conversion to the practical salinity scale (units), and graphing for initial data perusal. Once exported to Microsoft Excel, data were checked for errors and analyzed using a variety of basic statistical methods and database techniques. More complex statistical methods were done using R and Matlab software products.

CHAPTER IV – SEDIMENTARY RESULTS AND DISCUSSION

Results are presented and discussed in paired sections in the following order: sediment color, organic matter content, carbonate content, magnetic susceptibility, and particle size.

4.1 Munsell Color

4.1.1 Results

A total of 67 samples were collected for sedimentary analysis. These samples were kept moist for color analysis. All results in Table 4.1 through Table 4.4 include approximate RGB equivalent color representation derived from Munverter software.

Table 4.1 *Bayou Heron*

Shallow Piezometer (0.75 m)			
Interval (m)	**Notation**	**Color Name**	**RGB Color Sample**
0.0	10YR 3/2	Very Dark Greyish Brown	
0.5	10YR 3/2	Very Dark Greyish Brown	
0.7	2.5Y 4/1	Dark Grey	
Intermediate Piezometer (1.5 m)			
Interval (m)	**Notation**	**Color Name**	**RGB Color Sample**
0.0	10YR 3/2	Very Dark Greyish Brown	
0.5	10YR 4/1	Dark Grey	
0.9	10YR 4/1	Dark Grey	
1.1	7.5YR 5/1	Grey	
1.4	10YR 6/1	Grey	
Deep Piezometer (2.25 m)			
Interval (m)	**Notation**	**Color Name**	**RGB Color Sample**
0.0	10YR 2/2	Very Dark Brown	
0.5	5Y 4/1	Dark Grey	
0.8	10YR 3/1	Very Dark Grey	
1.0	10YR 4/1	Dark Grey	
1.5	10YR 6/1	Grey	
1.8	10YR 6/1	Grey	
2.2	10YR 6/1	Grey	
2.4	10YR 6/1	Grey	

Table 4.2 *Salt Pan*

Shallow Piezometer (0.75 m)			
Interval (m)	**Notation**	**Color Name**	**RGB Color Sample**
0.0	2.5Y 3/1	Very Dark Grey	
0.4	2.5Y 2.5/1	Black	
0.7	2.5Y 4/1	Dark Grey	
Intermediate Piezometer (1.5 m)			
Interval (m)	**Notation**	**Color Name**	**RGB Color Sample**
0.0	5Y 2.5/1	Black	
0.3	5Y 3/1	Very Dark Grey	
0.7	5Y 5/1	Grey	
1.0	2.5Y 4/4	Olive Brown	
	* 2.5Y 6/8	Olive Yellow	*
1.16	2.5Y 5/4	Light Olive Brown	
1.2	5Y 6/1	Grey	
	* 2.5Y 6/8	Olive Yellow	*
1.5	Gley1 7/N	Light Grey	
	* 2.5Y 6/6	Olive Yellow	*
Deep Piezometer (2.25 m)			
Interval (m)	**Notation**	**Color Name**	**RGB Color Sample**
0.0	10YR 3/1	Very Dark Grey	
0.4	7.5YR 3/1	Very Dark Grey	
0.8	2.5Y 3/1	Very Dark Grey	
1.0	2.5Y 4/1	Dark Grey	
1.3	5Y 4/3	Olive	
	* 2.5Y 6/6	Olive Yellow	*
1.7	5Y 7/1	Light Gray	
2.0	Gley1 6/10Y	Greenish Grey	
	* 10YR 6/8	Brownish Yellow	*
2.4	Gley1 6/10Y	Greenish Grey	
	* 5Y 5/4	Olive	*

* indicates a redoximorphic accessory color or other minor distinct color.

Table 4.3 *Middle Bay*

Shallow Piezometer (0.75 m)			
Interval (m)	**Notation**	**Color Name**	**RGB Color Sample**
0.0	10YR 2/2	Very Dark Brown	
0.4	10YR 3/2	Very Dark Greyish Brown	
0.7	10YR 2/2	Very Dark Brown	
Intermediate Piezometer (1.5 m)			
Interval (m)	**Notation**	**Color Name**	**RGB Color Sample**
0.0	2.5Y 3/2	Very Dark Greyish Brown	
0.5	2.5Y 3/2	Very Dark Greyish Brown	
0.9	10YR 2/2	Very Dark Brown	
1.2	10YR 2/2	Very Dark Brown	
1.5	10YR 5/1	Grey	
	* 2.5Y 4/1	Dark Grey	*
Deep Piezometer (2.25 m)			
Interval (m)	**Notation**	**Color Name**	**RGB Color Sample**
0.0	10YR 3/2	Very Dark Greyish Brown	
0.4	10YR 3/2	Very Dark Greyish Brown	
0.8	2.5Y 3/1	Very Dark Grey	
1.0	10YR 2/2	Very Dark Brown	
1.5	5Y 6/1	Grey	
	* 2.5Y 2.5/1	Black	*
1.9	Gley1 6/N	Grey	
	* 5Y 6/1	Grey	*
2.1	Gley1 6/N	Grey	
	* 10YR 6/8	Brownish Yellow	*
2.3	5Y 6/1	Grey	
	* 10YR 6/8	Brownish Yellow	*
	* 2.5Y 2.5/1	Black	*

* indicates a redoximorphic accessory color or other minor distinct color.

Table 4.4 *Spartina*

Shallow Piezometer (0.75 m)			
Interval (m)	**Notation**	**Color Name**	**RGB Color Sample**
0.0	5Y 2.5/2	Black	
0.4	5Y 3/2	Dark Olive Gray	
0.8	5Y 4/2	Olive Grey	
Intermediate Piezometer (1.5 m)			
Interval (m)	**Notation**	**Color Name**	**RGB Color Sample**
0.0	Gley1 2.5/10Y	Greenish Black	
0.4	5Y 3/2	Dark Olive Gray	
0.8	5Y 4/2	Olive Grey	
	* 7.5YR 5/8	Strong Brown	*
1.3	Gley1 7/N	Light Grey	
	* 10YR 5/4	Yellowish Brown	*
	* 10R 4/8	Red	*
1.5	Gley1 6/N	Grey	
	* 2.5Y 6/4	Light Yellowish Brown	*
	* 2.5YR 5/6	Red	*
Deep Piezometer (2.25 m)			
Interval (m)	**Notation**	**Color Name**	**RGB Color Sample**
0.0	Gley1 2.5/10Y	Greenish Black	
0.4	5Y 4/1	Dark Grey	
0.7	5Y 4/2	Olive Grey	
1.0	2.5Y 5/3	Light Olive Brown	
1.3	Gley1 6/10Y	Greenish Grey	
	* 2.5Y 6/6	Olive Yellow	*
	* 10YR 6/4	Light Yellowish Brown	*
	* 10R 4/8	Red	*
1.5	Gley1 7/N	Light Grey	
	* 2.5YR 5/8	Red	*
1.8	2.5Y 5/6	Light Olive Brown	
	* Gley1 7/10Y	Light Greenish Grey	*
2.1	Gley1 6/10Y	Greenish Grey	
2.4	Gley1 6/10Y	Greenish Grey	

* indicates a redoximorphic accessory color or other minor distinct color.

4.1.2 Discussion

The Munsell colors in Table 4.1 through Table 4.4 facilitate interpretation of geochemical conditions and organic matter preservation. Reducing conditions are typically indicated by the combination of a Munsell value of 4 or more and a chroma of 2 or less resulting in a grey or gleyed color. High values and low chroma indicate prolonged saturation and long duration reducing conditions resulting in an absence of Fe/Mn oxides. If the chroma is slightly greater than 2, long duration saturation and reducing conditions was likely accompanied by shorter duration oxidizing conditions. If the chroma is considerably greater than 2, oxidizing conditions are dominant. However, it is important to remember that a value of less than 4, regardless of chroma, generally implies an accumulation of high organic content and relatively balanced oxidation/reduction conditions (Vepraskas, 2014).

Redoximorphic features are created through cycles of reduction, oxidation, and saturation. Redoximorphic features include nodules, concretions, masses, and stains of either highly reduced or highly oxidized material. These features typically form a contrasting coloration often exemplified by a red or orange concentration of oxidized iron surrounded by a very light grey as seen in Figure 4.1. Staining occurs as intermixed patches or mottled colorations caused by the movement of iron oxides or the diffusion of reduced iron.

Figure 4.1 *Redoximorphic Mottling*

This sample from Spartina Intermediate shows strong yellow colors indicative of oxidation as well as greens and greys indicating reduction. Also visible is some black plant debris in the center.

There are two basic redoximorphic feature types: redox concentrations and redox depletions. Redox concentrations form when organic material such as roots or decaying debris along with sufficient active bacteria are present in saturated aerobic conditions. The oxygen is typically supplied by flowing oxygenated water or the active input of oxygen from the plant root. Reduced iron diffuses toward the dissolved oxygen in the soil solution and precipitates an immobile iron oxide. Thereby, a concentration of iron occurs around the oxygen source or live organism(s) resulting in the surrounding sediment being depleted of iron.

Redox depletions form when organic material such as roots or decaying debris along with sufficient active bacteria are present in saturated anaerobic conditions. There is no active supply of dissolved oxygen, and any oxygen present is quickly depleted leading to reducing conditions. Redox depletions can only form after soil becomes both saturated and reduced. Much like an inverse of redox concentrations, depletions form by a local reduction of the iron state. Thereby, the reduced iron can then be further

concentrated if it diffuses into the surrounding sediment. The increasingly limited availability of organic carbon and dissolved oxygen with greater depths results in longer times required to create redox depletions (Vepraskas, 2014).

The Spartina site exhibited numerous redoximorphic features and the largest range in chroma. Mottling characteristics for short periods of oxidation were prevalent in the lower half of the intermediate and deep piezometer cores. In various intervals, this mottling, which is seen as the yellows and browns in Figure 4.1, was also accompanied by strong red-colored nodules or masses indicative of redoximorphic concentrations. These redox features in the 1–1.5m depth range are likely associated with a buried deltaic soil that was previously exposed prior to marsh colonization. Alternatively, vertical percolation of oxygenated marine water during high tides in this outermost, energetic site could also infuse sufficient oxygen for redox concentrations. However, reduction colors dominate throughout the lowermost profile of the deep core yielding greys and light greys characteristic of prolonged saturation and long duration reduction as is expected with depth.

The Middle Bay Juncus site exhibited redoximorphic concentration and depletion only at the deepest two intervals, likely indicating a buried deltaic soil that was previously exposed. These redox features include brownish-yellow mottles interspersed in the dominant colorations of various greys. Interestingly, this site also had considerable organic content throughout the profile such that there were no light greys. Several intervals including the deepest had observable organic debris and concentrations of black organic matter. Overall, this was the most organic-rich profile.

The Salt Pan site, like Spartina, included a few intervals dominated by oxidation coloration. However, these colorations are more analogous to the yellows and browns of Middle Bay Juncus. No nodules were visible, but masses of browns, greys, and yellows were intermixed. Although primarily a reduced profile, this site is clearly representative of periodic oxidizing conditions lasting longer than those indicated in the Middle Bay Juncus profile. Also, this site is less organic-rich than Spartina or Middle Bay Juncus. Interestingly, Salt Pan was the only site to prevalently exhibit olive colors throughout the profile; though the reason remains uncertain, the color could be due to a salt-tolerant microbe or algae.

There is no oxidation coloration at the Bayou Heron site. In fact, Bayou Heron has the most 'grey' colors of any site. There are a variety of reasons for grey coloration including reducing conditions and sediment composition. Prolonged reduction is plausible if the flow of oxygen in the water is too slow compared to the availability of organic material, but the rapid inflow of groundwater observed at the time of installation suggests ample dissolved oxygen likely passes through the system. It is possible that periods of stagnation could reduce the dissolved oxygen and permit prolonged reduction, but permeation of surface oxygen into the groundwater would still occur due to the lack of an impermeable clay boundary layer at this site. Thus, composition is more likely the dominant factor in color at the Bayou Heron site.

The red hue and the grey colors at the Bayou Heron site have less to do with redox conditions than with the sediment source and particle size. As discussed in the upcoming magnetic susceptibility and particle size sections, the Bayou Heron site is dominated by fine sands. These sands are primarily quartz in composition and have little

to no source material for iron or manganese to be oxidized. Though generally grey, nearly all colors at Bayou Heron are on the 10YR hue suggesting some red coloration from the presence of iron oxides, so very small amounts of iron or manganese may be present in the limited silt particles.

Overall, the marsh demonstrated several surprising trends. First, the gleyed colors were not as prevalent or dominant as expected and were often deeper than expected. Second, the presence of strong colors from redox and oxidation features were typically at the lower depths. This was contrary to the expectation that oxidation would occur nearer the surface where periods of unsaturated conditions are more likely. However, there are no oxidation colors within the top 0.75m at any site. This supports the idea of rapidly buried previously exposed deltaic soil horizons. Those soil horizons when exposed would have oxidized. When buried rapidly by fine sands and silts, the oxygen mobility might be decreased to the extent that oxidation features remain relatively unchanged by reducing conditions above. Alternatively, this may indicate that either the seasonal fluctuations of the water table can be much larger than previously assumed, or the oxidation or redox reaction may be triggered by some other process such as occasional rapid flushing of oxygenated water through the soil during periods of surface inundation. Furthermore, there may be less iron to oxidize due to the composition of the source material or due to mobilization of soluble iron immediately following reducing conditions. Thus, the third marsh-wide trend was the progression of accessory, minor, or redox colors from the strongest reds and browns at Spartina to the yellows at Middle Bay Juncus to the yellows and greens of Salt Pan and ending in greys at Bayou Heron.

Munsell characterization is very useful for gaining valuable insight to the geochemical processes of this estuarine system. Though some assumptions had to be made, the marsh is dominated by reducing conditions and most oxidation colors are a result of redoximorphic concentrations of iron and magnesium oxides. However, there could be complicated interplay with other ions, nitrox, sulfates, or salts which may not be represented in the oxidation colorations. Finally, colors identified in these samples represent the conditions at the time of sample collection and do not represent the total history of redox. Hydrologic analyses including dissolved oxygen, pH, temperature, and dissolved organic compounds could be used to determine more about the reactions and even constrain the rates of reduction. Furthermore, it is possible that other geochemical processes or seasonal cycles could be involved but are not evident in this analysis.

4.2 Organic Matter

4.2.1 Results

Organic matter contents (% by mass) displayed in Figure 4.2 indicate variable content generally less than 10% with a greater proportion measured in some samples. The average value of 4.6% in the collected samples indicates that inorganic sediments dominate the marsh subsurface. Notably, the sites range from very low organic content at Bayou Heron to more than 10% of some samples from Spartina and Middle Bay Juncus. Spartina and Middle Bay have highly variable organic matter contents, whereas samples from Salt Pan and Bayou Heron are roughly consistent with depth. Despite generally low organic content at Bayou Heron, a thin layer of wood debris was observed at 2m (not indicated by the OM test methods). Overall, there was expected variation in organic

content between cores at each site with those cores at Spartina showing the largest variation throughout the depth profile.

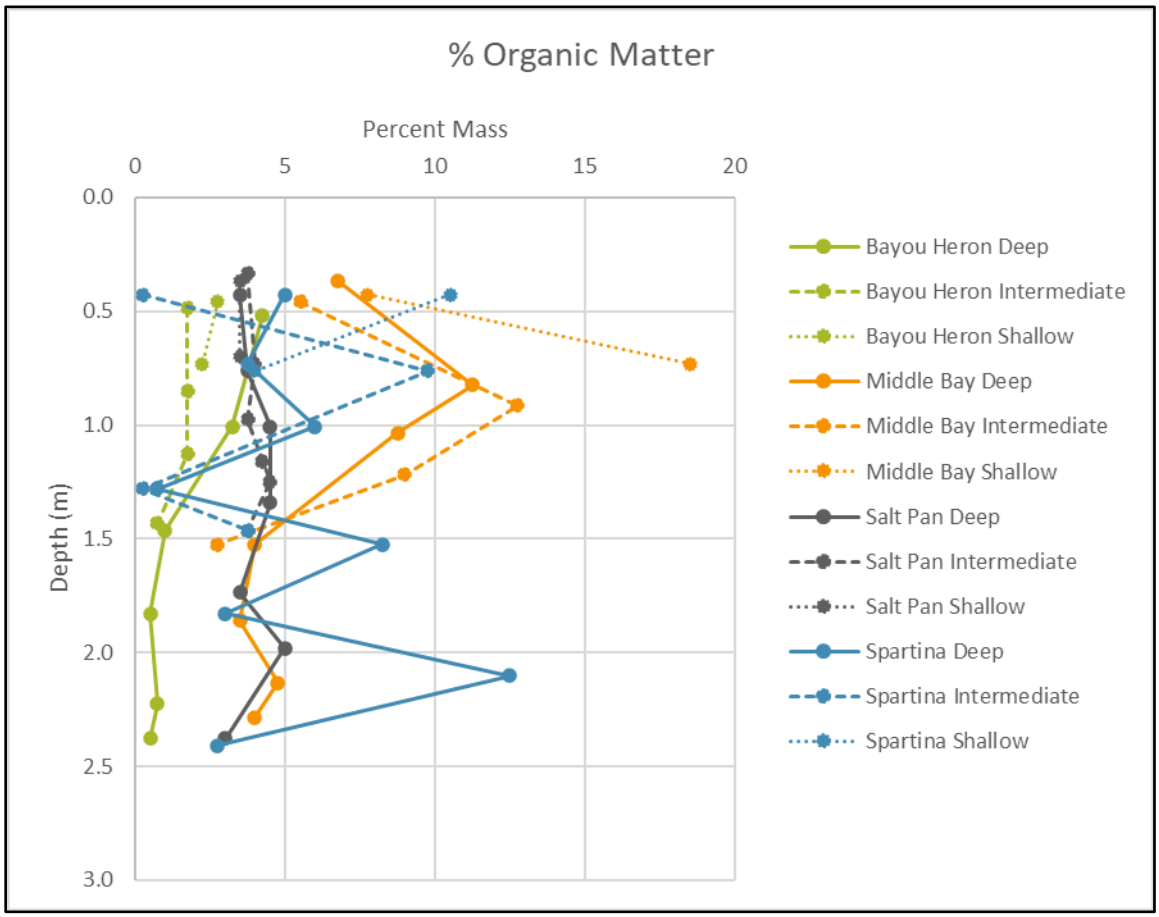

Figure 4.2 *Depth Profiled Organic Matter By Percent Mass*

4.2.2 Discussion

Organic material has many roles in the soil environment. Organic matter typically accounts for less than 6% by weight of a well-drained soil but has a disproportionate impact on soil properties. Organic material helps loosen the soil and promotes malleability rather than forming hard cloddy structures that would otherwise inhibit the favorable growth of microbes and plants. The loose granular soil structure and the organic materials allow for increased soil water capacity throughout the marsh. This

results in a larger portion of plant available water and nutrient availability (Oades, 1984; Brady and Weil, 2010).

As organic material breaks down, nutrients such as phosphorus, sulfur, and nitrogen are released as soluble ions into the soil solution which can be absorbed by roots, microbes, or adsorbed to colloidal particles such as clays or humus. Humus, complex organic compounds resistant to decay, has the greatest ability to attract and bind with water and nutrient ions. Thus, even a small amount of organic material can greatly enhance the pH buffering capacity of the soil water or increase plant and microbial productivity (Brady and Weil, 2010). With an average of 4.6 % mass throughout the core depths, the organic carbon contained in the marsh sediments is quite substantial. Sediment cores at the Spartina and Middle Bay Juncus sites exhibit the highest organic contents, 10–12%, within the top meter of sediment. Organic mass within the first meter of the surface provides the vegetation a substantial buffer to drying and inundation events, which can significantly affect the salinity of the plant available water.

Soil organisms and the breakdown of complex organic materials also produce organic substances capable of binding together mineral particles into granular soil structures. This glue-like function of organic matter provides the soil with stability and reduces the negative effect of rapid wetting (Oades, 1984). The frequent storm and tidal fluctuations in the marsh are often accompanied by rapid changes in water depth especially where the surface elevation is very low. Additionally, this could likely have significant benefits for Spartina and Middle Bay, which are most vulnerable to erosion but have high organic content.

The Middle Bay and Spartina sediment cores have relatively large variance of organics with depth suggesting event-related depositional controls (i.e., episodes of rapid sediment deposition). In contrast, Bayou Heron and Salt Pan have only limited variation, but this does not exclude the possibility of event-related deposition rather just spatial variation in marsh deposition. Most of this variance with depth is likely attributable to the additional clay and silt content found in layers at Middle Bay and Spartina. The uncharacteristic absence of organic material at Spartina around 1.3m (4.2ft) corresponds to the greatest oxidation attributed colors noted in Munsell data of any site. Whereas, Bayou Heron is uniquely lower in organic content throughout, but Bayou Heron lacks the silt of the Spartina 1.3m sample. Clay and fine silt particles have a much greater ability to retain organic material than fine sands and large silts (Brady and Weil, 2010).

Notably, the samples containing more than approximately 10% were also noted to have large leafy or woody debris during initial collection. Although no leafy or woody debris was notable in the samples used for testing, the presence of the debris suggests rapid burial or mixing occurred such that there was insufficient oxygen for this debris to be broken down through aerobic microbial processes. Furthermore, the largest peak in content at the Spartina site was found in a layer with woody debris of several centimeters as well as infrequent gravels uncharacteristic of the sedimentary layer. This supports the possibility of storm deposition accounting for the presence of increased organic carbon content and indicates sediment deposition at a rate significantly more than typical conditions at present (Tornqvist et al., 2007). The source of the woody material and gravel is likely the back marsh and pine savannah. Whether the deposition was hurricane sourced or due to riverine flooding remains unknown (Turner et al., 2006).

4.3 Carbonate Content

4.3.1 Results

The carbonate mass loss of samples ranged from 0.0g to 0.3g or 0% to 6.82%, respectively. A change in sample mass of 0.1g calculates to an equivalent calcium carbonate percent of 2.27%. Therefore, any carbonate percent less than 2.27% was below detection limits with available instrumentation and thus indistinguishable from 0%. However, it is worth noting that the 2.07% average and 2.3% median of all samples indicate slightly more carbonate is likely present. This calculation is a valid estimation of calcium carbonate based on the reaction of all calcium and magnesium calcites. Thus, greater accuracy by using more sample mass and higher precision scales would yield better resolution but not affect the general conclusion of limited carbonate content as all sediment samples contained less than 10%.

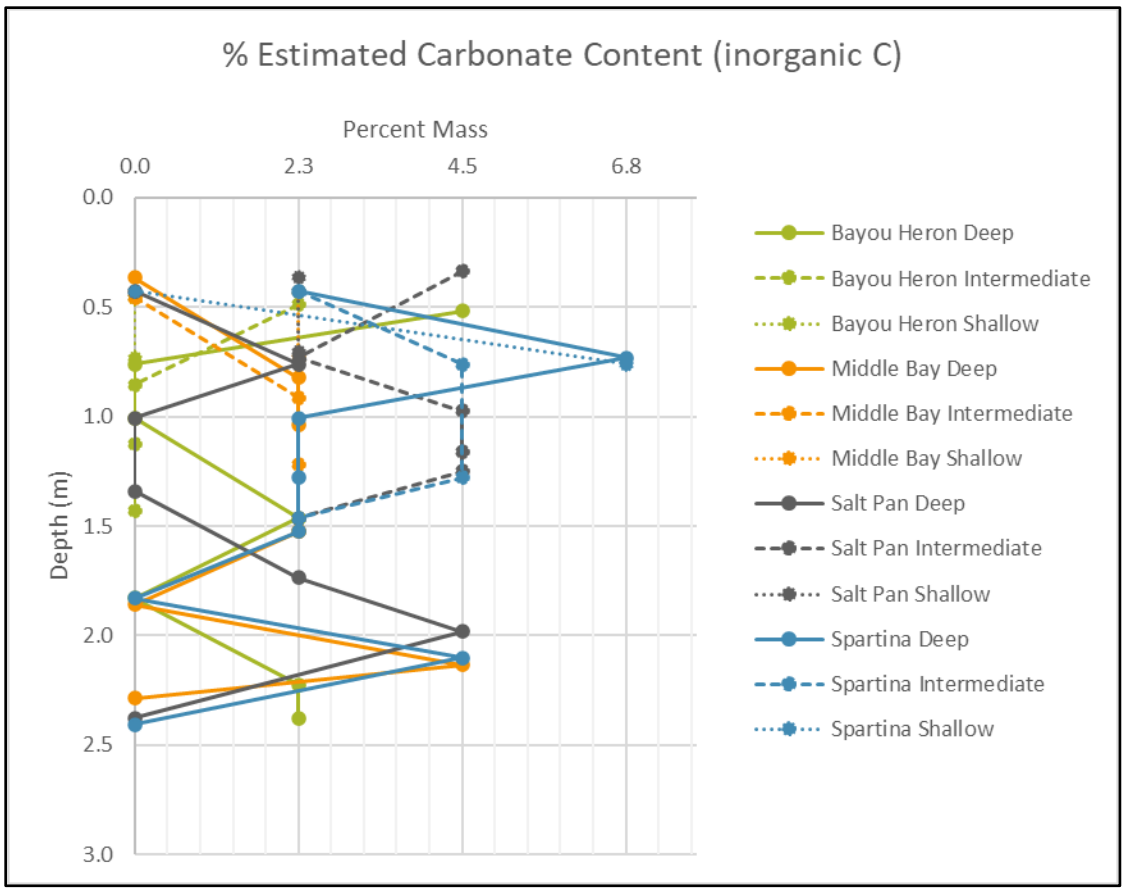

Figure 4.3 *Depth Profiled Carbonate Content by Percent Mass*

The alignment of values occurred due to limited sample material processed combined with limited scale precision. 2.27% is equivalent to a loss of 0.1g sample mass.

4.3.2 Discussion

Carbonates are typically present in soils among the other mineral grains as cements and sometimes as fine particles. Carbonates can serve to buffer the pH of the soil solution and neutralize organic and inorganic acids (Brady and Weil, 2010). In coastal sediments, carbonates are present as cements, large debris or shell hash, and even sand particles capable of dune formation. These biogenic and inorganic carbonates can act as a sediment source for areas without appreciable terrestrial input. Thus, the results in Figure

4.3 indicate a smaller percent than one might expect to find in a marsh with mollusk colonies such as Grand Bay. However, this may be a high percentage given additional marsh factors present.

Carbonates are typically found as shell hash in coastal marshes. However, there was little shell hash visible in samples. Thus, the carbonate content of less than 10% was qualitatively verified in the field. Carbonate is a natural buffer for acids and a nutrient for shell growth. The amount of carbonate is affected by a variety of factors such as acidic anthropogenic wastewater runoff, the influx of organic acids and tannins in the brackish water of Bayou Heron, or fluctuations in mollusk population. Periods of high temperature surface water and anoxic conditions as well as the erosion of hard substrates are likely contributing factors that could reduce the mollusk population and associated input of shell hash sediments. If carbonates are diminished, marsh vegetation could be affected by a either a decrease of pH if anthropogenic runoff increases or an increase of pH as more basic marine waters encroach on the marsh.

4.4 Magnetic Susceptibility

4.4.1 Results

Analysis of the magnetic susceptibility results, as shown in Figure 4.4, reveals that magnetic susceptibility is higher in the Salt Pan and Spartina sites compared to Bayou Heron. Magnetic susceptibility at the Middle Bay site increases steadily with depth. The magnetic susceptibility of Bayou Heron remains low throughout. Overall, the samples ranged from 0.00013 to 0.00091 SI with the greatest range at beyond 2 meters depth.

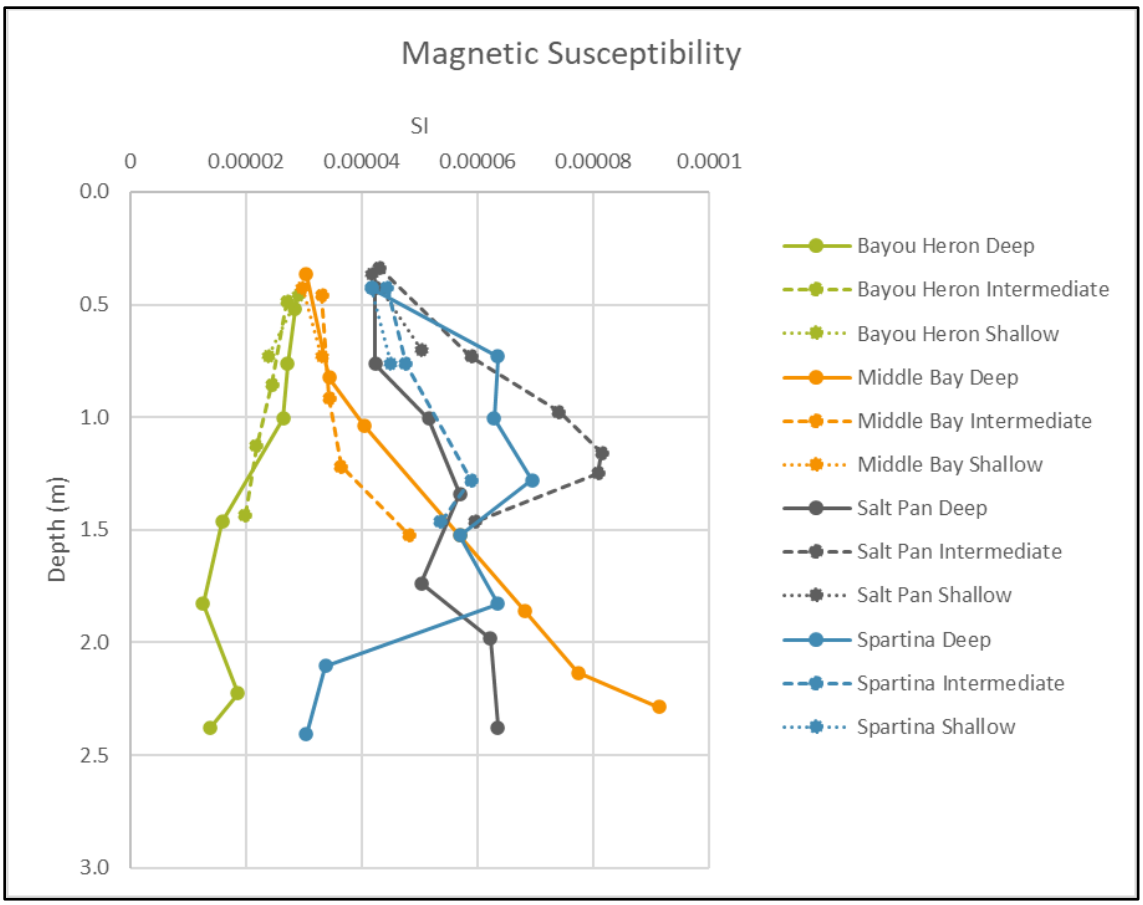

Figure 4.4 *Depth Profiled Magnetic Susceptibility*

Higher values are representative of paramagnetic minerals generally from terrestrial source materials. Lower values represent likely marine sourced materials. Values are dimensionless proportions and are identified as susceptibility index units (SI) representing material response to applied magnetic fields.

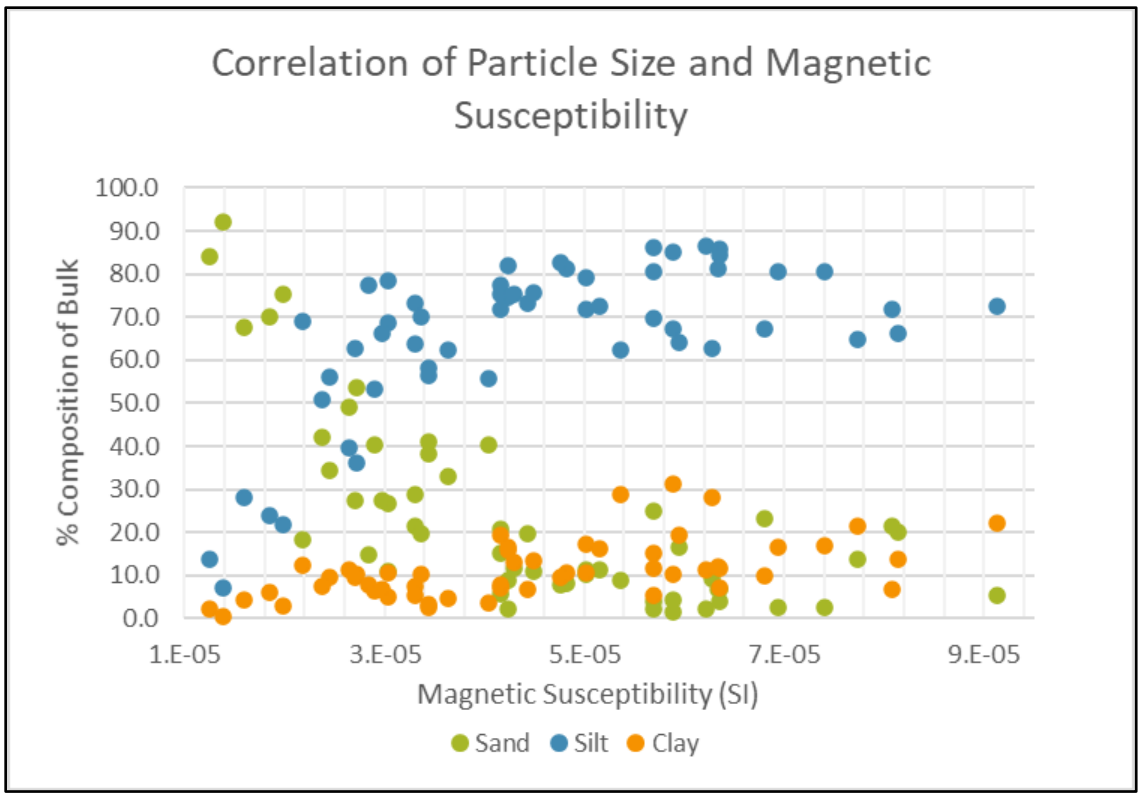

Figure 4.5 *Correlation of Magnetic Susceptibility to Bulk Composition*

Samples from all stations are shown as three points in vertical alignment. Color differentiates the particle size faction.

4.4.2 Discussion

While of limited use for this thesis, magnetic susceptibility data can be useful for evaluating bulk mineralogy, comparing sediment provenance, and distinguishing areas in an environment with higher erosion potential even within the same lithologic unit. Thus, all samples were analyzed for provenance implications and to provide a basis of comparison for further studies. The results shown in Figure 4.4 were produced from the mass-based magnetic susceptibility method. When the bulk sediment samples were tested using a volumetric method, there was no distinguishable pattern found in the data. This was likely due to the limited differences in particle size among many of the samples,

which has been found to reduce the reliability of bulk sediment data (Crockford and Fleming, 1998).

Magnetic susceptibility increases with decreased frequency of sand sized particles. This trend relates to the nature of particle size and the ability of smaller particles to have greater surface area and surface charges than larger particles. Thus, iron, titanium, and other metals are commonly retained in finer particles more easily than in loose sands (Hatfield et al., 2010). As displayed in Figure 4.5, there is a strong correlation between samples with greater percentages of silt and increased magnetic susceptibility. Additionally, the figure illustrates the clay particles are not a controlling factor of magnetic susceptibility. The particle size analysis, discussed at depth in 4.5.2, expands upon this reasoning, and additional correlations and statistical matrices are presented in Appendix C. Notably, samples from Salt Pan, Middle Bay Juncus, and Spartina converge from a depth of 1.3m to 1.5m with values ranging from 0.00048 to 0.00057 SI. This corresponds to the anomalous layer of similar composition and color as mentioned above. Bayou Heron does not indicate magnetic susceptibility convergence due to the sand content. Thus, a uniform deposition of the layer across the entire marsh is unlikely. Additionally, all samples are convergent near the surface with magnetic susceptibility ranging from 0.00027 to 0.00044. This overall convergence likely indicates the depositional source is becoming increasingly constrained with time and may suggest decreasing erosion within the marsh (Hatfield et al., 2010).

Finally, correlation between magnetic susceptibility and particle size has been found to be a robust method of sourcing sediments to specific environmental sources. The higher magnetic susceptibility of samples at depth is suggestive of paramagnetic minerals

from more terrestrial source materials in the past, such as previously vegetated deltaic soils, compared to the recent marsh surface (Hatfield and Maher, 2009). As further research is completed, these samples could be compared with other adjacent coastal samples to verify the source environment.

4.5 Particle Size

4.5.1 Results

Particle-size analyses using the Malvern Mastersizer generated detailed particle size results. These results were simplified to standard distribution values (μm) listed in Table 4.5. The percentages of clay, silt, and sand were computed from the detailed measurements.

Table 4.5 *Particle Size Analysis*

Sample Name	Depth (m)	Dx (10)	Dx (16)	Dx (50)	Dx (84)	Dx (90)	Clay %	Silt %	Sand %
BHER DEEP_1.7'	0.5	4.86	7.10	19.69	58.57	85.13	7.7	77.4	14.9
BHER DEEP_2.5'	0.8	3.75	7.57	73.20	182.88	216.79	10.3	36.2	53.5
BHER DEEP_3.3'	1.0	3.06	6.71	60.01	155.96	184.99	11.4	39.6	49.0
BHER DEEP_4.8'	1.5	10.26	19.00	98.03	182.88	210.62	4.3	28.1	67.6
BHER DEEP_6.0'	1.8	42.33	63.11	127.59	214.28	243.26	2.1	13.7	84.2
BHER DEEP_7.3'	2.2	10.84	31.57	94.50	170.22	196.61	6.0	23.8	70.2
BHER DEEP_7.8'	2.4	69.98	86.28	156.85	265.27	303.22	0.6	7.2	92.2
BHER MED_1.6'	0.5	4.14	6.99	25.56	98.54	125.82	9.6	62.9	27.6
BHER MED_2.8'	0.9	4.16	7.10	31.77	113.95	141.11	9.5	56.2	34.3
BHER MED_3.7'	1.1	2.96	5.12	18.85	69.90	93.93	12.5	69.2	18.4
BHER MED_4.7'	1.4	19.43	41.72	105.34	186.64	215.53	3.0	21.7	75.3
BHER SHAL_1.5'	0.5	6.09	9.65	44.00	128.41	159.63	6.6	53.2	40.2
BHER SHAL_2.4'	0.7	5.28	8.51	45.45	126.48	150.99	7.3	50.7	41.9
MBAY DEEP_1.2'	0.4	6.16	8.95	33.46	83.95	103.96	4.9	68.6	26.5
MBAY DEEP_2.7'	0.8	13.33	20.65	52.86	107.78	134.67	2.5	56.4	41.0
MBAY DEEP_3.4'	1.0	9.44	14.32	48.94	118.95	148.63	3.7	55.9	40.4
MBAY DEEP_5.0'	1.5	7.32	12.00	36.19	78.41	94.47	5.3	69.6	25.0
MBAY DEEP_6.1'	1.9	3.97	5.81	21.34	81.28	102.11	9.8	67.1	23.1

Table 4.5 (continued)

MBAY DEEP_7.0'	2.1	0.90	2.58	12.54	55.01	78.26	21.4	64.9	13.8
MBAY DEEP_7.5'	2.3	0.94	2.69	9.74	29.62	41.78	22.2	72.4	5.4
MBAY MED_1.5'	0.5	4.98	7.61	36.70	85.78	103.67	7.5	63.7	28.8
MBAY MED_3.0'	0.9	9.92	14.78	46.40	134.75	236.81	3.3	58.2	38.4
MBAY MED_4.0'	1.2	7.54	11.69	40.26	100.23	126.22	4.8	62.3	32.9
MBAY MED_5.0'	1.5	3.72	5.40	15.63	41.49	55.98	10.6	81.1	8.2
MBAY SHAL_1.4'	0.4	5.14	7.38	31.08	85.61	104.50	6.6	66.1	27.3
MBAY SHAL_2.4'	0.7	6.40	9.63	29.35	76.56	107.95	5.3	73.4	21.3
SALT DEEP_1.4'	0.4	1.88	3.76	14.82	43.99	58.31	16.6	74.7	8.8
SALT DEEP_2.5'	0.8	2.15	3.95	13.09	29.83	37.00	15.9	81.8	2.3
SALT DEEP_3.3'	1.0	2.29	3.86	14.50	49.51	67.19	16.2	72.5	11.3
SALT DEEP_4.4'	1.3	2.61	4.08	13.54	33.37	42.46	15.3	80.6	4.1
SALT DEEP_5.7'	1.7	3.76	5.14	15.60	47.46	63.21	10.6	79.2	10.2
SALT DEEP_6.5'	2.0	3.69	4.73	11.90	28.19	35.37	11.2	86.7	2.1
SALT DEEP_7.8'	2.4	4.78	6.73	20.24	44.78	54.59	7.3	85.9	6.9
SALT MED_1.1'	0.3	2.79	4.91	17.88	51.52	68.73	13.0	75.2	11.8
SALT MED_2.4'	0.7	0.65	0.93	9.40	25.33	31.15	31.1	67.4	1.4
SALT MED_3.2'	1.0	2.12	3.73	12.44	30.18	37.91	16.8	80.7	2.5
SALT MED_3.8'	1.2	2.90	4.52	19.05	72.97	93.67	13.7	66.3	20.0
SALT MED_4.1'	1.2	6.00	9.97	32.00	73.06	89.57	6.7	71.8	21.5
SALT MED_4.8'	1.5	1.84	3.29	13.28	63.92	85.29	19.3	64.2	16.5
SALT SHAL_1.2'	0.4	0.99	2.65	15.14	38.73	49.13	19.2	75.2	5.6
SALT SHAL_2.3'	0.7	1.80	3.60	15.33	49.77	66.42	17.2	71.7	11.2
SPAR DEEP_1.4'	0.4	5.62	9.16	29.18	73.13	92.25	7.2	71.9	20.9
SPAR DEEP_2.4'	0.7	3.34	5.31	15.66	34.10	42.57	11.7	84.3	4.0
SPAR DEEP_3.3'	1.0	0.77	1.55	9.88	41.78	59.32	28.0	62.8	9.2
SPAR DEEP_4.2'	1.3	2.84	3.81	10.09	27.58	36.14	16.7	80.6	2.7
SPAR DEEP_5.0'	1.5	3.66	4.65	10.97	25.83	33.33	11.5	86.2	2.3
SPAR DEEP_6.0'	1.8	3.53	4.75	13.15	38.60	51.77	11.8	81.3	6.8
SPAR DEEP_6.9'	2.1	3.87	5.02	16.76	71.35	88.94	10.2	70.0	19.8
SPAR DEEP_7.9'	2.4	3.78	4.78	12.41	47.79	65.32	10.7	78.4	10.8
SPAR MED_1.4'	0.4	5.82	9.64	30.56	70.84	92.42	6.7	73.4	19.9
SPAR MED_2.5'	0.8	4.09	6.70	20.62	45.13	56.18	9.6	82.7	7.8
SPAR MED_4.2'	1.3	3.85	5.03	13.37	34.05	43.99	10.3	85.3	4.5
SPAR MED_4.8'	1.5	0.57	0.80	13.95	46.42	59.50	28.8	62.2	9.0
SPAR SHAL_1.4'	0.4	4.61	6.47	21.69	60.30	76.17	7.7	77.2	15.0
SPAR SHAL_2.5'	0.8	2.86	4.64	15.33	46.68	65.94	13.4	75.8	10.8

The preceding table gives standard cumulative distribution bin values in µm. Percentages represent % of total sample volume.

Traditional particle distribution curves fail to show modality clearly and are difficult to compare samples to identify changes. Other commonly used curves such as particle frequency curves show modality clearly but fail to be comparable across large sample sets when viewed two dimensionally. Particle size distribution surface plots are the ideal solution for comparisons of multiple samples by using one axis as the sample identity (in this case depth), the second axis as the particle size classes, and the final axis as the frequency (Beierle et al., 2002). Color fields allow changes in frequency from one sample to the next to be easily compared visually while still representing the results two-dimensionally. In Figure 4.6 through Figure 4.13, the Intermediate and Deep sediment profiles for each site are shown using the surface plot method. Additional examples using traditional methods are available in Appendix B.

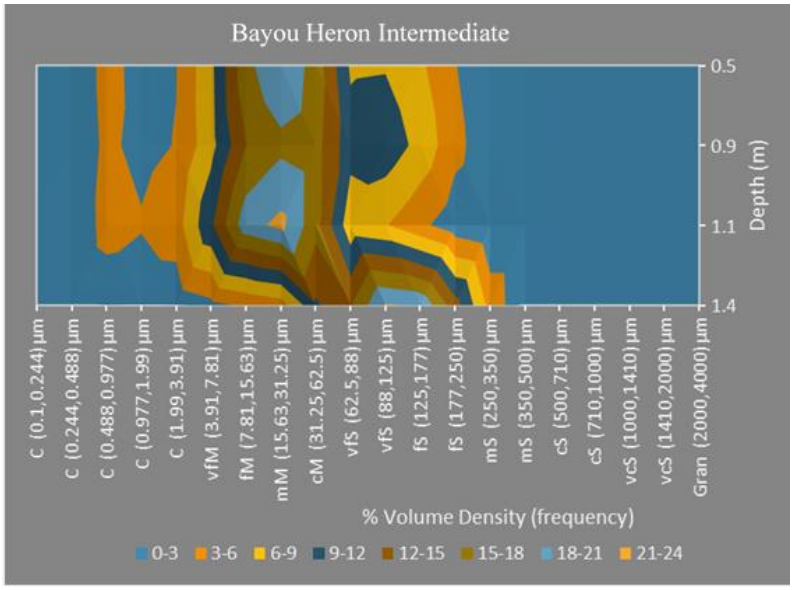

Figure 4.6 *Particle Size Distribution of Bayou Heron Intermediate*

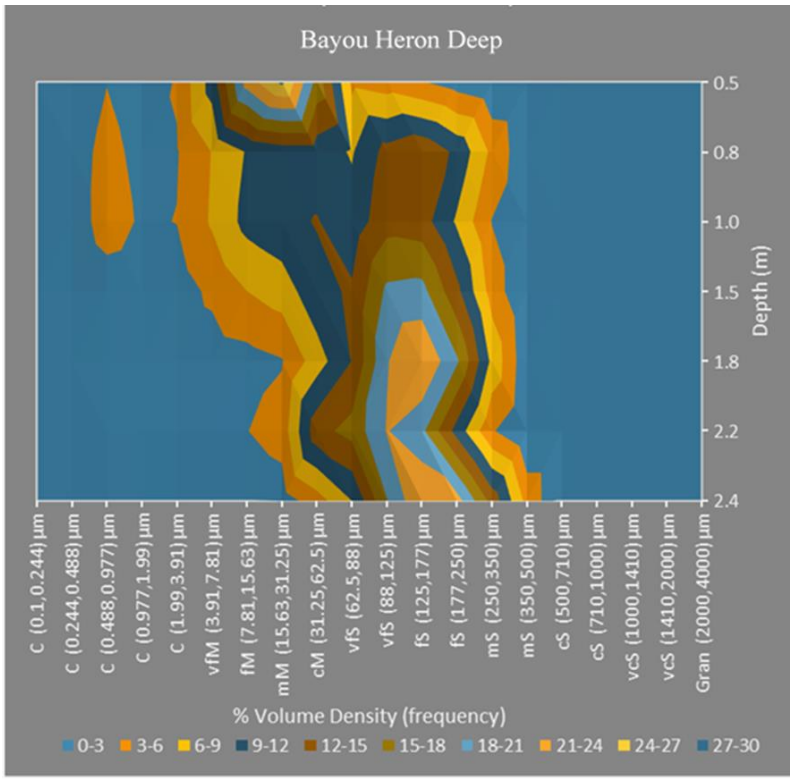

Figure 4.7 *Particle Size Distribution of Bayou Heron Deep*

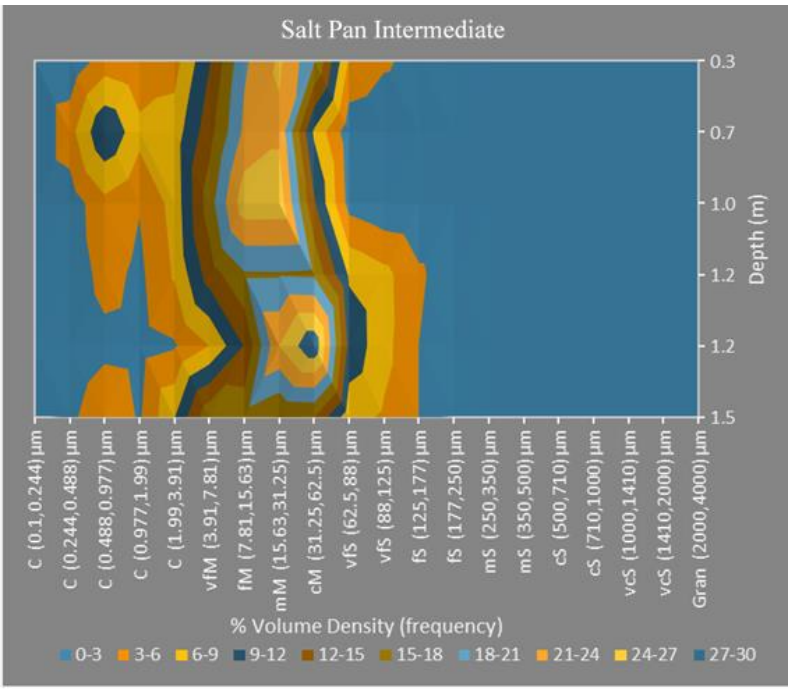

Figure 4.8 *Particle Size Distribution of Salt Pan Intermediate*

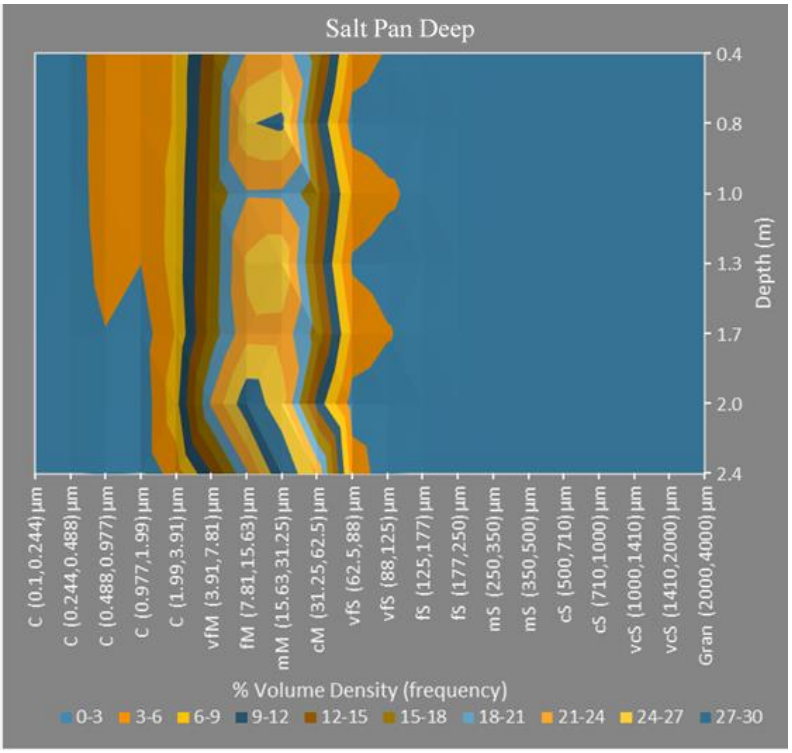

Figure 4.9 *Particle Size Distribution of Salt Pan Deep*

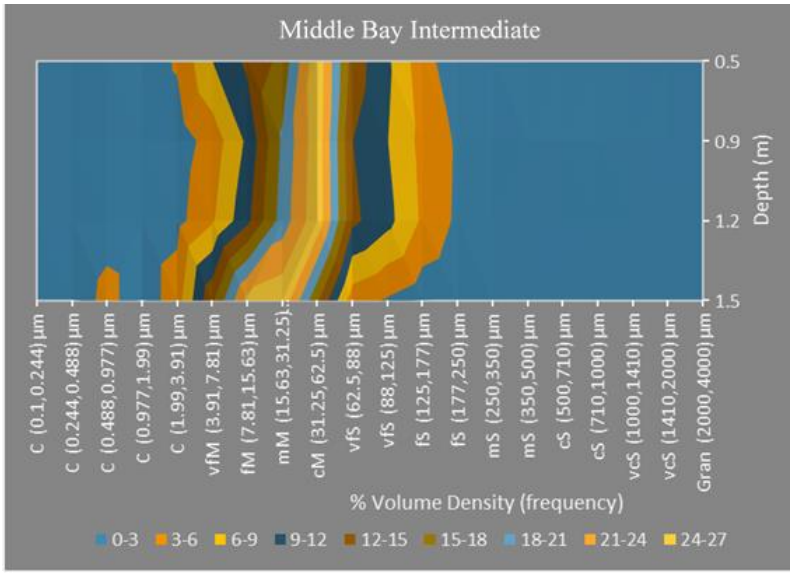

Figure 4.10 *Particle Size Distribution of Middle Bay Intermediate*

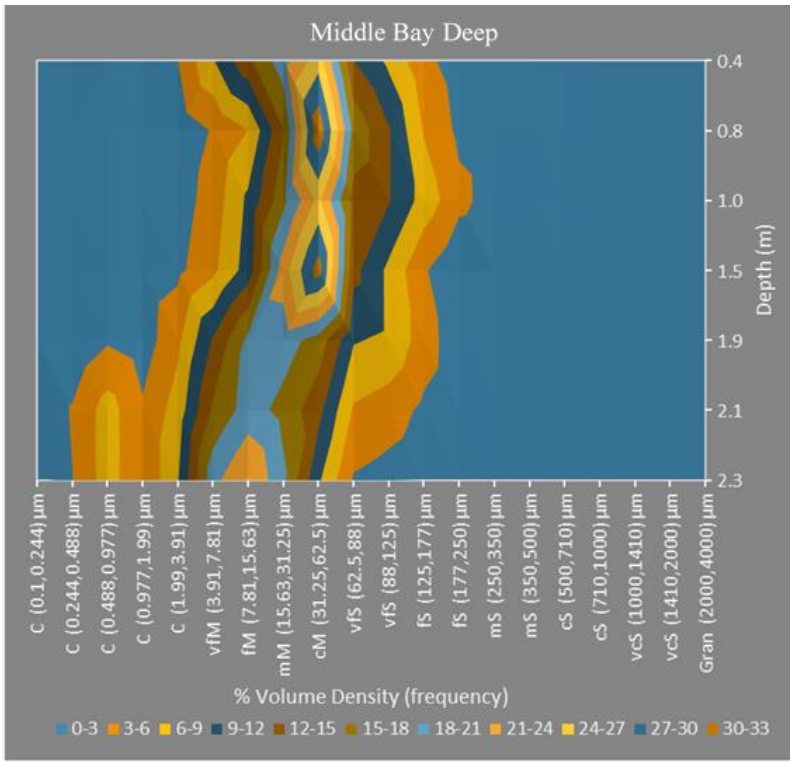

Figure 4.11 *Particle Size Distribution of Middle Bay Deep*

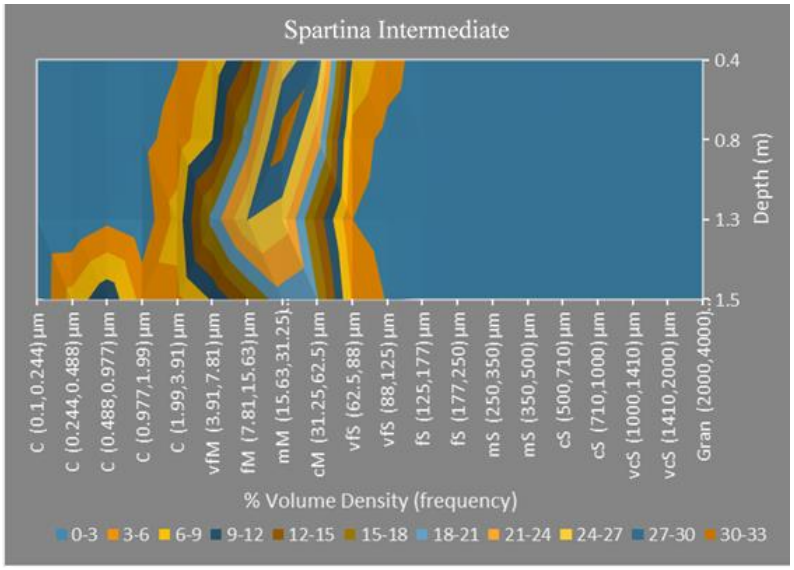

Figure 4.12 *Particle Size Distribution of Spartina Intermediate*

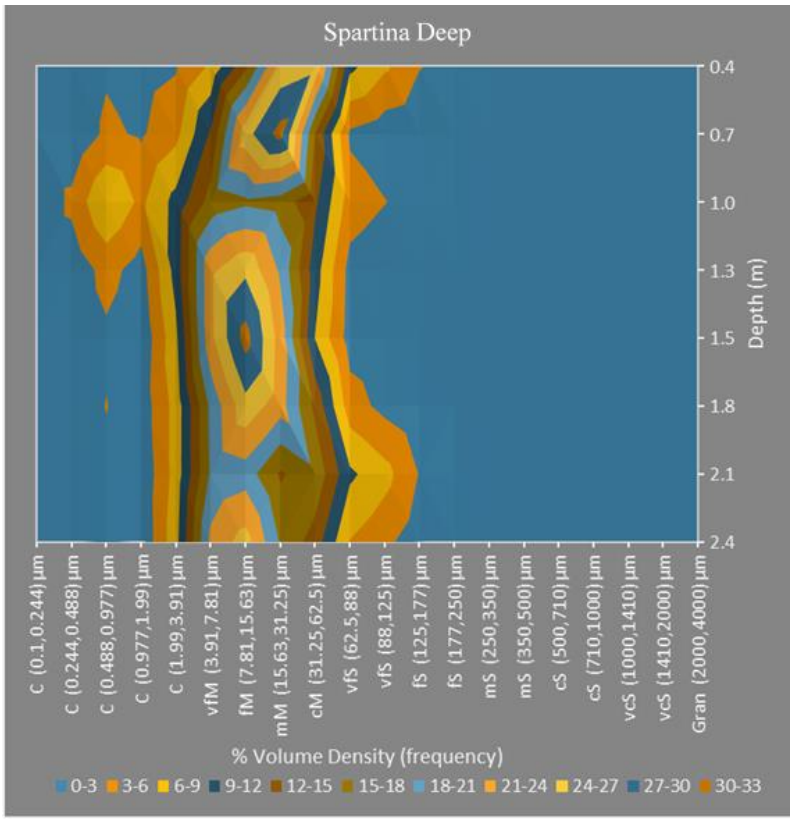

Figure 4.13 *Particle Size Distribution of Spartina Deep*

4.5.2 Discussion

The Bayou Heron site shows a lower abundance of clay and silt sized particles compared to the other sites. Bayou Heron also has larger size sands on average than the other sites. From this result alone, there exists a potential for greater hydraulic conductivity through the sediment at Bayou Heron. This hypothesis is consistent with both observed characteristics of the sediment and water flow at the time of piezometer installation as well as with continued observations with the CTD instrumentation. The installations at this site were challenging because of the rapid collapse of the borehole sidewalls if left without reinforcement between auger sample collections. Within seconds, the sidewalls of the hole would collapse and fill with a quicksand-like solution from the surrounding material. Furthermore, this high hydraulic conductivity could also be seen in the hydrologic records (Chapter V). In several instances, rapid changes in water depths were recorded at the deep or intermediate Bayou Heron piezometers. These changes were likely rapid drainage events from surface waters further inland in the marshy areas and pine savannas north of the Bayou Heron site. These flushing events likely indicate that the unit(s) of fine sand are intermittent but extensive fill deposits from previous stream channels across the former Escatawpa River delta.

Overall, the Spartina and Salt Pan sites have nearly identical sedimentary particle size profiles suggesting that each site lies along the same or similar structural features of the former delta. Both sites are dominantly comprised of medium silt and some clay and are best described overall as silty loam as displayed in Figure 4.14. Several sample intervals can be described as silty clay loam. Therefore, the past deposition of these sites

occurred in a lower energy regime than Bayou Heron, which has a greater percentage of coarser particles indicative of higher energy channel deposits.

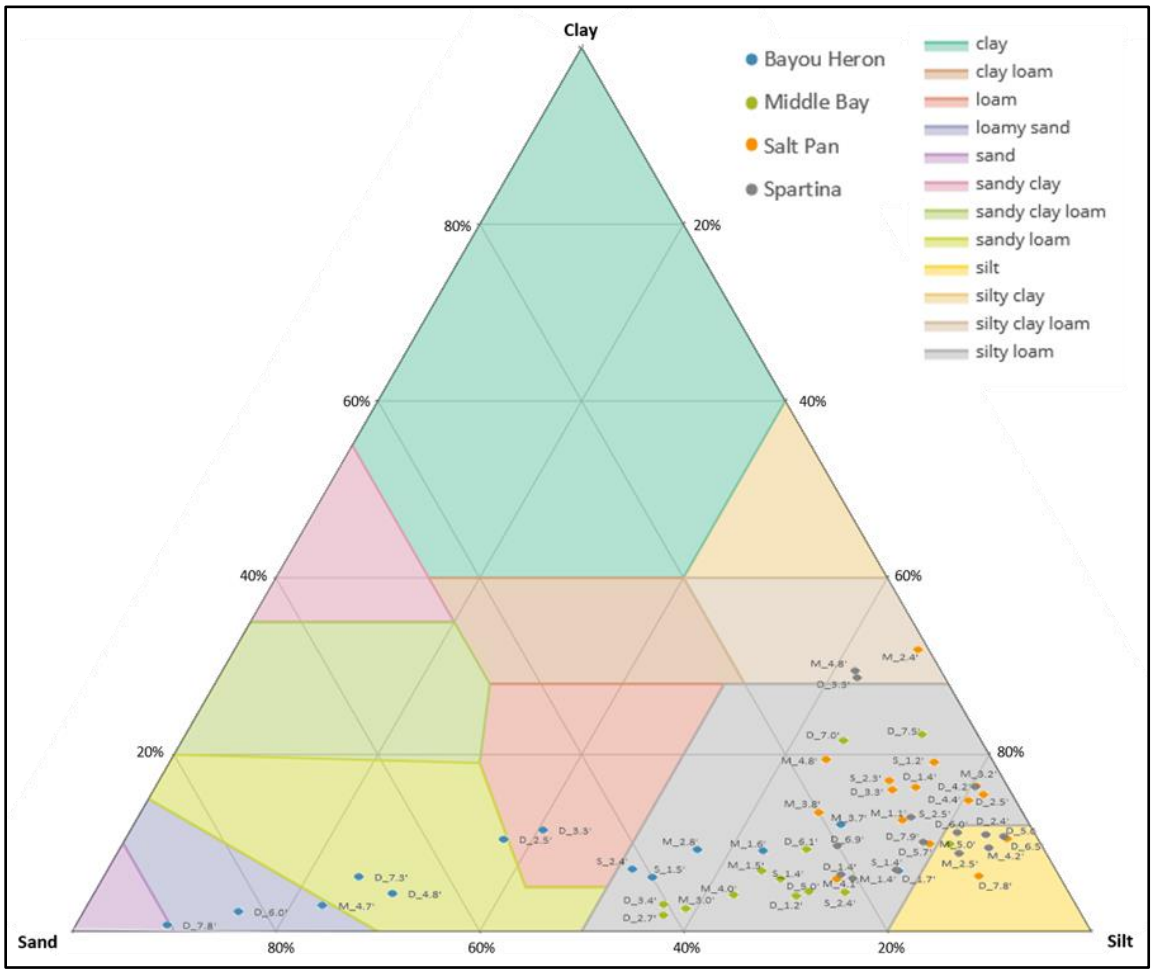

Figure 4.14 *USDA Soil Classifications*

Marsh sediment specimens are identified by color for site, "S_" (Shallow), "M_" (Intermediate), "D_" (Deep) for piezometer identification, and a number to indicate the depth of the sample interval.

Middle Bay also falls within the silty loam characterization. Overall, it has less clay than Salt Pan and less clay than many sample intervals of Spartina. However, several sample intervals of Middle Bay have a distinctly higher clay content of more than 20%, which significantly reduces the hydraulic conductivity. These sample intervals, along with the similar intervals from Salt Pan and Spartina, are not enough to form a confined

aquifer but do function effectively as a nearly occlusive barrier to surface infiltration and vertical mixing. These clay-rich layers provide significant short-term benefits to vegetation by buffering rapid changes due to inundation events.

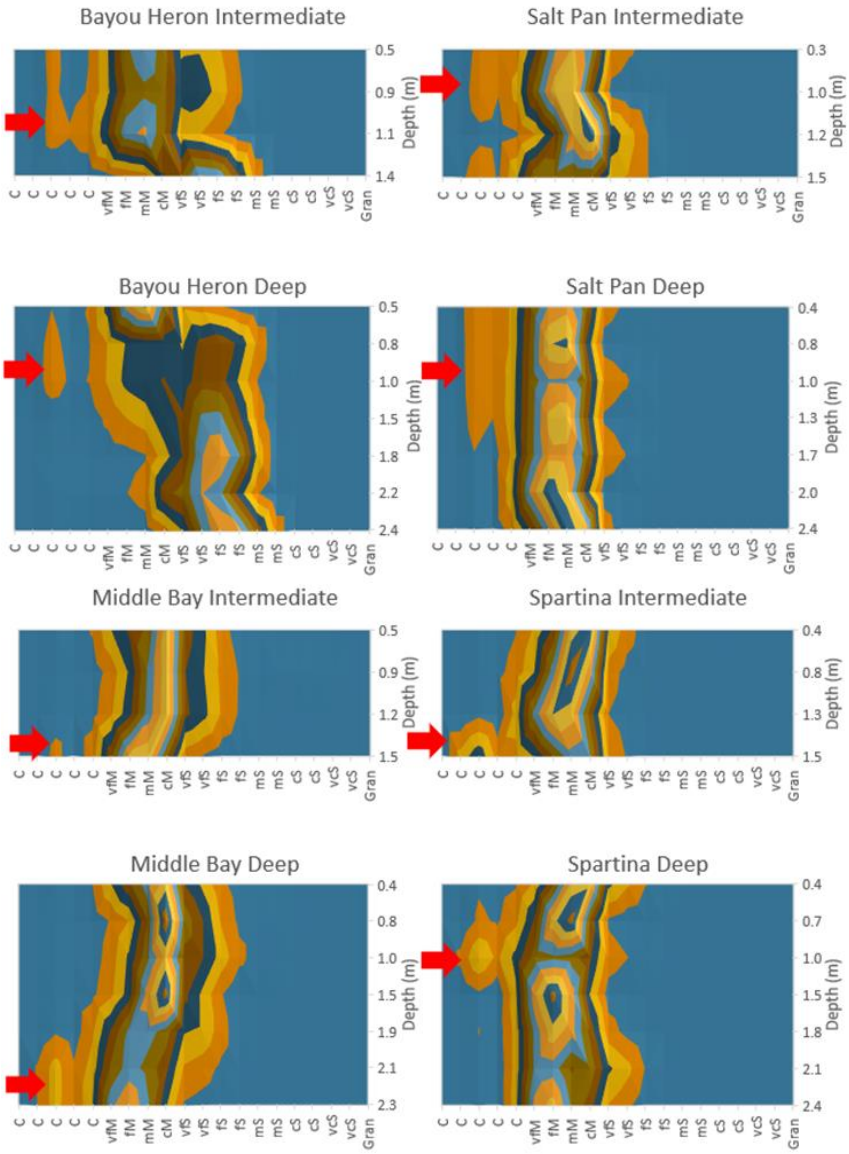

Figure 4.15 *Distinctive Low Permeability Layers*

Distinctive low permeability clay layers are indicated by red arrows. There are other low permeability layers present (not indicated) as a result of well mixed particle sizes and fine silts. Particle size increases from left to right of each subplot. C, M, S are abbreviations for clay, silt, and sand respectively.

Understanding the sedimentary factors likely to exhibit control of groundwater hydrology required multivariable analysis. Principle component analysis included analysis of sedimentary characteristics tested above and including sediment particle classifications as additional factors. The first analysis in Figure 4.16 treated each sediment sample as completely independent data points. Whereas the second analysis used the sample's site of origin as a factor in Figure 4.17. Position relative to an assumed salinity gradient was excluded as a factor. The first analysis clearly indicates only particle size factors as major axes with all three size groups being major components. The second analysis indicates that sand content specifically has the greatest control over sample characteristics. Depth is also a strong component. Ultimately, these indicate that sediment control over hydrologic behavior is likely strongly influenced by the relative proportion of sand to clays and silts. Furthermore, the strong depth component suggests the presence of sedimentary control corresponding to various depths which could affect permeability.

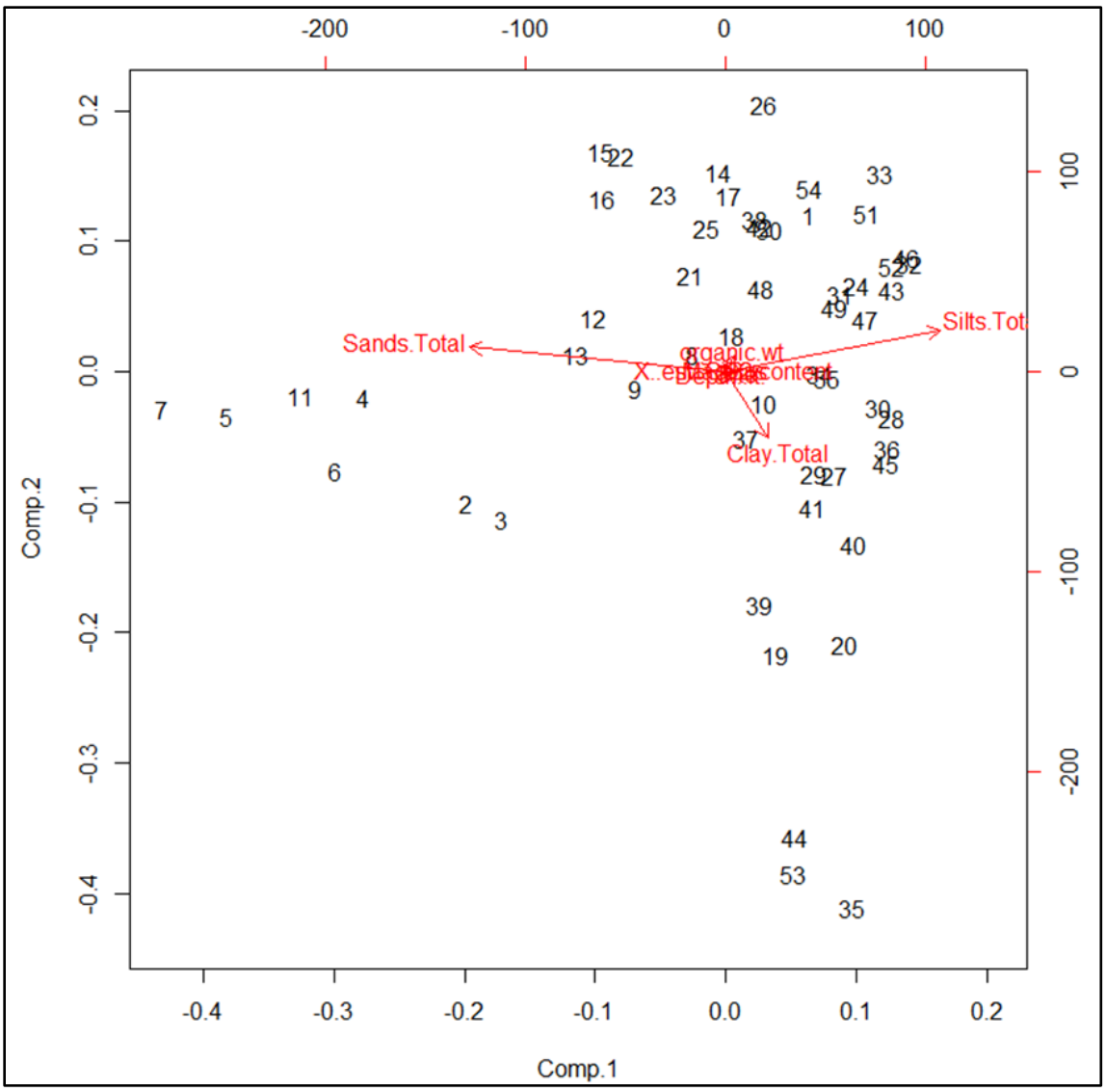

Figure 4.16 *Principle Components Analysis Site Independent*

Principle components analysis showing the relation of factors excluding location or salinity. The major axes are particle size factors. All other factors were minor axes of minimal magnitude. Analyses were conducted in the Rattle package of R.

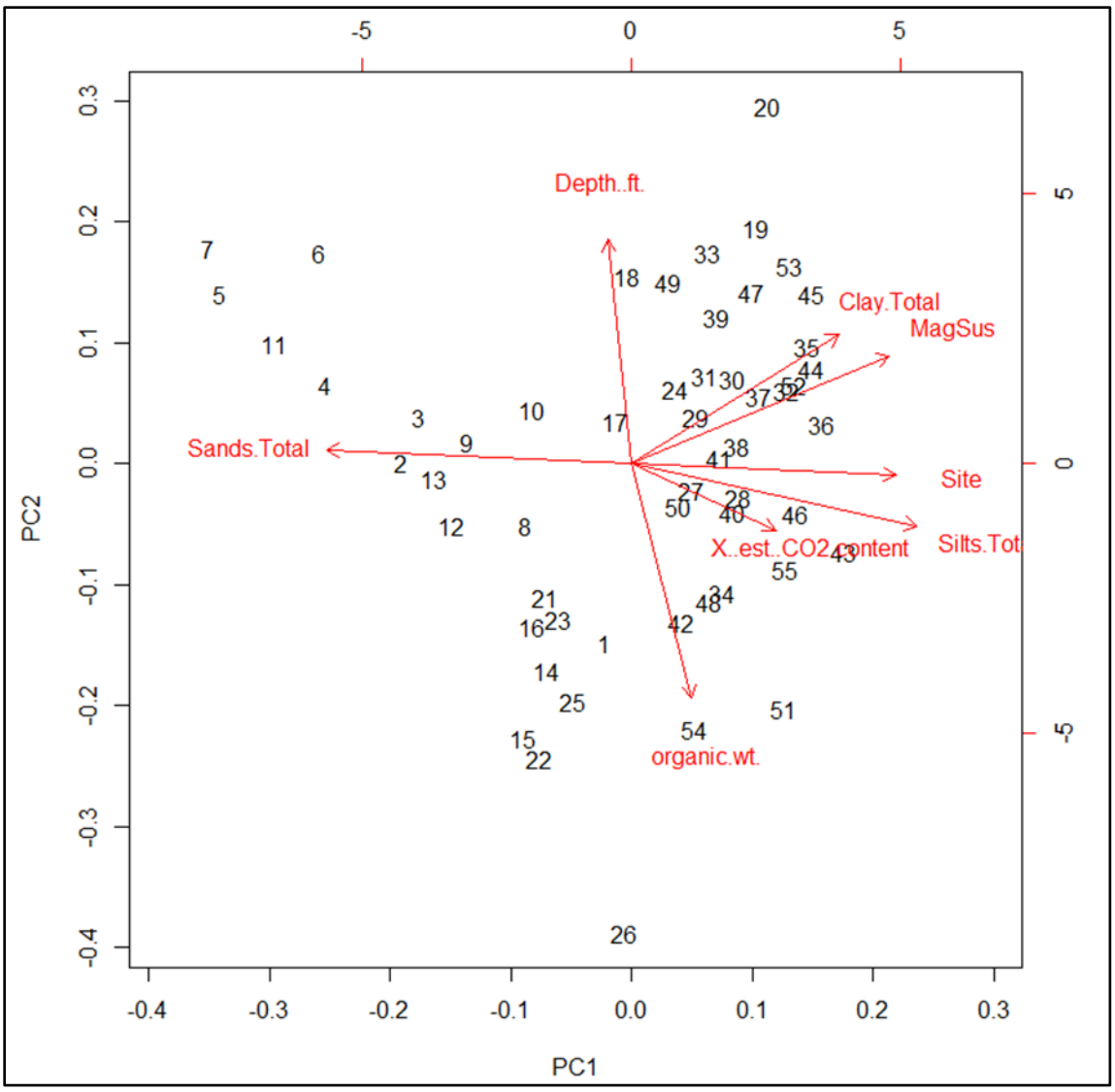

Figure 4.17 *Principle Components Analysis Site Factored*

Principle components analysis showing the relation of factors including site as a factor. The major axes of note are sands and depth. All other factors are represented as major axes but are either an opposing component factor or do not represent strong independent control. Analyses were conducted in the Rattle package of R.

CHAPTER V – HYDROLOGICAL RESULTS AND DISCUSSION

The hydrological results will be given separately for surface water followed by shallow groundwater. The discussion section will be similar with an emphasis on the trends and responses observed for diurnal, seasonal, and storm events.

5.1 Surface Water Results

The following data show the surface water characteristics at each site. These data were recorded by sensors installed adjacent to the intermediate piezometer standpipes on the sediment surface at each site. When water levels were at least 5cm above the marsh sediment surface, the sensors were sufficiently submerged to collect viable data for the surface waters including temperature, level, and conductivity. Figure 5.1 through Figure 5.4 represent the overall records available for each piezometer site. Detailed comparisons for individual parameters across multiple sites are represented in subsequent figures. Some figures include additional data from the adjacent sentinel sites for further comparison. All data representing water levels are given relative to the Earth Gravimetric Model 96 verticle datum which is a regionally accurate approximation of mean sea level.

5.1.1 Data Collected by Site

5.1.1.1 Bayou Heron

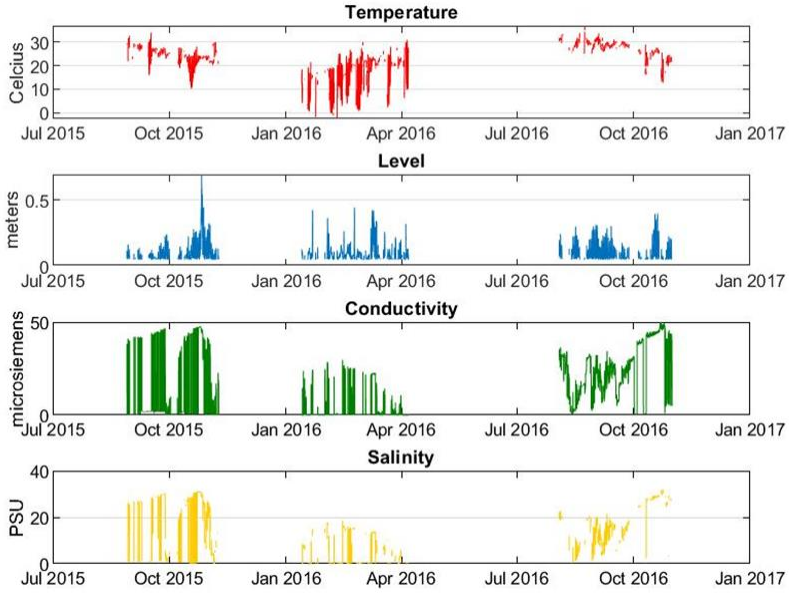

Figure 5.1 *Bayou Heron Combined Surface Records*

5.1.1.2 Salt Pan

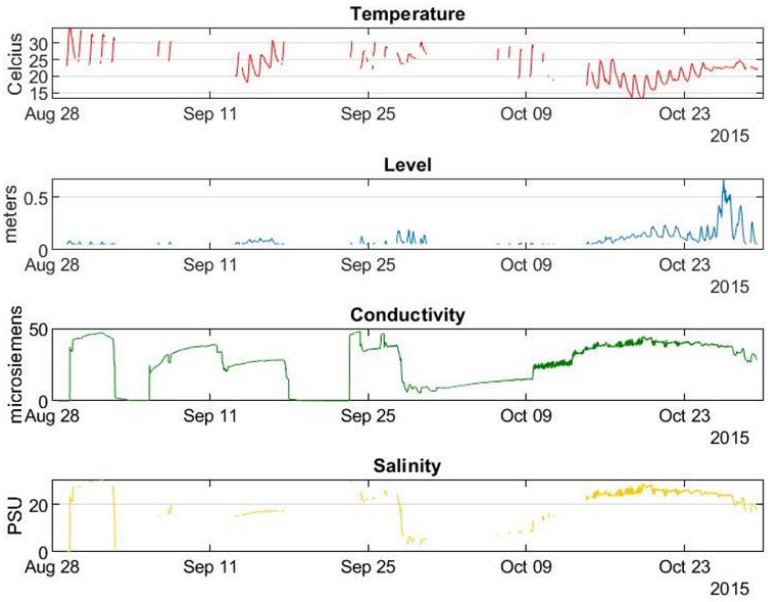

Figure 5.2 *Salt Pan Combined Surface Records*

5.1.1.3 Middle Bay Juncus

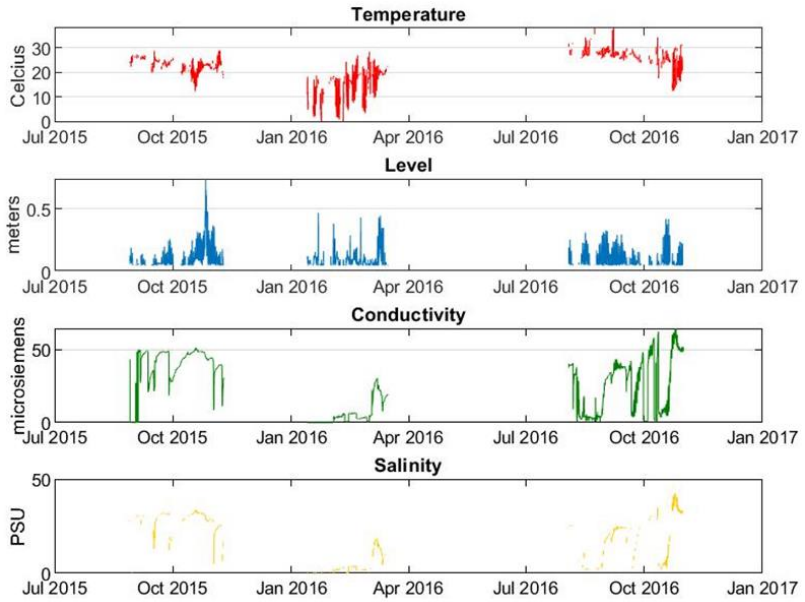

Figure 5.3 *Middle Bay Juncus Combined Surface Records*

5.1.1.4 Spartina

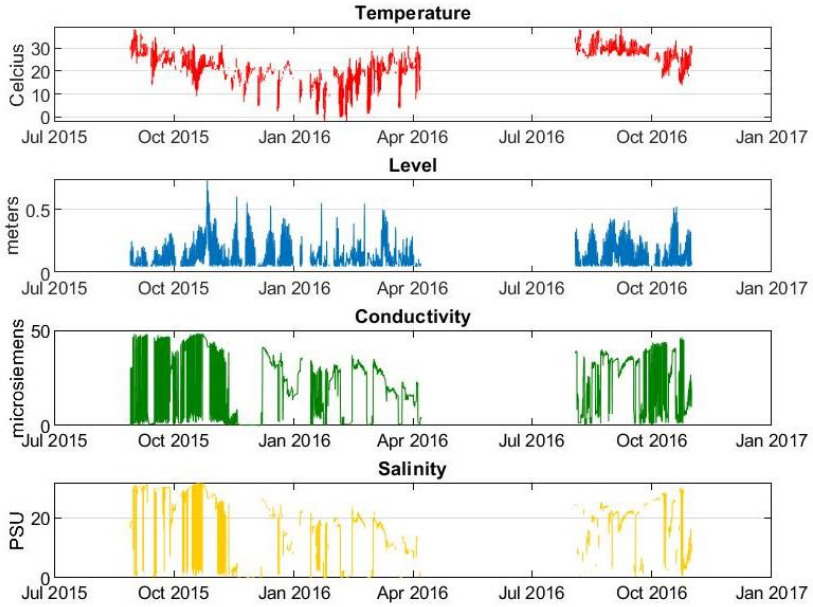

Figure 5.4 *Spartina Combined Surface Records*

5.1.2 Surface Water Levels

Table 5.1 *Surface Water Elevation Statistics relative to EGM96*

	Site	Mean (m)	Median (m)	Maximum (m)	Range (m)
Summer 2015	Bayou Heron	0.25	0.25	0.34	0.11
	Middle Bay Juncus	0.12	0.12	0.23	0.14
	Salt Pan	0.40	0.40	0.44	0.06
	Spartina	0.18	0.16	0.32	0.20
	WQBH	1.20	1.20	1.61	0.99
	WQPC	1.34	1.34	1.69	0.81
Fall 2015	Bayou Heron	0.32	0.29	0.87	0.64
	Middle Bay Juncus	0.20	0.17	0.78	0.69
	Salt Pan	0.47	0.45	1.00	0.62
	Spartina	0.25	0.22	0.81	0.69
	WQBH	1.34	1.33	2.15	1.32
	WQPC	1.44	1.44	2.20	1.20
Winter ’15-‘16	Bayou Heron	0.29	0.27	0.62	0.39
	Middle Bay Juncus	0.16	0.14	0.51	0.42
	Salt Pan	--	--	--	--
	Spartina	0.22	0.19	0.62	0.50
	WQBH	1.19	1.18	1.99	1.60
	WQPC	1.33	1.33	2.09	1.43
Spring 2016	Bayou Heron	0.26	0.25	0.50	0.27
	Middle Bay Juncus	--	--	--	--
	Salt Pan	--	--	--	--
	Spartina	0.18	0.18	0.36	0.24
	WQBH	1.30	1.30	1.89	1.18
	WQPC	1.36	1.39	1.98	1.35
Summer 2016	Bayou Heron	0.31	0.30	0.50	0.27
	Middle Bay Juncus	0.19	0.17	0.37	0.28
	Salt Pan	--	--	--	--
	Spartina	0.25	0.24	0.50	0.37
	WQBH	1.21	1.21	1.61	0.72
	WQPC	1.24	1.21	1.71	0.73
Fall 2016	Bayou Heron	0.29	0.27	0.57	0.35
	Middle Bay Juncus	0.16	0.14	0.46	0.37
	Salt Pan	--	--	--	--
	Spartina	0.24	0.22	0.59	0.47

Values in Table 5.1indicate that the average surface water levels across the marsh are higher in the fall and spring seasons and lower in the winter and summer seasons. The Salt Pan site typically has the smallest range. For comparison, the open channels at the Bayou Heron water quality station and the Point aux Chenes water quality station have the highest water level range indicative of surface water runoff associated with precipitation events. This demonstrates the effects of vegetation, elevation, and distance as reducing factors of tidal and storm inundation.

5.1.3 Surface Water Temperature

The surface water temperatures have been statistically grouped in Figure 5.5 and Figure 5.6. The surface water temperatures were f highly variable. The Salt Pan site should be viewed and compared with caution as limited data availability due to sensor failure makes overall comparison with other sites statistically limited beyond the fall season. However, statistics on all available data for each site individually are shown. For general perspective, temperature data from the sentinel water quality stations (sampling channel surface waters) were included.

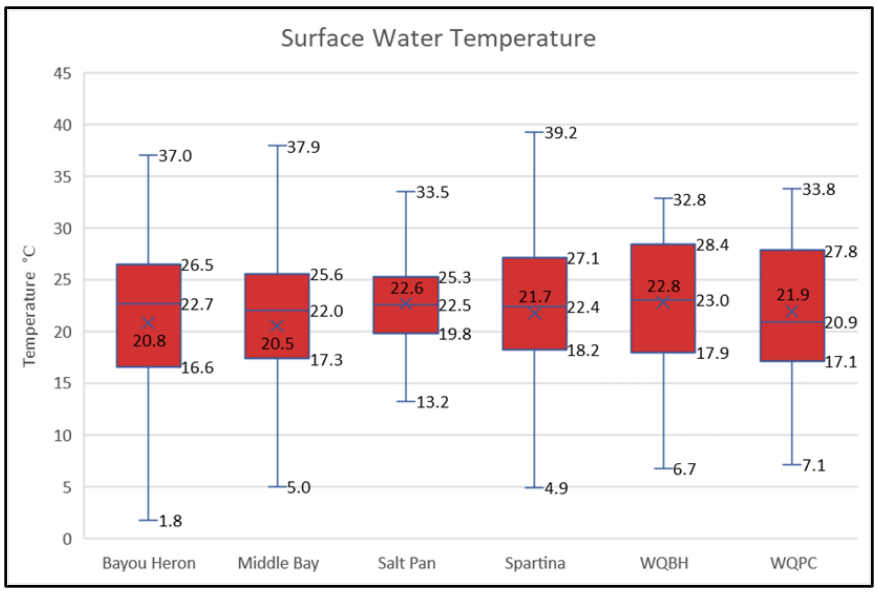

Figure 5.5 *Surface Water Temperature Statistics by Site*

These statistics include all valid records. The number of valid data points varies widely. X marks the mean.

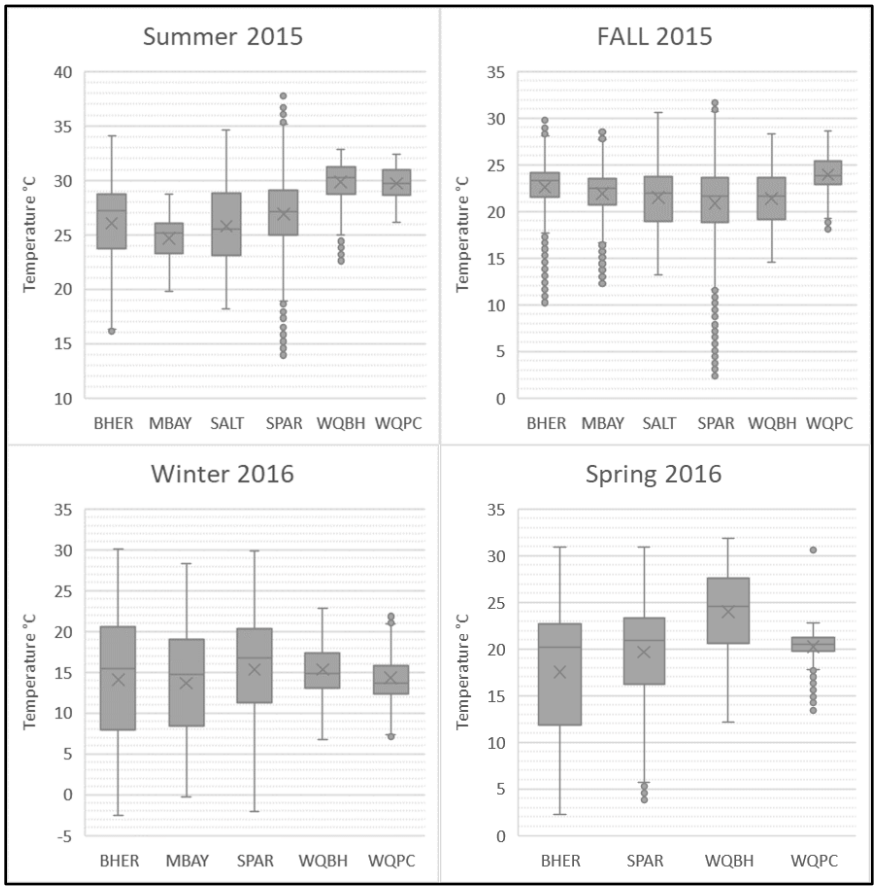

Figure 5.6 *Surface Water Temperature by Season*

5.1.4 Surface Water Salinity

Figure 5.6 displays surface water conductivity records by site converted to salinity measured in practical salinity units. Available records for Salt Pan are limited and likely strongly underestimate the maximum surface salinity common at the site during dry periods. The surface salinity gradient demonstrates an increased surface salinity in the mid marsh area that likely skewed higher than Salt Pan due to the limitations of sensor recording. In order to record surface salinity, the sensor must be submerged. Thus precipitation events at Salt Pan, which is slightly elevated, may wash away salinity in the terrestrial runoff prior to the sensor being submerged. Spartina is clearly the most variable site. However, it is important to note there is not a large difference in surface salinity across the entire marsh area.

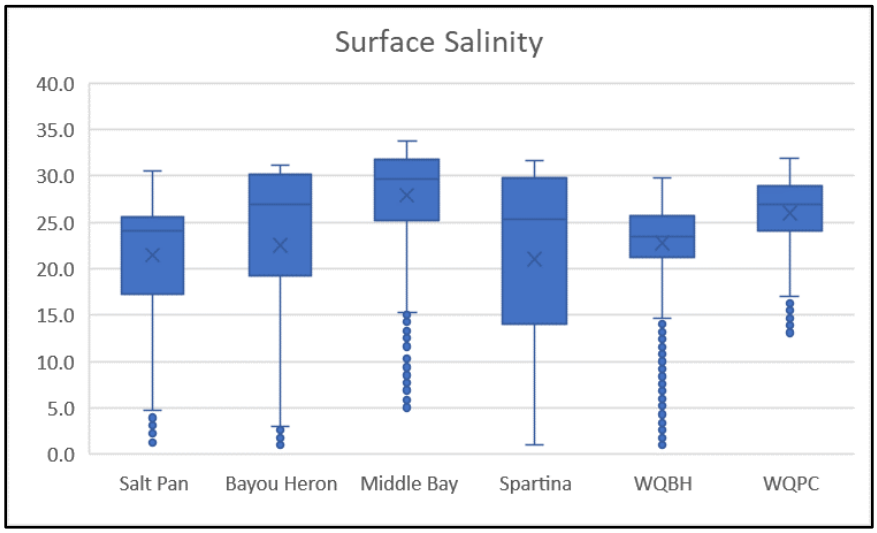

Figure 5.7 *Surface Water Salinity by Site*

All available valid conductivity data was converted to the practical salinity scale.

5.2 Shallow Groundwater Results

The following tables and charts represent the entire duration of record for each shallow groundwater station at shallow (~0.75 m below surface), intermediate (~1.5 m below surface) and deep (~2.25 m below surface) levels. Temperature, total pressure, and conductivity were recorded by the sensor; total pressure was converted to hydrostatic pressure by barometric pressure compensation. The subsurface water levels represent the depth in terms of the height of the water column above the sensor at the bottom of the piezometer. These depths are not the distance from surface to groundwater nor a statement of relative elevation of the water table throughout the marsh. However, all water levels in the discussion sections have be converted to elevation relative to mean sea level using the Earth Gravitation Model 96. Salinity was calculated from these records using Solinst Levelogger software. Where a full season of data was not available, tables included all available data within the season.

5.2.1 Data Collected by Site

5.2.1.1 Bayou Heron

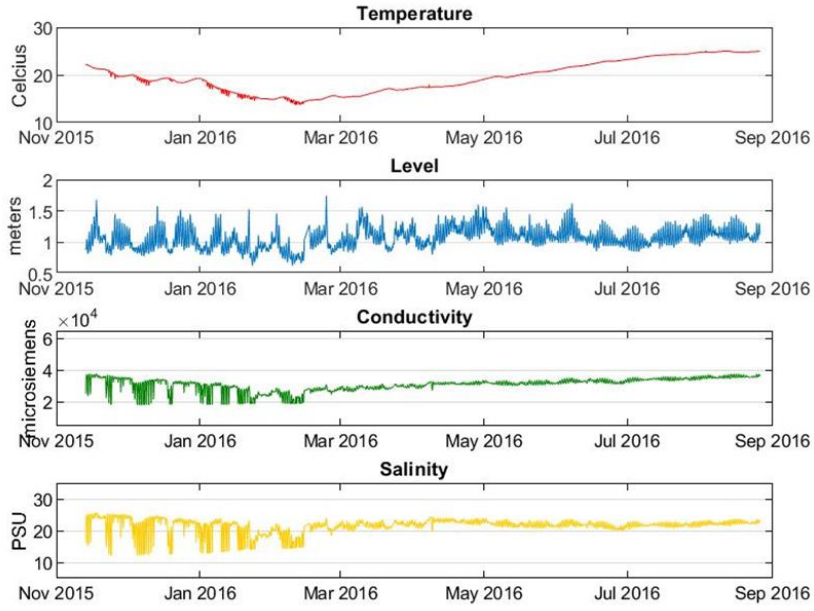

Figure 5.8 *Bayou Heron Intermediate Combined Groundwater Records*

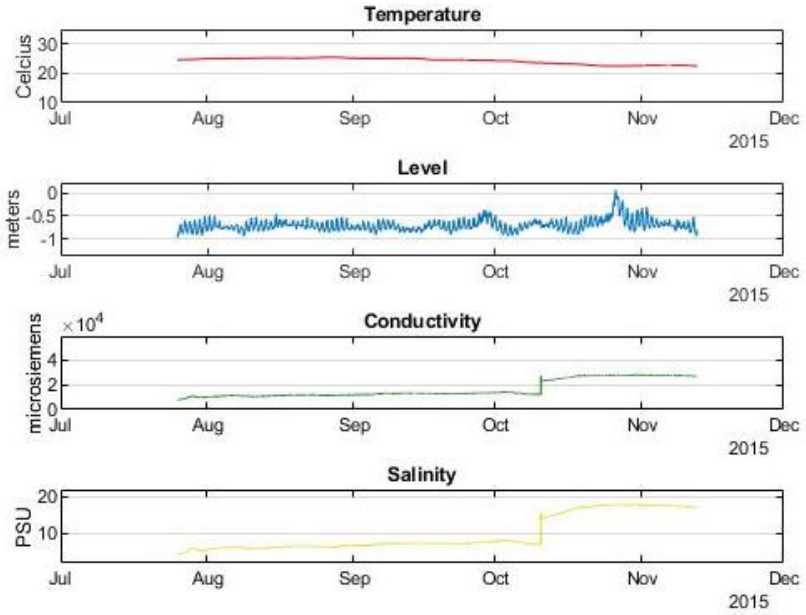

Figure 5.9 *Bayou Heron Deep Combined Groundwater Records*

The record for Bayou Heron Deep was short due to the nature of the highly mobile sandy sediment slowly filling in the piezometer. In mid-November, the sensor was pulled and repurposed as the Bayou Heron Intermediate sensor (previous figure).

5.2.1.2 Salt Pan

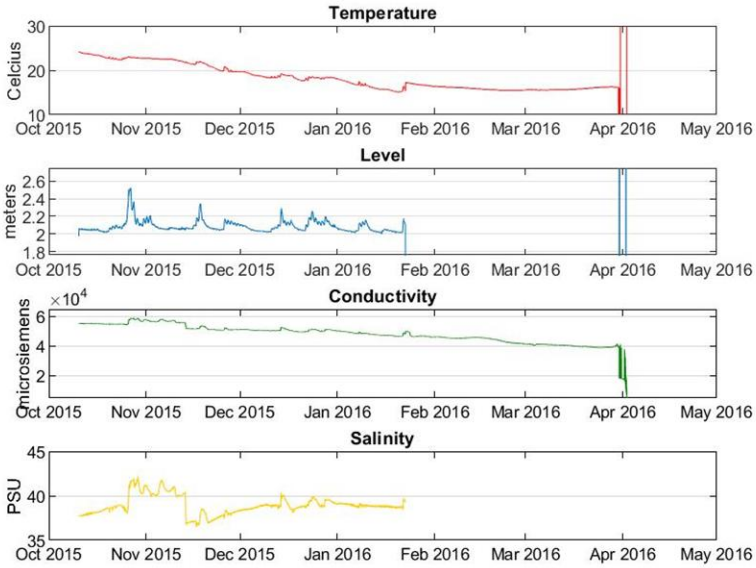

Figure 5.10 *Salt Pan Deep Combined Groundwater Records*

This record illustrates the failure of the pressure transducer component of the sensor on January 22, 2016. Salinity is calculated from temperature, pressure, and conductivity. Therefore, both depth and salinity fail validation beyond that time. The failure of the electro-optical sensor for measuring temperature and conductivity occurs on March 29, 2016, rendering the last few days invalid. Some invalid values remain in the figure above for illustration but were not included in the calculations for the table values.

5.2.1.3 Middle Bay Juncus

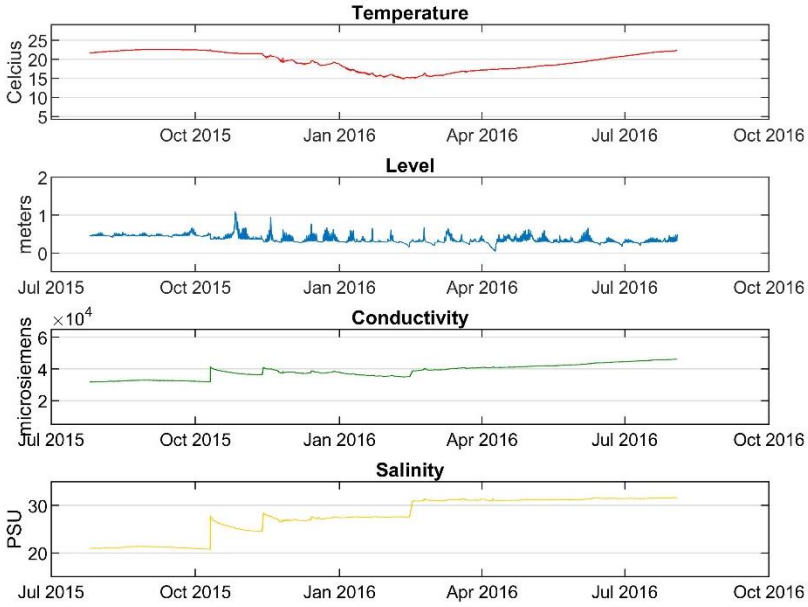

Figure 5.11 *Middle Bay Intermediate Combined Groundwater Records*

Following a few sensor failures, a redistribution of functional sensors was intended to record data at unmonitored stations including Middle Bay Juncus Deep. This sensor was also not checked for conductivity calibration at that time. Unfortunately, the sensor did not remain functional and limited valid data could be salvaged from the sensor. However, the short duration of valid data represents a clear view of tidal influence at this station.

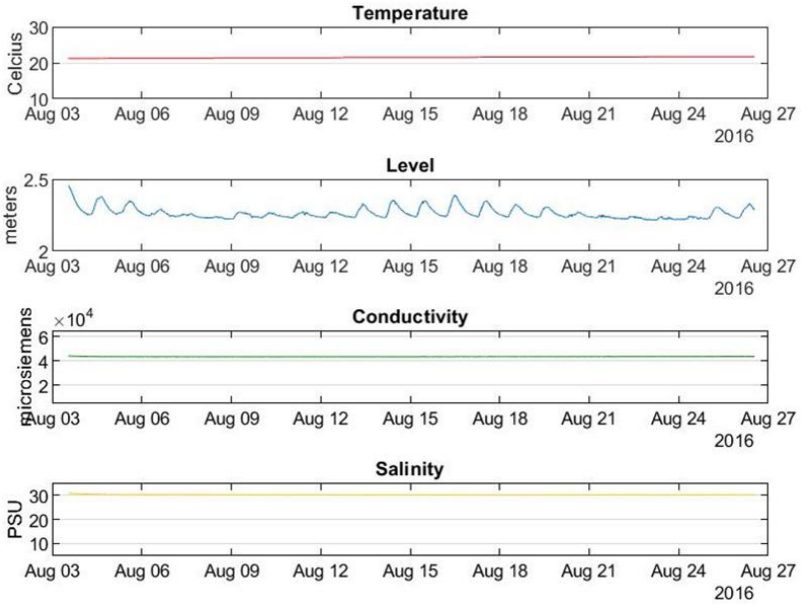

Figure 5.12 *Middle Bay Deep Combined Groundwater Records*

5.2.1.4 Spartina

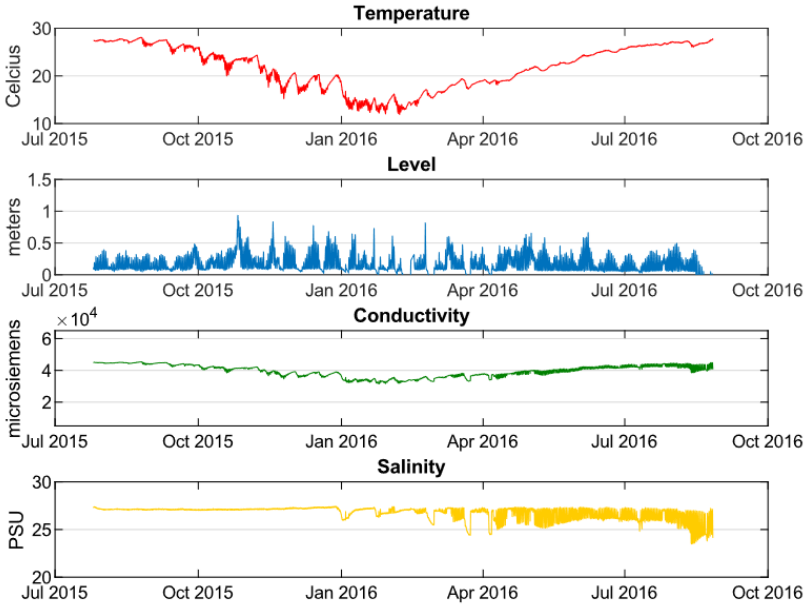

Figure 5.13 *Spartina Shallow Combined Groundwater Records*

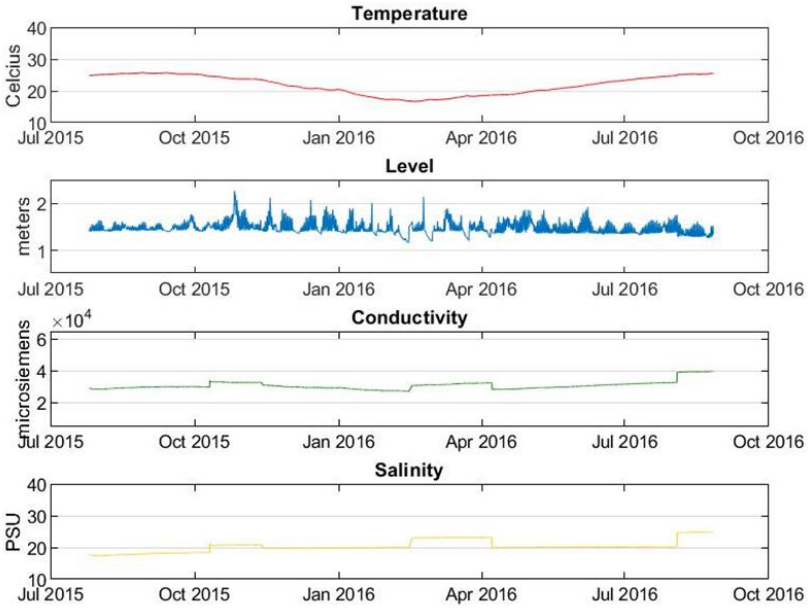

Figure 5.14 *Spartina Intermediate Combined Groundwater Records*

5.3 Surface Water Discussion

Data availability for surface water across all sites is limited to Summer 2015 and Fall 2015. More limited site comparisons are available thereafter due to sensor failures. However, various surface water trends were apparent very early in the study. All sites experience frequent inundation lasting for hours to days, especially during the wetter months as seen in the surface water site data above (Figure 5.1through Figure 5.4). A strong diurnal tidal signal was observed at all surface water sensors. This diurnal signal was most strongly represented in the water levels (as discussed below and in Figure 5.16) but was also observed clearly in the water temperature (Figure 5.19). A lag of the tidal peak through the marsh was observed. There was little difference in the outer marsh but significant delay for the inner marsh of more than one hour at Salt Pan (Figure 5.15). Wind direction and other atmospheric factors likely affect the lag between sites as water is forced through channels and around landforms. Tidal influence on surface salinity was present but complicated by evapotranspiration differences, precipitation, and other factors such as terrestrial runoff and mixing.

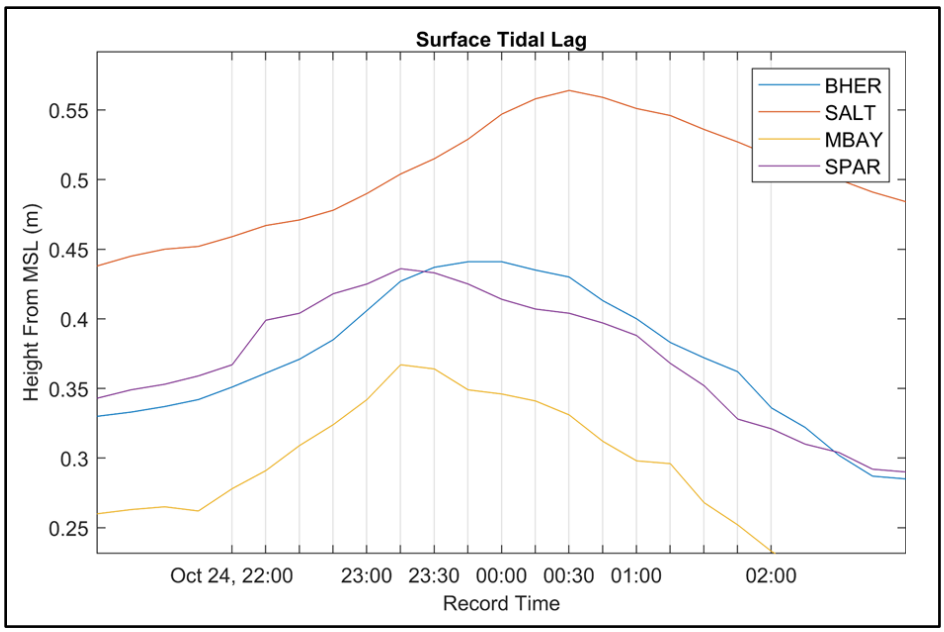

Figure 5.15 *Surface Tidal Lag*

Surface water tidal peak timing through marsh reveals a significant delay for Salt Pan.

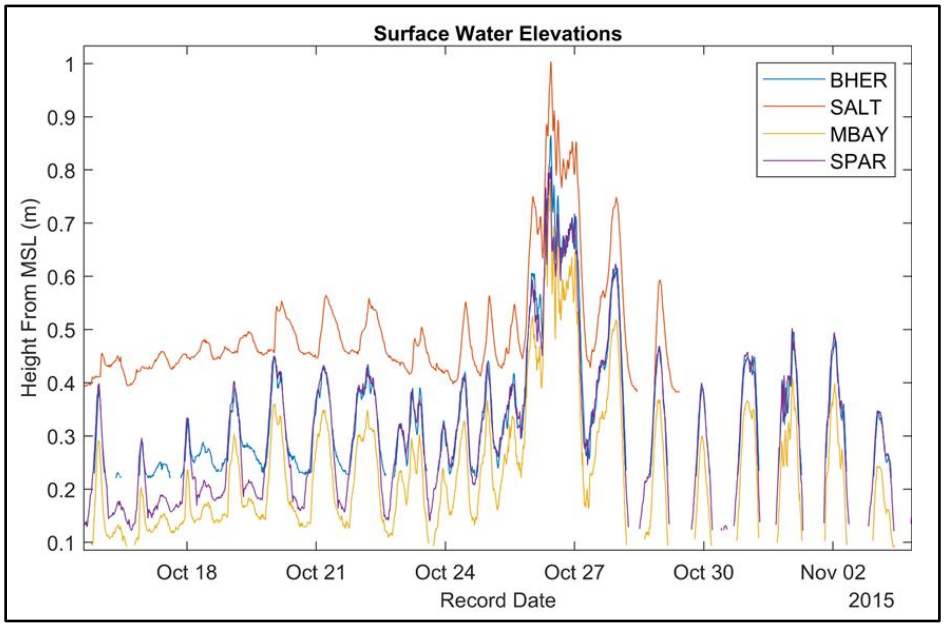

Figure 5.16 *Surface Water Elevations*

Surface water levels in late October indicating significant storm surge.

Though the surface water levels would recede below the viable surface sensor height, field visits revealed several centimeters of standing water was common such that drying events were rare except at Salt Pan due to its slightly higher overall elevation about 15cm higher than Bayou Heron (Table 3.1). During drier periods, a salty crust could be observed at Salt Pan. This was a stark contrast to the Middle Bay Juncus site where the low elevation commonly resulted in extensive ponding of water and highly saturated surface sediments. Middle Bay surface water salinity is affected by evapotranspiration rates and is elevated during hot summer days. Furthermore, the dense vegetation at Middle Bay provides some thermal stabilization by slowing surface water mixing and insulating the surface. The less dense vegetation cover at Salt Pan combined with the elevation allows precipitation events to flush the surface salts thereby lowering surface salinity. In Figure 5.17 below, afternoon showers cause incremental short-term decreases in surface salinity followed by more substantial decreases caused by a prolonged precipitation event discussed below.

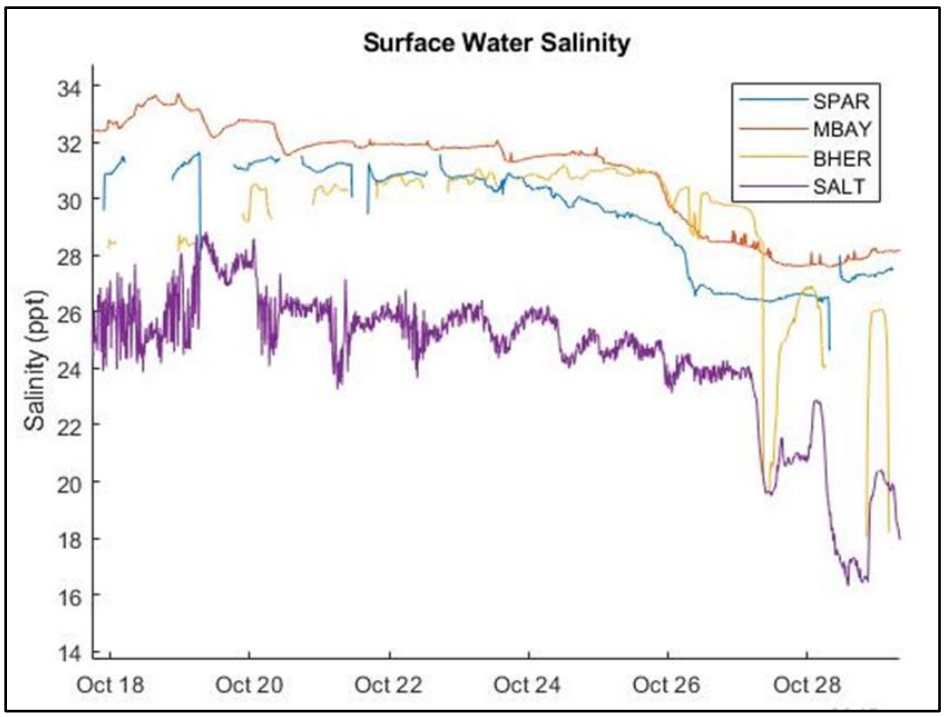

Figure 5.17 *Surface Water Salinity*

Surface water salinity drops sharply with storm precipitation in late October.

In late October 2015, observations included the impacts of a hybrid weather system formed from the remnants of Hurricane Patricia and a low-pressure system over Louisiana. The combined system was accompanied by heavy precipitation and high winds along the Gulf Coast causing storm surge coincident with spring tides. Average tidal range is 0.6m; the surge was approximately 0.5m above the average high. As indicated in Figure 5.16 above, the storm surge levels increased significantly early October 26th with the low barometric pressure. Then levels peaked as the wind driven water is forced into the marsh. Debris rafts, primarily of Juncus, were deposited as the surge receded (Figure 5.18).

Figure 5.18 *Storm Debris*

Debris deposited in thick mats by storm surge from Patricia remnant system. Photograph adjacent to Middle Bay site representative of areas throughout outer marsh.

Following the storm peak, surface water returned to average levels within 48 hrs. The surface salinity at all sites was observed to decrease with the increased precipitation and storm water runoff, especially as storm surge receded from the marsh. Surface temperatures stabilized during the storm such that the normal day and night heating cycle was undetectable, and the temperature cycles did not return until after the surface water receded (Figure 5.19).

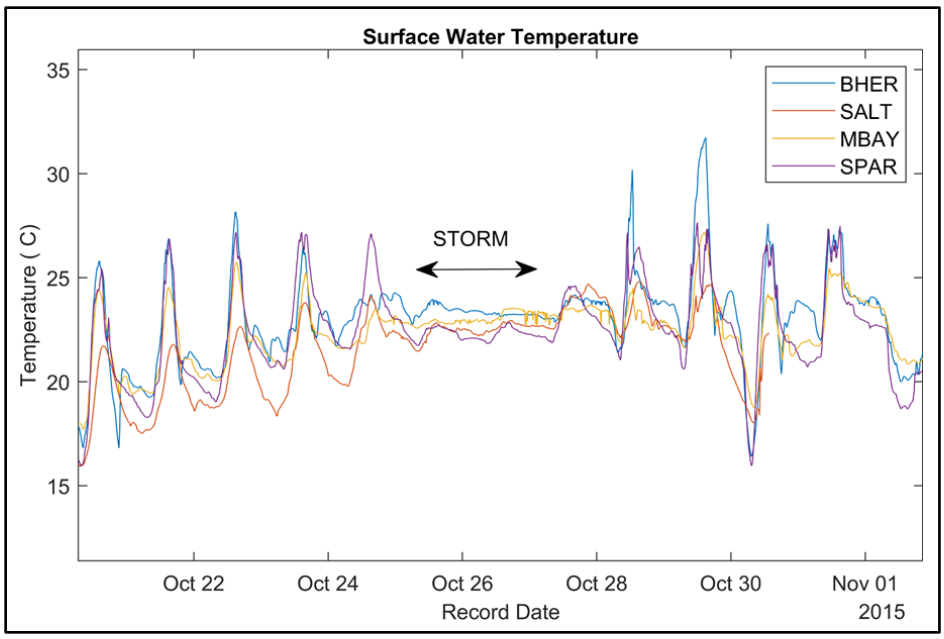

Figure 5.19 *Surface Water Temperature*

Surface water temperatures indicate strong diurnal signals preceeding and following the storm event.

This storm serves as an important example for episodic interruptions to diurnal and seasonal trends in shallow groundwater processes and characteristics. Storms of significant strength and multiday duration have the greatest potential for inundation to the marshlands creating conditions similar to a small change in relative sea level (Figure 5.20). This storm demonstrates that cloud cover and precipitation have the potential to reduce daily thermal cycling of surface waters. Furthermore, storm surge or rSLR will damage vegetative cover and affect surface water mixing and salinity flushing. Further groundwater effects are discussed below.

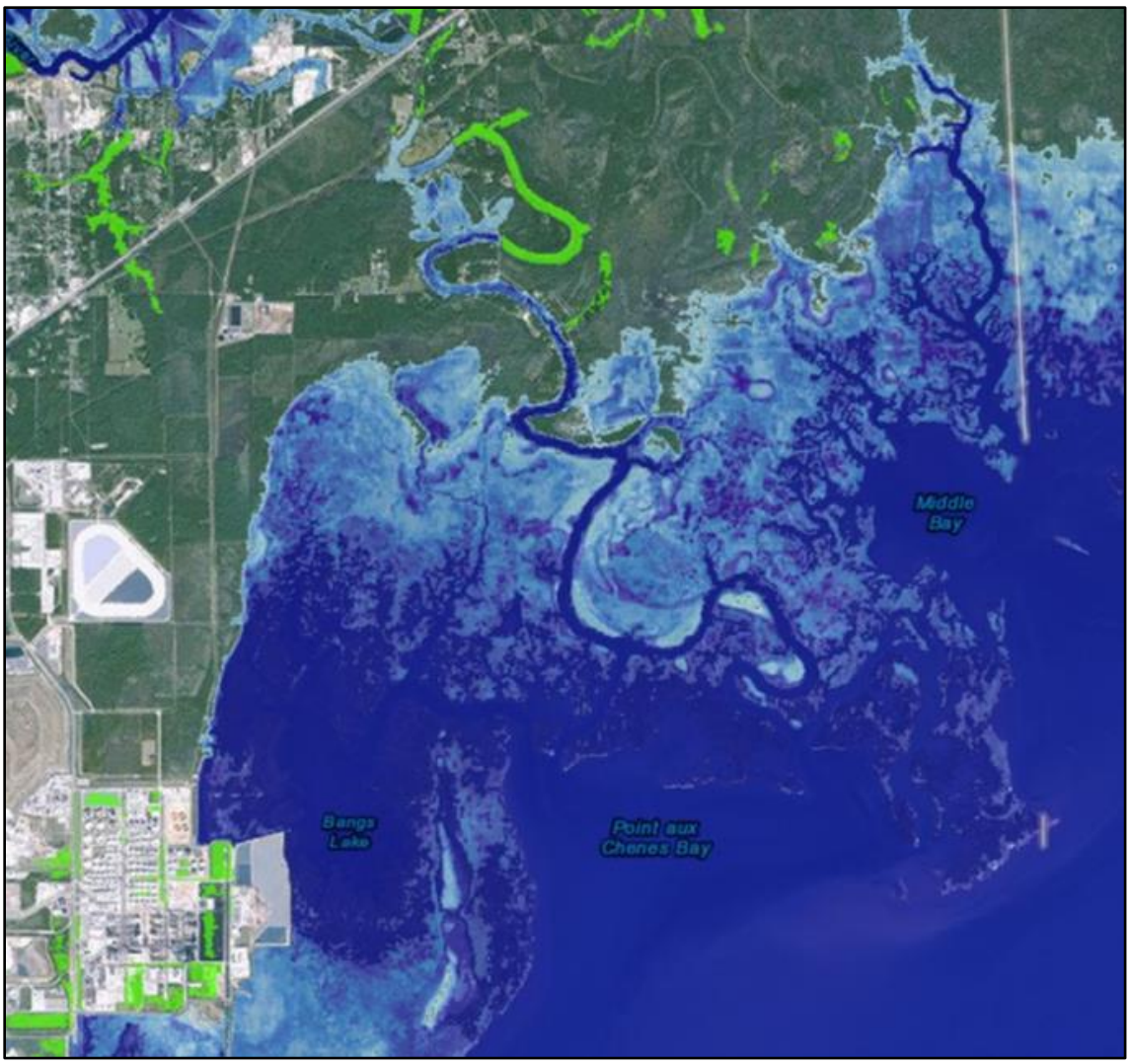

Figure 5.20 *Inundation Example Model*

NOAA Flood Prediction Model demonstrates a 1-meter rise of relative sea level. Areas in light blues are submerged in this scenario.

(Coast.NOAA.gov/SLR)

5.4 Shallow Groundwater Discussion

Barometrically corrected records show strong signals of tidal fluctuations in the shallow groundwater at all stations. This diurnal signal is present only in the groundwater levels and not in the temperature or salinity signals at most piezometers. Only limited tidal influence on salinity could be identified as communication with surface waters in the outer marsh at the shallow Spartina piezometer. Therefore, this diurnal signal is more indicative of a discrete groundwater body rather than an expression of direct and continuous surface water communication and mixing. The range of the tidal signal at each station is locally consistent but varies across the marsh system. No practical difference in groundwater level response could be identified between the intermediate and deep piezometers within any site (Figure 5.21). However, differences between the intermediate and shallow depths were evident. An example of this is observed at Bayou Heron, where the shallow tidal peak lags from the intermediate peak by roughly 45 minutes (Figure 5.22). Additional lag is observed between sites, such as the 4 to 5 hour lag at Salt Pan after the peaks at Spartina. The variation by depth within a site is likely controlled by the sediment composition or depositional structures.

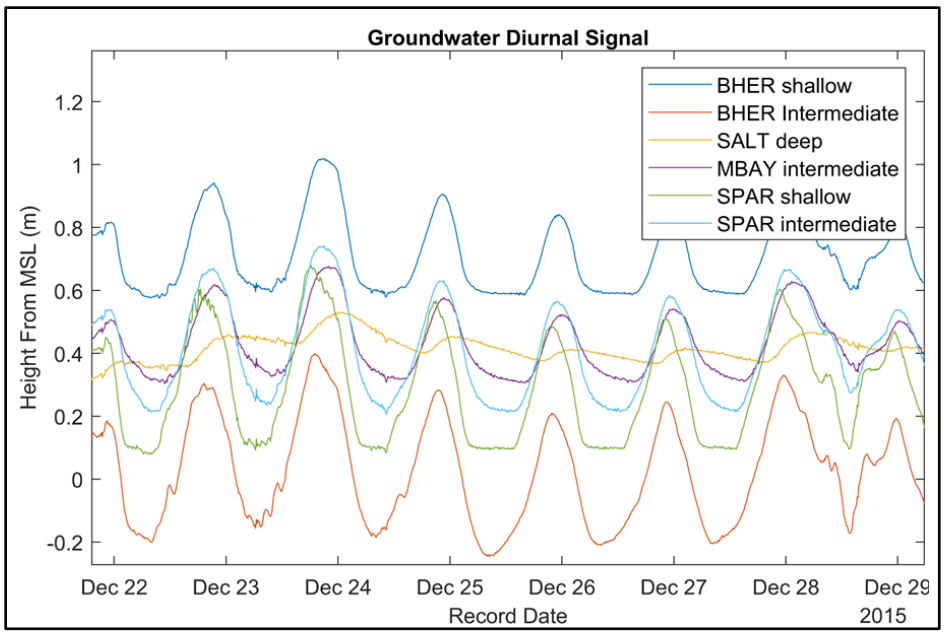

Figure 5.21 *Groundwater Diurnal Signal*

Diurnal tidal signals in the groundwater level at all sites are fluctuating consistent with the surface diurnal tidal cycles. Deeper piezometers demonstrate negligible attenuation compared to intermediate depth signals.

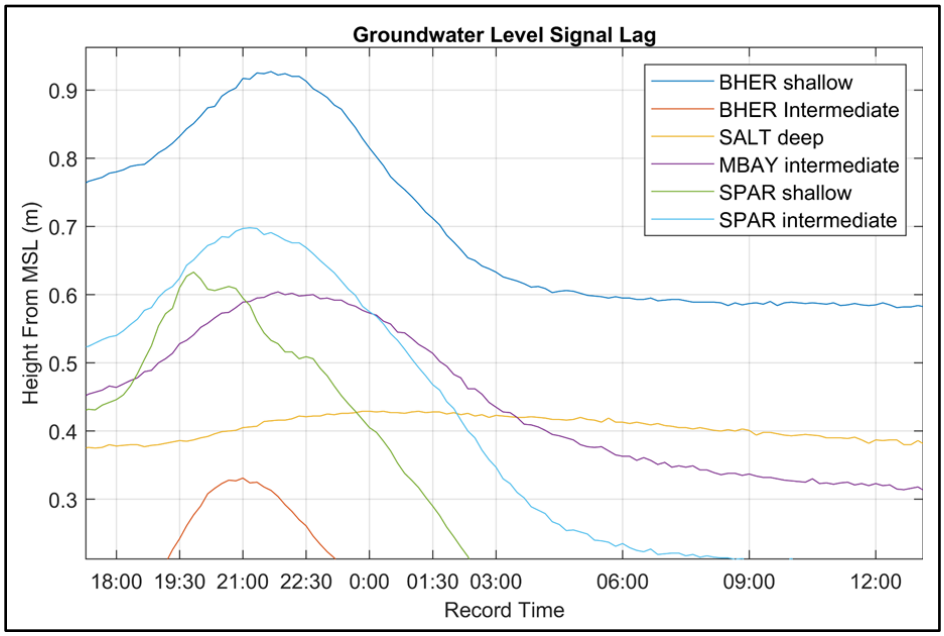

Figure 5.22 *Groundwater Diurnal Peak Signal Lag by Site*

The variation within a site as well as between sites is clearly observed at high tide on a non-event day.

Temperature is relatively steady in the marsh subsurface (Figure 5.23). Temperature fluctuations are rarely more than a degree in 24 hrs. These fluctuations notably decrease with depth showing the most extreme case at the Spartina site (Figure 5.24) Temperature at depth not only fluctuated less in the short-term, but also had a reduced overall range with lower summer and higher winter temperatures. Surface vegetation density is likely an additional influence on shallow groundwater temperature but likely has little to no impact on deeper groundwater temperatures. Storm events producing a long duration of heavy precipitation can lower the groundwater temperature faster than typical daily or seasonal fluctuation alone.

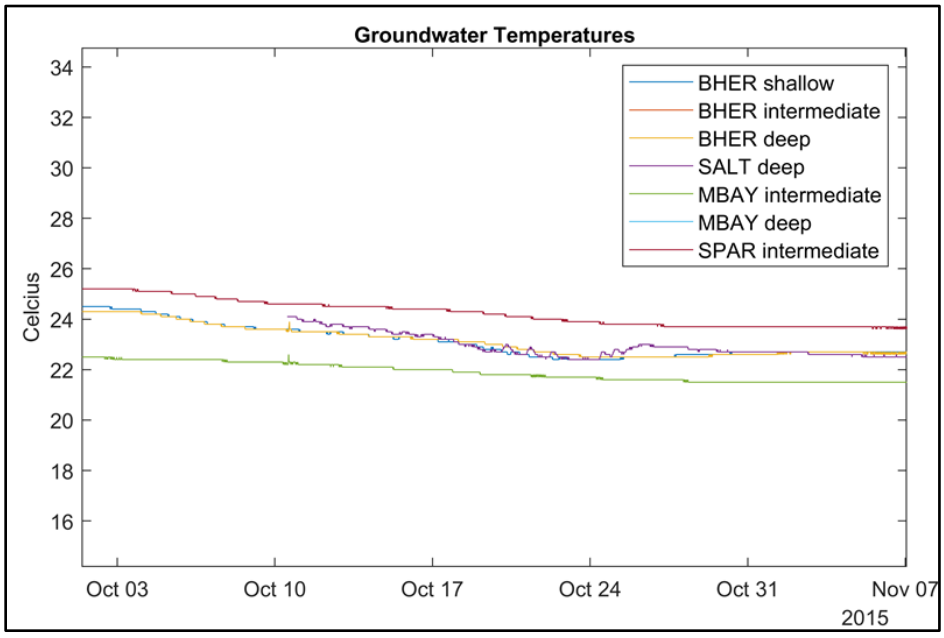

Figure 5.23 *Groundwater Temperature Fluctuations*

The temperature is observed to be generally steady throughout the marsh where no direct mixing with the surface occurs. Note the declining trend due to seasonal cooling and the slightly faster decrease at Salt Pan as the storm front arrives. The slight increase at Salt Pan with the storm corresponds to heavy precipitation and slow infiltration of warmer surface water.

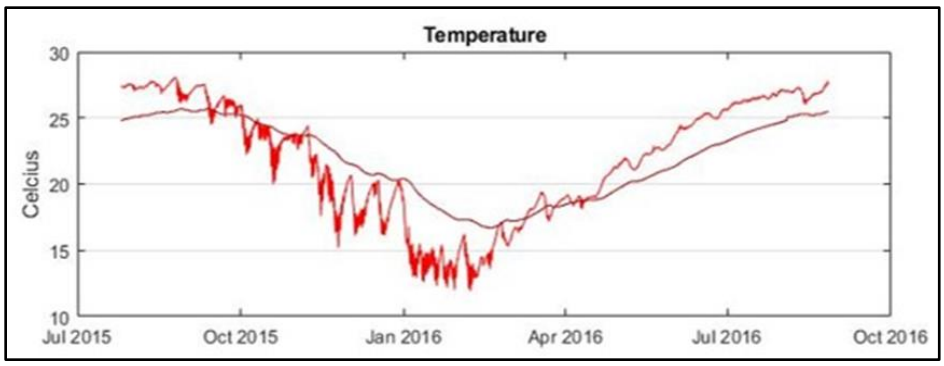

Figure 5.24 *Temperature Signal Attenuation with Depth*

This example from Spartina shows shallow groundwater temperatures-the most extreme fluctuations of all groundwater- compared against intermediate groundwater temperatures.

Shallow groundwater conductivity and salinity also generally decrease with depth at all sites suggesting seaward flow of fresher subsurface waters. The salinity difference with depth also suggests potential for vertical osmotic water movement that may benefit deep rooted vegetation. However, this vertical movement may be significantly limited by clay-rich and otherwise low permeability layers. This may be most important at Middle Bay and Spartina wherein short-term inundation events had little impact on groundwater salinity suggesting the low permeability sediments and clays resist surface infiltration and rapid salinity changes.

Additionally, the decreased salinity at depth could suggest that a seaward flow of lower salinity water exists in the shallow subsurface resisting the penetration of the higher density saline surface water. This is supported by the flushing events seen most readily in the Bayou Heron data wherein salinity rapidly and temporarily decreases after some precipitation events seen in Figure 5.25. This subsurface flushing is enabled by the permeable sand-rich layers and semi-isolated from the surface by thin deposits of less permeable silts and clays. While subsurface flushing is present at Salt Pan, limited data shows that precipitation can also wash surface salts into the groundwater such that an

increase in salinity is observed as discussed below. The presence of this deeper lower salinity water could serve to protect vegetation from rapid shifts in surface salinity. Though this effect may depend greatly upon the precipitation occurring in the pine savannahs to the north as opposed to local surface precipitation.

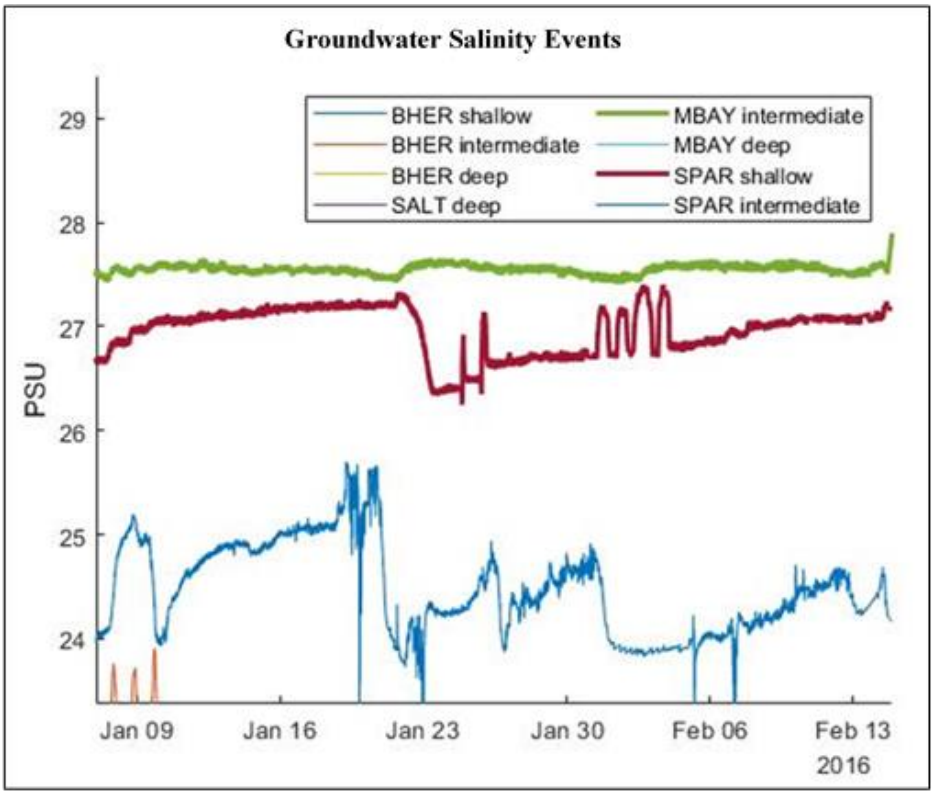

Figure 5.25 *Rapid Salinity Changes with Precipitation*

Increased precipitation, lower atmospheric pressure, landward wind-driven water volume, and other storm influences can increase groundwater levels and alter the salinity profile but have negligible effect on subsurface temperatures. During the October storm system, groundwater levels increased nearly as much as the surface levels (Figure 5.26), but low tide signals were weakened likely as a result of the low-pressure front and prolonged precipitation. Following the storm peak, groundwater levels took up to approximately 72hrs to return to nominal levels. Effects on groundwater temperatures

were not observed and varied no more than 1 degree Celsius during the storm in stark contrast to the strong influence observed in surface water temperatures.

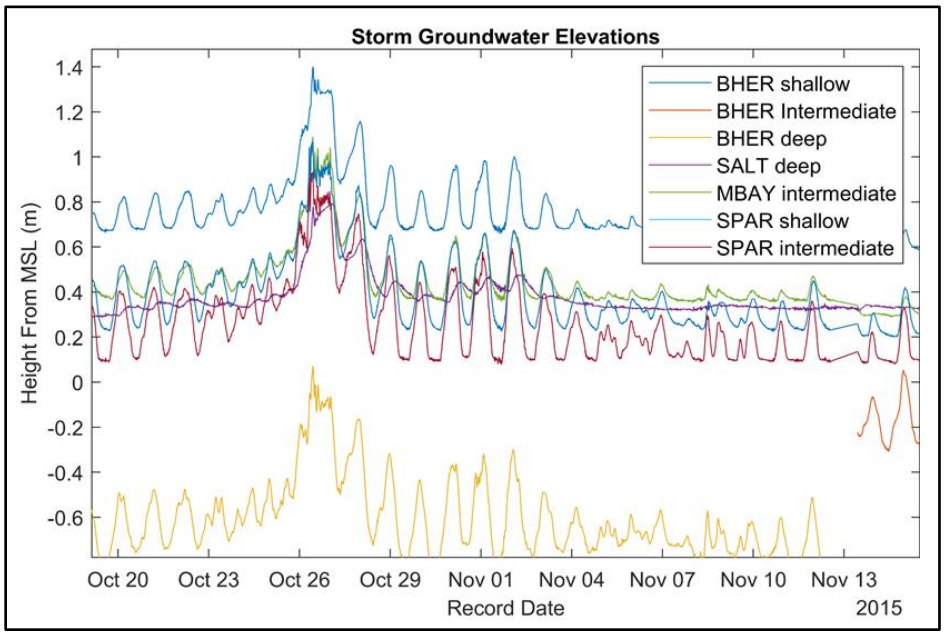

Figure 5.26 *Groundwater Storm Levels*

Additional impacts were seen at Salt Pan where surface salinity was washed into the ground water by the precipitation (Figure 5.27). The ground water salinity at all sites and piezometers other than Salt Pan remained relatively stable. Only a very slight decrease throughout and after the storm was observed at Middle Bay, but this decrease was likely typical seasonal change due to temperature, rainfall and evapotranspiration as discussed below rather than a direct storm response.

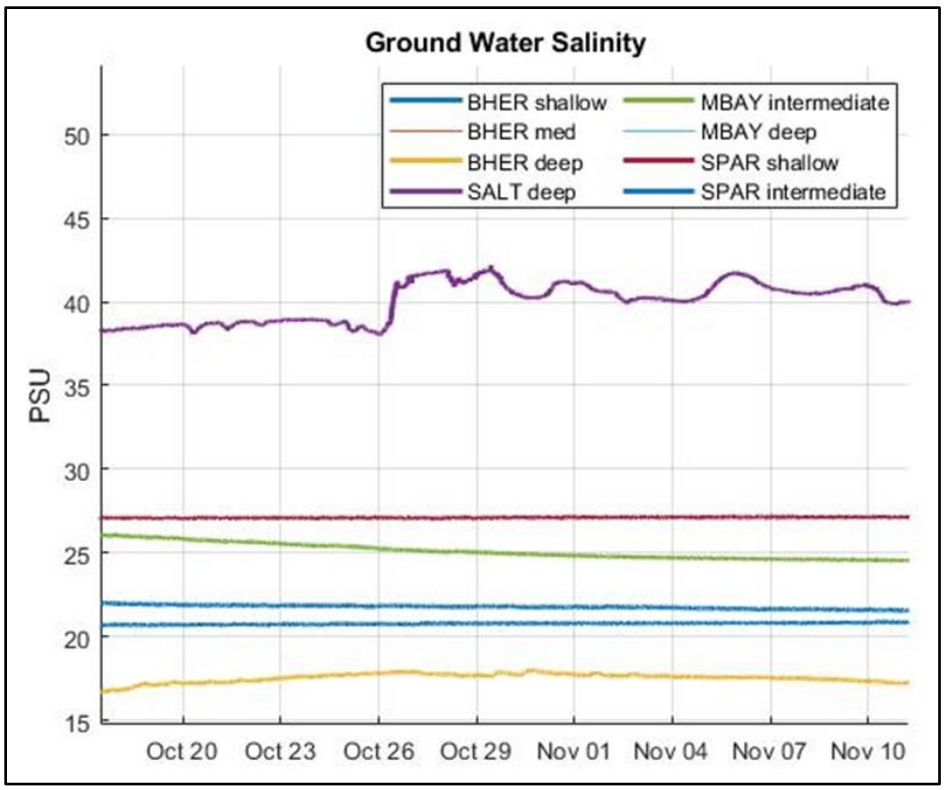

Figure 5.27 *Groundwater Salinity Stability and Storm Response*

Note the increase at Salt Pan likely due to storm water dissolution of surface salts and 2 day percolation

Conductivity generally follows the expected salinity gradient across the marsh. Conductivity decreases with depth, distance from open ocean, and seasonal precipitation. It is typically slow to fluctuate and does not show a strong diurnal tidal signal. Exceptions may include where very loose and organic surface materials allow for deeper surface water influence as observed at the shallow Spartina piezometer. Seasonally, there are long periods in winter and early-summer with lower tidal ranges and periods of reduced precipitation resulting in lower water levels. Conductivity can increase when surface tidal heights and precipitation are low. During these drier periods, the salinity gradient can shift more to the median of the marsh such that the salinity is higher through the mid marsh area than in the more open-ocean exposed areas (Figure 5.28). This partial gradient reversal is likely the result of evapotranspirationally-increased surface salinity. Late

summer thunderstorms and early fall cyclones provide regular precipitation and inundation events maintaining the normal salinity gradient, which increases seaward (Figure 5.29). Salt Pan tends to behave somewhat independently as it is generally higher salinity than the normal gradient range.

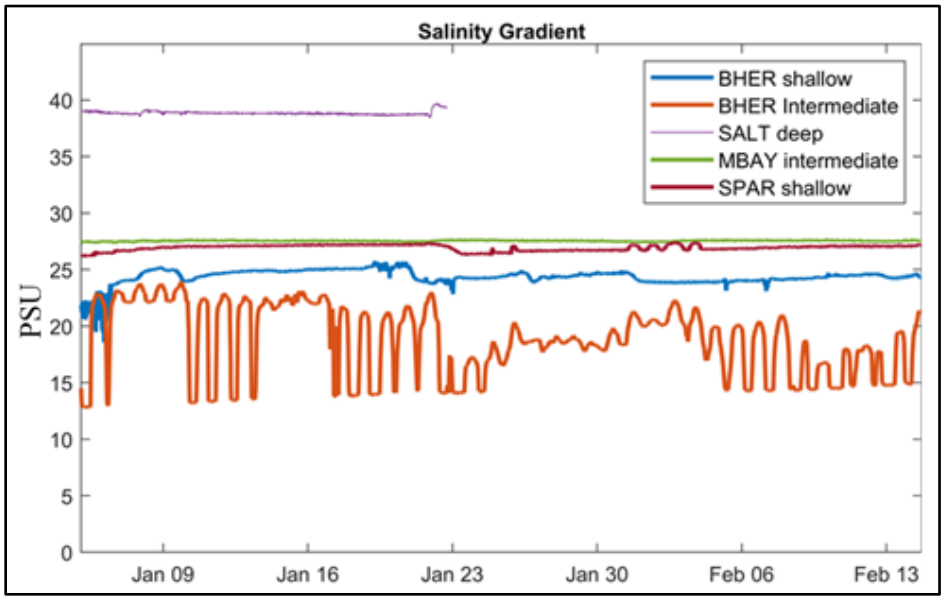

Figure 5.28 *Altered Groundwater Salinity Gradient (Dry Period)*

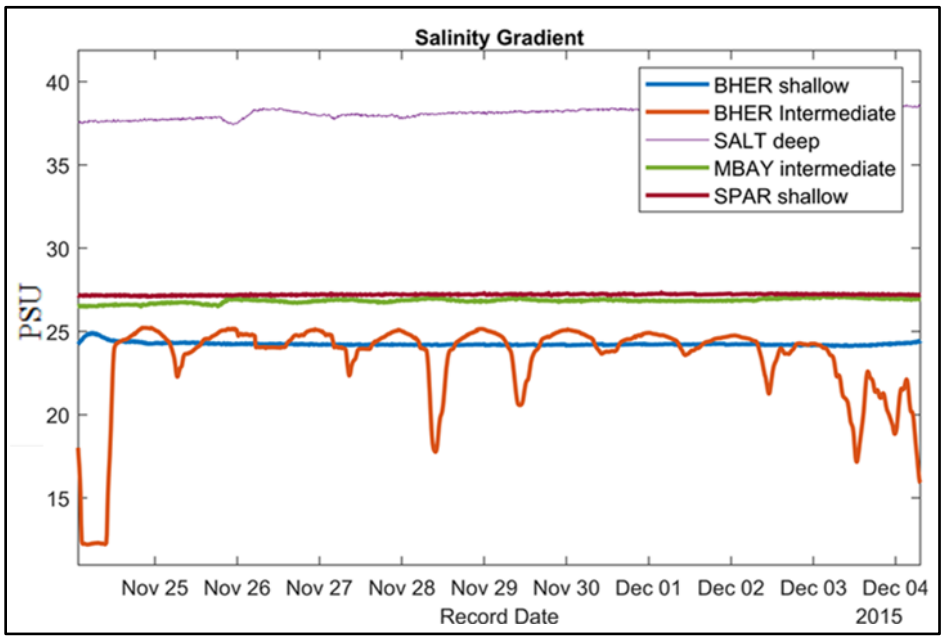

Figure 5.29 *Normal Groundwater Salinity Gradient (Wet Period)*

CHAPTER VI – CONCLUSIONS

6.1 Sedimentary Conclusions

In conclusion, a successful baseline of the current overall marsh system has been established. The relative percent of sand sized particles to silt and clay sized particles is the most significant control on many of the other soil and hydrologic characteristics. This is attributable to the greater permeability and porosity provided by the sands. In an estuarine environment with significant water movement from tides and storms, any increase in sand or relative decrease of smaller silt and clay particles results in leaching or loss of soluble ions and nutrients. This is seen in the organic content and magnetic susceptibility data. Most notably, Bayou Heron is distinct in this regard and represents the significant presence of fine sands and relative lack of silts and clays. It is characterized by a lack of colors, organic carbon, lower average carbonate, and significantly lower magnetic susceptibility. The proximity to the surface water channel of Bayou Heron is likely intertwined with the sand content and therefore also these other characteristics. The nearby Salt Pan site is a stark contrast. Having considerably less sands, Salt Pan is dominated by silts and has redoximorphic colorations, nearly double the organics and carbonate content, and significantly higher magnetic susceptibility.

Throughout the marsh, Munsell color analysis revealed an overall trend of reducing colors and the presence of redoximorphic features such as mottling. The organic matter analysis revealed an average content of 4.6% mass across all samples with a much higher content in the outer marsh samples. This high organic content provides a significant source of nutrients and plant available water. The carbonate content is low with an average of approximately 2% indicative of the tannic and acid surface runoff and

limited shell hash. Magnetic susceptibility analysis revealed a trend of decreasing terrestrial sediment supply as well as probable buried previously exposed vegetated soils. Particle size analysis revealed an overall lack of course grained material. Several clay layers were found that act to reduce permeability and resist the infiltration of higher salinity surface waters. There is strong evidence suggesting sedimentary structures and redox features indicative of rapid depositional events and buried deltaic surface soil horizons. These sediment composition and depositional structures play critical roles in the groundwater hydrology of the marsh.

6.2 Hydrology Conclusions

As expected, hydrology results are far more variable on the surface than the subsurface. I did not expect to see as much low salinity data at all the sites, but surface ponding may occur and allow rainfall to quickly fill the depressions with freshwater. Barometrically corrected records show strong signals of diurnal fluctuations in the shallow groundwater levels at all stations. Diurnal signaling was negligible in the shallow groundwater conductivity or temperature and present only in the outer marsh. This suggests that a hydrostatic pressure equilibrium generally exists between the surface and shallow groundwater. Salinity generally followed an increasing gradient seaward except during seasonal dry periods or at the Salt Pan site. During dry periods, salinity is observed to increase toward the middle marsh in excess of the Spartina site likely due to evapotranspiration. Variations among stations are likely controlled by sediment composition or depositional structures including observed clay layers and low permeability silts. Shallow groundwater conductivity and salinity generally decrease with

depth at all sites suggesting seaward flow of fresher subsurface waters and limited vertical mixing due to sedimentary controls.

Storm influences were present in surface and groundwater records. Low pressure storm systems increased surface and groundwater levels. Surface temperatures were observed to stabilize during the storm and return to daily solar cycles after flood water recession. Groundwater temperatures were unaffected by most storms and typically fluctuated no more than 1 degree Celsius per day. However, long duration precipitation events lowered the groundwater temperatures more rapidly than typical seasonal or daily fluctuations. Groundwater conductivity and salinity was generally stable and not significantly affected by storms except when heavy precipitation flushed limited surface salts into the shallow groundwater at the Salt Pan site. Middle Bay and Spartina exhibited no significant salinity change from short-term inundation events and further suggests low permeability sediments and clays resist surface infiltration and rapid salinity fluctuations Surface water salinity decreased with significant precipitation, but groundwater salinity was not significantly affected suggesting most surface salinity was removed in surface water runoff.

6.3 Broader Impacts

Based on the results obtained over the course of the study, I propose that further investigation is needed to understand the complex nature of the marsh hydrological system and its changes. The unfortunate gaps in hydrological data of the Salt Pan site leave many questions unresolved. The continued monitoring of hydrologic data has the potential to resolve some of these questions. The potential recording of additional

significant events similar even larger than Patricia could greatly increase our understanding of the possible future conditions in Gulf Coast marshes. Further study and more analysis from a multidisciplinary perspective may be needed to eliminate these unknowns and define these complicated marsh processes.

Understanding the sediment structure could allow for more accurately assessing the potential rates and significance of erosion, saline infiltration, and saline migration in shallow groundwater. The resultant understanding of erosion potential and saline migration would allow for more effective marsh conservation and restoration projects. The effectiveness of these have a direct impact on the health of the estuarine ecosystem, which serves as a feeding and breeding environment vital to many species that are commercial and recreationally fished.

Additional developments in scientific understanding of these underlying marsh systems will greatly enhance scientific research leading to more effective ecological management plans, hazard impact preparedness and recovery, property protection, carbon and nutrient cycle modeling, and storm impacts on marsh processes. In turn, each advancement allows for additional focused study of coastal processes and more accurate modeling of the potential responses to and impacts of climate and sea level change. This research is just one aspect of a larger multidisciplinary effort and will directly impact all aspects of that effort.

APPENDIX A – USGS Particle Size Classification

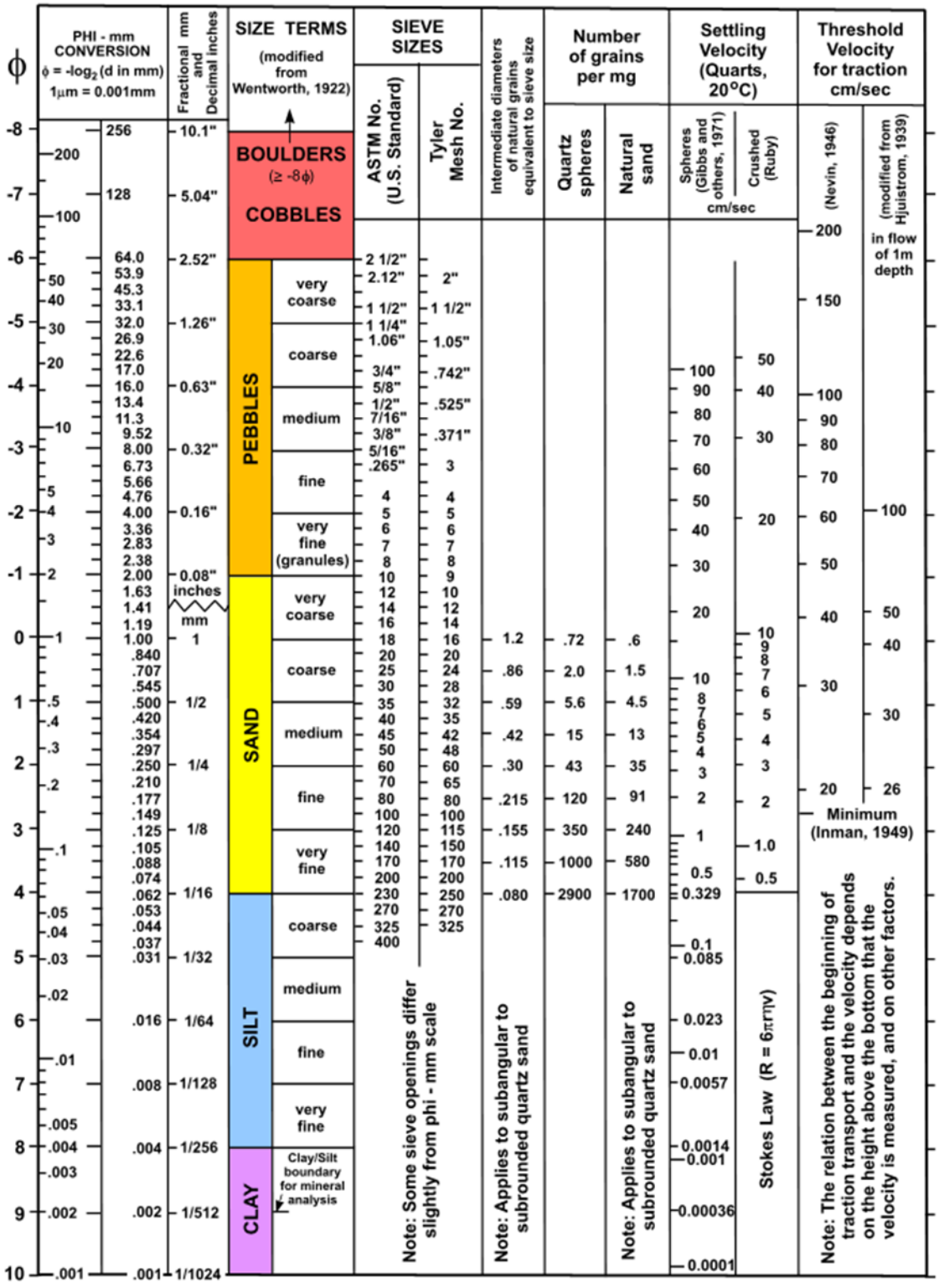

Figure A.1 *USGS Particle Size Conversion Scale*

APPENDIX B – Particle Size Distribution Curves

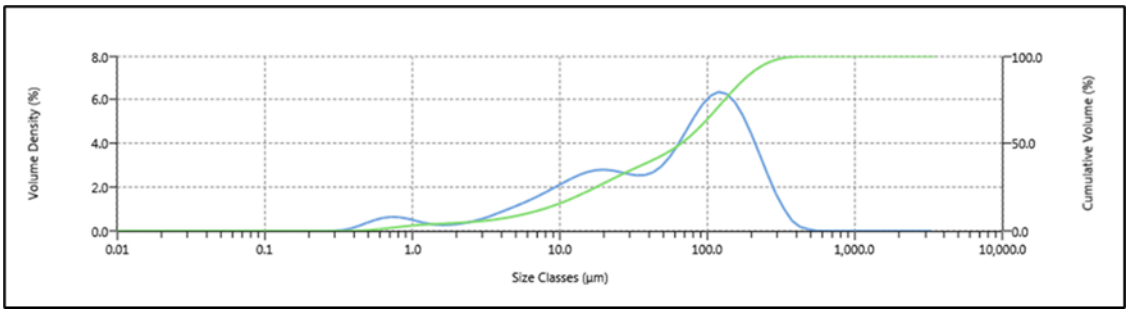

Figure B.1 *Average of All Bayou Heron Samples*

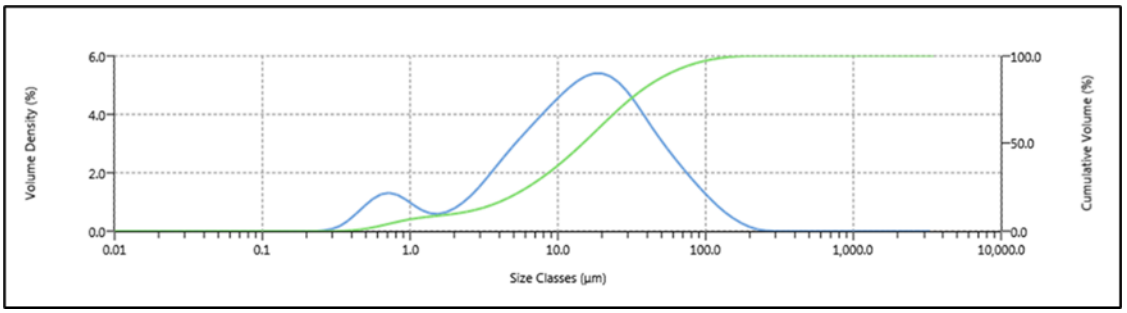

Figure B.2 *Average of All Salt Pan Samples*

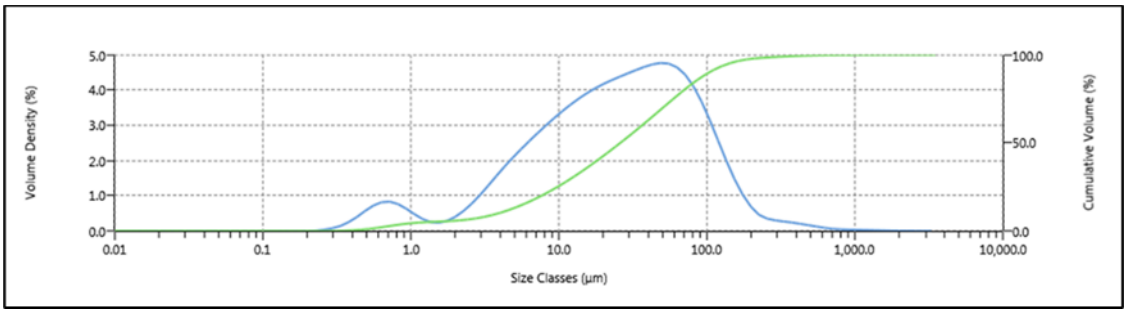

Figure B.3 *Average of All Middle Bay Juncus Samples*

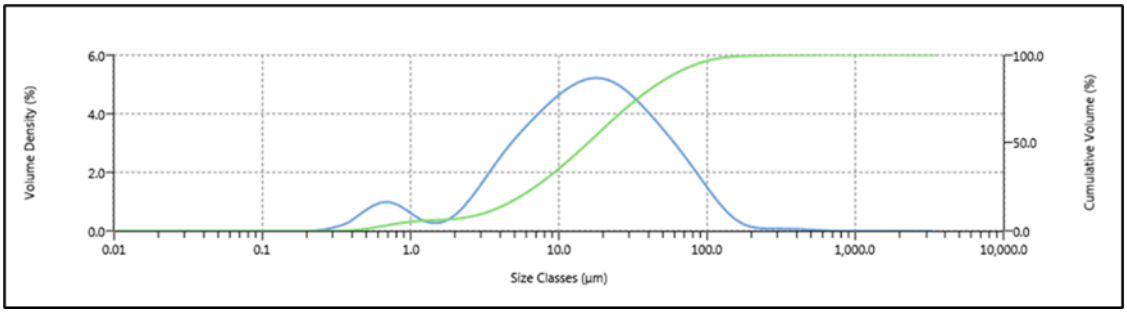

Figure B.4 *Average of All Spartina Samples*

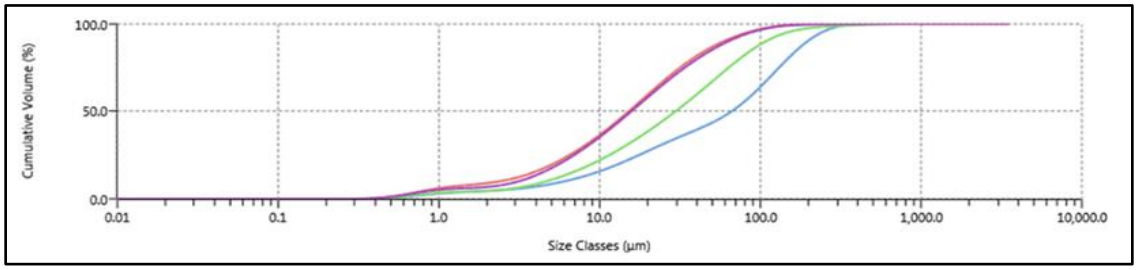

Figure B.5 *Site Average Comparison of Cumulative Volume*

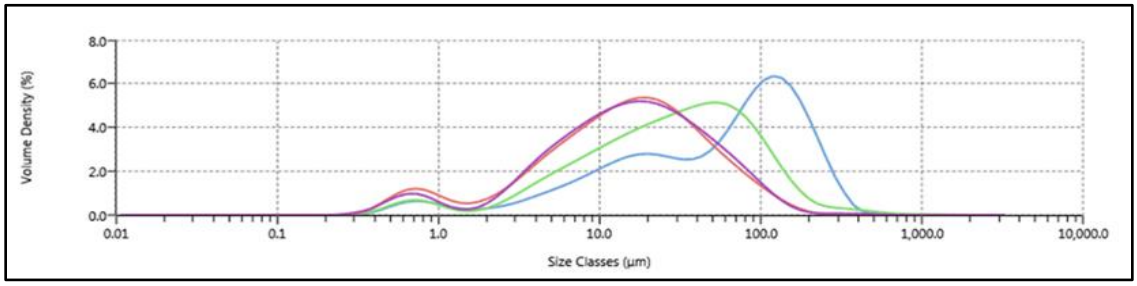

Figure B.6 *Site Average Comparison of Volume Density*

APPENDIX C – Correlation of Sedimentary Variables

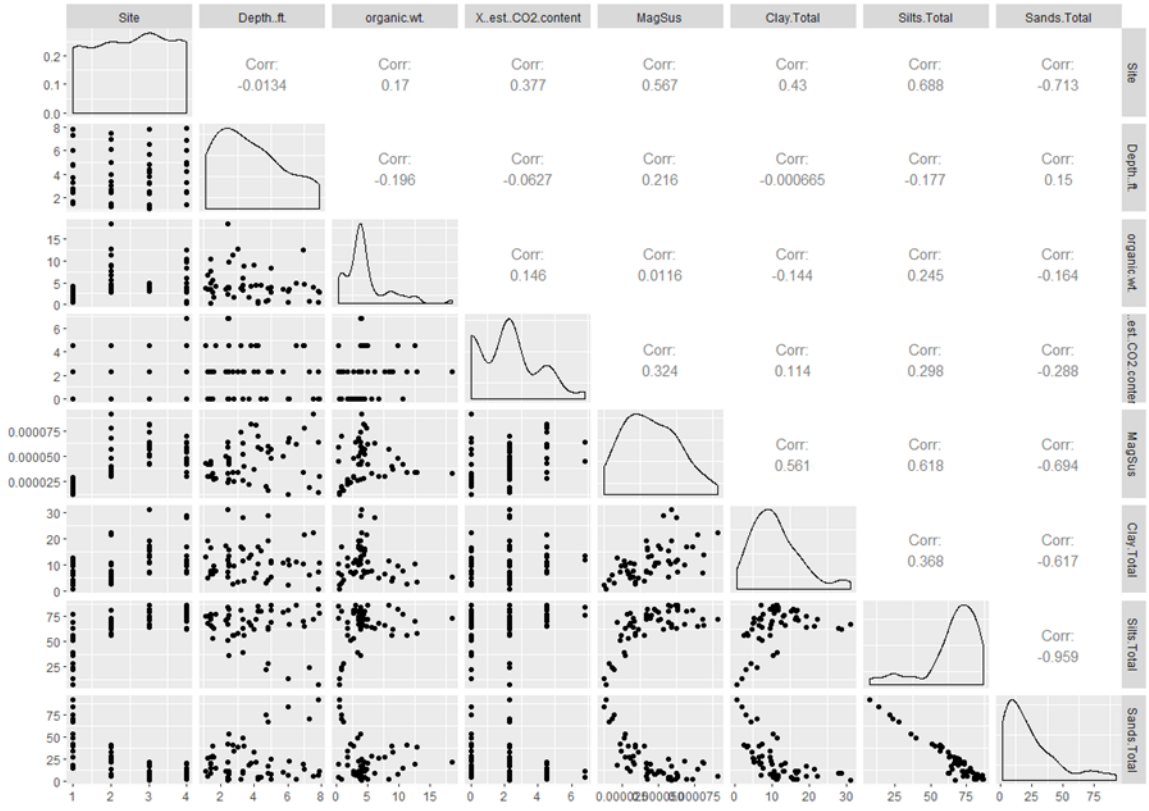

Figure C.1 *Cluster Analysis and Correlation of Sedimentary Biplots*

Produced with R using Rattle (Williams, 2011)

REFERENCES

Allison, L. E., & Moodie, C. D. (1965). Carbonate. In B. C.A. (Ed.), *Methods of Soil Analysis Part 2* (pp. 1279-1396). Madison: American Society of Agronomy.

Anderson, J. B., Wallace, D. J., Simms, A. R., Rodriguez, A. B., Weight, R. R., & Taha, Z. P. (2016, February). Recycling Sediments Between Source and Sink During a Eustatic Cycle: Systems of Late Quaternary Northwestern Gulf of Mexico Basin. *Earth-Science Reviews, 153*, 111-138.

ASTM. (2007). *D422-63(2007)e1, Standard Test Method for Particle-Size Analysis of Soils.* West Conshohocken, PA: ASTM International.

ASTM. (2011). *C25-11e2, Standard Test Methods for Chemical Analysis of Limestone, Quicklime, and Hydrated Lime.* West Conshohocken, PA: ASTM International.

ASTM. (2011). *F1647-11, Standard Test Methods for Organic Matter Content of Athletic Field Rootzone Mixes.* West Conshohocken: ASTM International. Retrieved from www.astm.org

Barbier, E. B., Hacker, S. D., Kennedy, C., Kich, E. W., Stier, A. C., & Silliman, B. R. (2011, May 01). Value of Estuarine and Coastal Ecosystem Services. *Ecological Monographs, 81*(2). doi:10.1890/10-1510.1

Beierle, B. D., Lamoureux, S. F., Cockburn, J. M., & Spooner, I. (2002). A New Method for Visualizing Particle Size Distributions. *Journal of Paleolimnology*(27), 279-283. doi:10.1023/A:1014209120642

Brady, N., & Weil, R. (2010). *Elements of the Nature and Properties of Soils* (3rd ed.). Upper Saddle River: Prentice Hall.

Carter, E., White, S., & Wilson, A. (2008). Variation in Groundwater Salinity in a Tidal Salt Marsh Basin, North Inlet Estuary, South Carolina. *Estuarine, Coastal and Shelf Science*(76), 543-552.

Cooper, J., & Pilkey, O. (2004). Sea-Level Rise and Shoreline Retreat: Time to Abandon the Bruun Rule. *Global and Planetary Change*(43), 157-171.

Craft, C. B., Seneca, E. D., & Broome, S. W. (1991, June). Loss on ignition and kjeldahl digestion for estimating organic carbon and total nitrogen in estuarine marsh soils: Calibration with dry combustion. *Estuaries, 14*(2), 175-179. doi:10.2307/1351691

Crockford, R. H., & Fleming, P. M. (1998). Environmental Magnetism as a Stream Sediment Tracer: an Interpretation of the Methodology and Some Case Studies. *Australian Journal of Soil Research, 36*(1), 167-184. doi:10.1071/S97040

Dolan, R., Hayden, B., & Lins, H. (1980). Barrier Islands: The Natural Processes Responsible for the Evolution of Barrier Islands and for Much of Their Recreational and Aesthetic Appeal Also Make Them Hazardous Places for Humans to Live. *American Scientist, 68*(1), 16-25.

Eleuterius, C., & Criss, A. (1991). *Point aux Chenes: Past, Present, and Future Perspective of Erosion.* Ocean Springs: Gulf Coast Research.

Goh, T. B., Arnaud, R. J., & Mermut, A. R. (1993). Carbonates. In M. Carter (Ed.), *Soil Sampling and Methods of Analysis* (pp. 177-180). Boca Raton: Lewis Publishers.

Gornitz, V. M., Daniels, R. C., White, T. W., & Birdwell, K. R. (1994). The Development of a Coastal Risk Assessment Database: Vulnerability to Sea-Level Rise in the U.S. Southeast. *Journal of Coastal Research, SI*(12. COASTAL HAZARDS: PERCEPTION, SUSCEPTIBILITY AND MITIGATION), 327-338.

Gosselink, J. G., Odum, E. P., & Pope, R. M. (1974). *The Value of the Tidal Marsh* (Vol. 3). Baton Rouge: Center for Wetland Resources, Louisiana State University.

Grand Bay National Estuarine Research Reserve. (2013). *Grand Bay National Estuarine Research Reserve Management Plan 2013-2018.* Grand Bay National Estuarine Research Reserve, Mississippi Department of Marine Resources. Moss Point, Mississippi: Mississippi Department of Marine Resources.

Hatfield, R. G., & Maher, B. A. (2009, June 16). Fingerprinting Upland Sediment Sources: Particle Size-Specific Magnetic Linkages Between Soils, Lake Sediments and Suspended Sediments. *Earth Surface Processes and Landforms*. doi:10.1002/esp.1824

Hatfield, R. G., Cioppa, M. T., & Trenhaile, A. S. (2010, November 15). Sediment Sorting and Beach Erosion Along a Coastal Foreland: Magnetic Measurements in Point Pelee National Park, Ontario, Canada. *Sedimentary Geology, 231*(3-4), 63-73.

Hilbert, K. (2006, November). Land Cover Change within the Grand Bay National Estuarine Research Reserve: 1974-2001. *Journal of Coastal Research, 22*(6), 1552-1557.

Hoyt, J. H. (1967). Barrier Island Formation. *Geological Society of America Bulletin, 78*(9), 1125-1135.

Maher, E., Harvey, A., & France, D. (2007). The Impact of a Major Quaternary River Capture on the Alluvial Sediments of a Beheaded River System, the Rio Alias SE Spain. *Geomorphology*(84), 344-356.

Malvern. (2015). *Mastersizer 3000 Basic Guide.* Worcestershire, UK: Malvern Instruments Ltd.

Melillo, J., Richmond, T., & Yohe, G. (2014). *Climate Change Impacts in the United States: The Third National Climate Assessment.* U.S. Global Change Reseach Program. doi:10.7930/J0Z31WJ2

Milliken, K., Anderson, J. B., & Rodrigues, A. B. (2008). A new composite Holocene sea-level curve for the northern Gulf of Mexico. In J. B. Anderson, & A. B. Rodriguez, *Response of Upper Gulf Coast Estuaries to Holocene Climate Change and Sea-Level Rise* (Vol. 443). Geological Society of America. doi:10.1130/SPE443

Morton, R. A., Miller, T., & Moore, L. (2005, July). Historical Shoreline Changes Along the US Gulf of Mexico: A Summary of Recent Shoreline Comparisons and Analyses. *Journal of Coastal Research, 21*(4), 704-709.

Morton, R., Miller, T., & Moore, L. (2004). *National Assessment of Shoreline Change: Part 1: Historical Shoreline Changes and Associated Coastal Land Loss Along the U.S. Gulf of Mexico.* Center for Coastal and Watershed Studies. St. Petersburg: U.S. Geological Survey.

Mudd, S. M., Howell, S., & Morris, J. T. (2009). Impact of Dynamic Feedbacks between Sedimentation, Sea-Level Rise, and Biomass Production on Near-Surface Marsh Stratigraphy and Carbon Accumulation. *Estuary, Coast and Shelf Science, 82*, 377-389.

Munsell Soil Color Charts. (2000). New Windsor: Munsell Color Company.

Munsell, A. H. (1907). *A Color Notation* (2nd ed.). Boston: Geo. H. Ellis Co.

National Data Buoy Center. (2009). *Handbook of Automated Data Quality Control Checks and Procedures.* U.S. Department of Commerce, National Oceanic and Atmospheric Administration. Stennis Space Center, MS: NDBC.

Nicholls, R. J., Leatherman, S. P., Dennis, K. C., & Volonte, C. R. (1995, Winter). Impacts and Responses to Sea-Level Rise: Qualitative and Quantitative Assessments. *Journal of Coastal Research, SI*(14), 26-43.

NOAA. (2017). *Coastal Fast Facts*. Retrieved from NOAA Office for Coastal Management: https://coast.noaa.gov/

Oades, J. M. (1984, February). Soil Organic Matter and Structural Stability: Mechanisms and Implications for Management. *Plant and Soil, 76*(1-3), 319-337. doi:10.1007/BF02205590

Office of Ocean and Coastal Resources. (2012). *Sentinel Sites Program Guidance for Climate Change Impacts.* Silver Spring: NOAA.

Otvos, E. (1985, March). Coastal Evolution - Louisiana to Northwest Florida: Guidebook. *American Association of Petroleum Geologists Annual Meeting*, pp. 27-29.

Passeri, D., Hagen, S., Medeiros, S., & Bilskie, M. (2015). Impacts of Historic Morphology and Sea Level Rise on Tidal Hydrodynamics in a Microtidal Estuary (Grand Bay, MS). *Continental Shelf Research, 111*, 150-158.

Pendleton, E., Thieler, E. R., & Williams, S. J. (2010, January). Importance of Coastal Change Variables in Determining Vulnerability to Sea- and Lake-Level Change. *Journal of Coastal Research, 26*(1), 176-183.

Perkin, R. G., & Lewis, E. L. (1980). The Practical Salinity Scale 1978: Fitting the Data. *IEEE Journal of Oceanic Engineering, 5*(1), 9-16. doi:10.1109/JOE.1980.1145441

R Core Team. (2017). *R: A Language and Environment for Statistical Computing.* R Foundation for Statistical Computing, Vienna, Austria. Retrieved from https://www.R-project.org/

Santisteban, J. I., Mediavilla, R., Lopez-Pamo, E., & et al. (2004). Loss On Ignition: A Qualitative or Quantitative Method for Organic Matter and Carbonate Mineral Content in Sediments. *Journal of Paleolimnology, 32*(3), 287-299.

Scavia, D., Field, J., Boesch, D., Buddemeier, R., Burkett, V., Cayan, D., . . . Titus, J. (2002, April). Climate Change Impacts on U.S. Coastal and Marine Ecosystems. *Estuaries, 25*(2), 149-164.

Schmid, K. (2000). *Shoreline Erosion Analysis of Grand Bay Marsh.* Mississippi Department of Environmental Quality, Office of Geology, Jackson.

Schmid, K., & Otvos, E. (2004, September 1). *Geology and Geomorphology of the Coastal Counties in Mississippi - Alabama.* Retrieved from Mississippi Department of Environmental Quality: http://geology.deq.state.ms.us/coastal/Pubs_Publications.htm

Schmidt, N. (1965). *A Study of the Isolation of Organic Matter as a Variable Affecting Engineering Properties of a Soil.* University of Illinois at Urbana-Champaign: ProQuest Dissertations Publishing.

Schwartz, M. L. (1967). The Bruun Theory of Sea-Level Rise as a Cause of Shore Erosion. *The Journal of Geology, 75*(1).

Stratton, P. (2014). Munsell Color Conversion. *Munverter*. Philadephia, PA, USA: Halescode Software. Retrieved 2015, from munverter.com

Strauss, B., Ziemlinski, R., Weiss, J., & Overpeck, J. (2002, March 14). Tidally Adjusted Estimates of Topographic Vulnerability to Sea Level Rise and Flooding for the Contiguous United States. *Environmental Research Letters, 7*, 12. doi:10.1088/1748-9326/7/1/014033

The National Climatic Data Center from NOAA. (2021). *Climate Pascagoula - Mississippi and Weather Averages*, 3. (Y. W. Service, Editor) Retrieved from U.S. Climate Data: https://www.usclimatedata.com/climate/pascagoula/mississippi/united-states/usms0281

Tornqvist, T. E., Paola, C., Parker, G., Liu, K.-b., Mohrig, D., Holbrook, J. M., & Twilley, R. R. (2007, April 13). Comment on "Wetland Sedimentation from Hurricanes Katrina and Rita". *Science, 316*(5822), 201. doi:10.1126/science.1136780

Turner, R. E., Baustian, J. J., Swenson, E. M., & Spicer, J. S. (2006, October 20). Wetland Sedimentation from Hurricanes Katrina and Rita. *Science, 314*(5798), 449-452. doi:10.1126/science.1129116

Vepraskas, M. (2014). *Redoximorphic Feature Formation and Interpretation.* NC State University, Department of Soil Science, Raleigh.

Wetlands Regulatory Assistance Program. (2000). *Installing Monitoring Wells and Piezometers in Wetlands.* Vicksburg: U.S. Army Engineer Research and Development Center.

White, W. A., & Tremblay, T. A. (1995, Summer). Submergence of Wetlands as a Result of Human-Induced Subsidence and Faulting Along the Upper Texas Gulf Coast. *Journal of Coastal Research, 11*(3), 788-807.

Williams, G. J. (2011). *Data Mining with Rattle and R: The Art of Excavating Data for Knowledge Discovery.* Springer.